

# Benchmarking Study of Various Commercial Polypropylene Raffia Grades Available in Indian Market

A Major Project Report submitted towards partial fulfillment of the requirement for the degree

of

**MASTER OF ENGINEERING  
IN  
POLYMER TECHNOLOGY**

*Submitted by*

**EHTESHAMUL ISLAM**

(University Roll No.9004)

*Under the able guidance of*

**Dr. G.L.Verma**

Head of the Department

Department of Applied Chemistry & Polymer Technology

Delhi College of Engineering, Delhi-110042

&

*Dr. G.S. Kapur and Dr. Shashikant*

Petrochemical & Polymer Department

R & D Centre, Indian Oil Corporation Ltd.

Faridabad -121007



**DEPARTMENT OF APPLIED CHEMISTRY & POLYMER TECHNOLOGY  
DELHI COLLEGE OF ENGINEERING  
UNIVERSITY OF DELHI, DELHI**

## **CERTIFICATE**

This is to certify that the M.E. major project entitled “Benchmarking Study of Various Commercial Polypropylene Raffia Grades Available in Indian Market” has been completed by MR. EHTESHAMUL ISLAM, a student of M.E. (Polymer Technology) in the Department of Applied Chemistry, of Delhi College of Engineering, Delhi University.

The original work has been carried out by him under our joint supervision and guidance for the partial fulfillment of the requirement of the M.E. Polymer Technology.

The project work has been carried out during the session 2010-2011.

To the best of our knowledge and belief the content therein is his own original work and has not been submitted to any other University or Institute for the award of any degree or diploma.

***DR. G.S. KAPUR***

Chief Research Manager  
Petrochemical & Polymer Department  
R&D Centre  
Indian Oil Corporation Limited  
Faridabad-121007

***DR. G.L. VERMA***

Head of the Department  
Department of Applied Chemistry  
Delhi College of Engineering  
Bawana Road, Delhi-110042

***DR. SHASHIKANT***

Deputy General Manager  
Petrochemical & Polymer Department  
R&D Centre  
Indian Oil Corporation Limited  
Faridabad-121007

## Acknowledgement

I would like to acknowledge all persons who have contributed directly or indirectly to the completion of my project and have seen its materialization in the form of this thesis.

First and foremost I would like to thank the management of Indian Oil R&D Centre, Faridabad, for giving me this opportunity to carry out this project work in their esteemed R&D Centre. I would like to express my gratitude to my external guide *Dr. G.S. Kapur (Chief Research Manager, Petrochemicals and Polymers, R&D center, IOCL)* for giving me an opportunity to complete my M.E. project-work under his selfless guidance. He not only proposed this project but also obliged me with his valuable suggestions at every step of the project. For me it was a privilege to work with his research team at the R&D Centre of IOCL, Faridabad. To him I owe more than I can say.

I would also like to thank *Dr. Shashikant (Deputy General Manager, R&D center, IOCL)* for not only providing me an opportunity to work at the reputable R&D Centre but also for his rigorous and fruitful discussions on the interpretation of experimental data and results. Truly, I have learnt a lot from him. His contribution was remarkable and memorable.

I would also like to thank my Institutional guide *Dr. G.L. Verma (H.O.D, Department of Applied Chemistry, Delhi College of Engineering, University of Delhi)*, for his care and guidance throughout my M.E. course and particularly for making it possible for me to have the time and quiet needed to involve myself in the activities-like, going through the literature, consequently leading to the completion of this assignment.

I would also like to thank *Mr. K.K. Vimal (Research Officer)* for his continuous guidance, advice, encouragement and most importantly for his patience. Without his consistent support this work wouldn't have been the same.

I also appreciate the way he made me understand the physical meaning of each concept and I owe a great deal to him providing me such a genial and cozy environment that I could expedite my work independently. Words are incapable to sufficiently indicate the extent to which obligations are due.

Yet I would like to take this opportunity of expressing my gratitude to Mr. *J.S. Dhaliwal (SRO)*, Dr. *K. Naresh Kumar (Research officer)*, and Mr. *M.S. Negi (Research officer)* for their useful suggestions and to make me learn how the things happen in the R&D Center. I would also like to thank Dr. *J. Christopher (CRM-AD)*, Dr. *Anil Yadav (SRO-AD)*, Dr. *Veena Bansal (SRM-AD)* and Dr. *Ravinder Singh (RO)*. All of them helped me in one way or another.

I would also like to acknowledge and appreciate the support of Mr. *S.M. Sanduja (Training Manager)* and Mr. *Sanjay Bhagat (Training Officer)* during the course of the project. And special thanks to Mr. *Anil Sharma*, Mr. *Ranbir Singh* and Mr. *Chander* for their kind co-operation during the experimental work.

Lastly I desire to record here my sincere thanks to my colleagues for their friendly co-operation and co-ordination, and also to all those whose names I forgot to mention but who in different ways have helped and encouraged me.

## **DEDICATION**

I would like to dedicate this work to my family, especially, to my mother *Mrs. Aseema Perveen Suraiya* and my father *Mr. Badre Alam*, who gave me the opportunities that they didn't have. I am also deeply indebted to my elder brother *Mr. Obaidullah Raihan*. He is the person who supported me throughout the course of my masters program.

## **Executive Summary**

Under this research work ten different commercially available polypropylene homopolymer Raffia grades were taken. The main objective of this study was to establish 'Structure-Property-Performance' relationship. "Performance" refers to their processability and runnability at higher line speed (Extrusion Tape Line). Therefore, trial runs were conducted on these PP raffia grades in order to analyze their performances. It was found that some grades, namely, PP/R/R-036 & PP/R/H-031 run very well at higher line speeds of 415mt/min and 365mt/min respectively, when compared to other grades, namely, PP/R/I-071, PP/R/I-075 and PP/R/I-027. The major problems found with PP/R/I-071, PP/R/I-075 and PP/R/I-027 grades during the trial run were the tape breakage, higher power consumption, higher water carry-over etc.

Therefore, to ascertain the root cause of the inferior performance of PP/R/I-071, PP/R/I-075 and PP/R/I-027 a detailed "Benchmarking" study on these PP-raffia grades, were undertaken. Each grade was characterized in detailed using MFI & MFR, Capillary Rheometer, Differential Scanning Calorimetry, Oxygen Index Test, Dynamic Mechanical Analyzer, Dynamic Rotational Rheometer and HT-GPC techniques. On comparing the characteristics of these grades it was found that the PP/R/R-036 and PP/R/I-089 grades were having the good combination of higher modulus; low melt viscosity, higher melt elasticity and high crystallinity, than other grades, mainly due to the differences in various aspects such as high molecular weight tail, high and low molecular weight fractions at very low concentration, molecular weight distribution. Polypropylene raffia grades such as PP/R/R-036 and PP/R/I-089 have very limited high molecular weight tail with moderately broad molecular weight distribution. It is worth mentioning here that PP/R/I-075, PP/R/I-071 and PP/R/I-027 comparatively have very high molecular weight tail. These long molecular weight fractions will reduce the overall crystallinity by reducing the enthalpy. In addition to that, grades with comparatively broad molecular weight distribution have shown better processability and flowability. The presence of high molecular weight fractions at low concentration also play detrimental role during the orientation and annealing process, as in the case of PP/R/R-036 and PP/R/I-089 in the tape extrusion process.

## **List of figures:**

1. **Figure.1:**  $3_1$  helix structure of Polypropylene, (H. Batzer [9]).
2. **Figure.1.1:** Chain folded lamella in semicrystalline polymers [10].
3. **Figure.1.2:** Isomerism in polypropylene. a) Isotactic polypropylene.  
b) Syndiotactic polypropylene. c) Atactic polypropylene as illustrated by Karger and Kocsis (1995).
4. **Figure 1.3:** The m, meso-diad and the r, racemic diad, depending on the relative position of the CH<sub>3</sub>- group as described by Busico and Cipullo (2001) [11].
5. **Figure.1.4:** The isotactic pentad (mmmm), and the syndiotactic pentad (rrrr) by Busico and Cipullo (2001) [11].
6. **Figure 1.5:** Extrusion Tape line [14].
7. **Figure 1.6:** Coat Hanger Die
8. **Figure 1.7:** Screen Changer, Melt pump and Die [14].
9. **Figure 1.8:** Rotatory Slitter [14].
10. **Figure 1.9:** Stretching and Annealing Godets [14].
11. **Figure.2:** Transition from lamellar to micro-fibril morphology (peterlin [1973])
12. **Figure.2.1:** Tape Winding
13. **Figure 2.2:** Woven Sacks
14. **Figure 2.3:** FIBC or Jumbo Bag [22].
15. **Figure 2.4:** PP monofilaments rope [23].
16. **Figure 2.5:** Furniture band made up of PP raffia [23].
17. **Figure 2.6:** Weaving pattern of PP raffia leno bags.
18. **Figure 2.7:** PP raffia leno bags.
19. **Figure.3:** Velocity, shear rate and shear stress profiles for flow between two parallel plates [24].
20. **Figure.3.1:** Typical GPC column with elution mechanism [26].
21. **Figure 3.2:** schematic of sinusoidal oscillating frequency to a sample and the corresponding sinusoidal response from the material [27].
22. **Figure.3.3:** Location of the cross-over point of G' and G'' gives information about the molecular weight and molecular weight distribution [28].
23. **Figure.3.4:** Thermal Curve of a Standard OIT Test.

24. **Figure.3.5.** Storage and loss;  $E'$  describe the stored energy while  $E''$  describe the loss energy due to internal motions and friction [27].
25. **Figure.3.6:** Stereodeflects in polypropylene chains after Busico and Cipullo (2001) [11].
26. **Figure.3.7:** Theoretically possible ten non-equivalent steric pentads Busico and Cipullo (2001) [11].
27. **Figure.4:** shear viscosity Vs shear rate graph of PP/R/R-036, PP/R/I-075, PP/R/H-031 and PP/R/L-035.
28. **Figure.4.1:** Shear viscosity Vs shear rate graph of PP/R/R-036, PP/R/I-075, PP/R/I-070 and PP/R/I-071.
29. **Figure.4.2:** shear viscosity Vs shear rate graph of PP/R/R-036, PP/R/I-027, PP/R/I-089 and PP/R/I-066.
30. **Figure.4.3:** shear viscosity Vs shear rate graph of PP/R/H-031, PP/R/I-027, PP/R/I-089 and PP/R/I-066 and PP/R/L-035.
31. **Figure.4.4:** shear viscosity Vs shear rate graph of all the PP raffia grades.
32. **Figure.5:** Shear viscosity Vs corrected shear rate graph for PP-raffia grades.
33. **Figure.5.1:** HT-GPC MWD chromatogram of PP/R/R-036 Vs PP/R/I-075.
34. **Figure.5.2:** Complex Viscosity Vs Angular Frequency of PP/R/R-036 and PP/R/I-075.
35. **Figure.5.3:** MWD from rheometry and HT-GPC of PP/R/R-036 Vs PP/R/I-075.
36. **Figure 5.4:** Storage Modulus ( $G'$ ) and Loss Modulus Vs Angular Frequency of PP/R/R-036 and PP/R/I-075.
37. **Figure 5.5:** HT-GPC MWD chromatogram of PP/R/H-031 Vs PP/R/I-075.
38. **Figure 5.6:** Complex viscosity Vs Angular frequency of PP/RH-031 and PP/R/I-075.
39. **Figure 5.7:** MWD from rheometry and HT-GPC of PP/R/H-031 and PP/R/I-075.
40. **Figure 5.8:** Storage Modulus ( $G'$ ) and Loss Modulus Vs Angular Frequency of PP/R/H-031 and PP/R/I-075.
41. **Figure 5.9:** HT-GPC MWD chromatogram of PP/R/I-075 Vs PP/R/I-071.
42. **Figure.6:** Complex viscosity Vs Angular frequency of PP/R/I-071 and PP/R/I-075.



43. **Figure.6.1:** MWD chromatogram from GPC and rheometry of PP/R/I-071 Vs PP/R/I-075.
44. **Figure.6.2:** Storage Modulus (G') and Loss Modulus Vs Angular Frequency of PP/R/I-071 and PP/R/I-075.
45. **Figure 6.3:** HT-GPC MWD chromatogram of PP/R/R-036 Vs PP/R/I-089.
46. **Figure.6.4:** Complex viscosity Vs Angular Frequency of PP/R/R-036 and PP/R/I-089.
47. **Figure 6.5:** Storage Modulus (G') and Loss Modulus Vs Angular Frequency of PP/R/R-036 and PP/R/I-089.
48. **Figure 6.6:** HT-GPC MWD curves of PP/R/I-089 and PP/R/I-027.
49. **Figure 6.7:** Complex viscosity Vs Angular Frequency of PP/R/I-089 and PP/R/I-027.
50. **Figure 6.8:** Storage Modulus (G') and Loss Modulus Vs Angular Frequency of PP/R/I-089 and PP/R/I-027.
51. **Figure.7:** DSC melting thermograms of PP/R/R-036, PP/R/I-075 and PP/R/H-031.
52. **Figure.7.1:** DSC melting thermograms of PP/R/R-036, PP/R/I-071, PP/R/H-031 and PP/R/I-070.
53. **Figure 7.2:** DSC melting and cooling thermograms of PP/R/I-089.
54. **Figure7.3:** DSC melting and cooling thermograms of PP/R/I-027.
55. **Figure7.4:** DSC melting and cooling thermogram of PP/R/I-066.
56. **Figure.8.** Storage modulus, Loss modulus and Tan delta curves of PP-raffia samples.
57. **Figure.8.1** Storage modulus, Loss modulus and Tan delta curves of PP-raffia samples.
58. **Figure.9:**  $^{13}\text{C}$ -NMR spectra of PP/R/R-032.
59. **Figure.9.1:**  $^{13}\text{C}$ -NMR spectra of PP/R/I-070.
60. **Figure.9.3:**  $^{13}\text{C}$ -NMR spectra of PP/R/I-075.
61. **Figure.9.4:**  $^{13}\text{C}$ -NMR spectra of PP/R/I-027.
62. **Figure.9.5:**  $^{13}\text{C}$ -NMR spectra of PP/R/I-089.

## **List of Tables:**

1. **Table.1:** Summary of the trial run on different polypropylene raffia grades.
2. **Table.1.1:** Nomenclature of the samples used in the study.
3. **Table.1.2:** End uses indication through MFI for various grades of polypropylene (Krassing et al (1984)).
4. **Table.1.3:** Xylene soluble fractions of all the ten grades.
5. **Table 1.4:** MFI, shear rate and shear viscosity values at 2.16kg of all the grades at 230°C.
6. **Table 1.5:** MFI values at 20.6kg of all the grades at 230°C.
7. **Table.1.6:** MFI and MFR of all the grades at 230°C.
8. **Table 1.7:** power law constants n and m calculated from MFI at 2.16 and 20.6 kg.
9. **Table.2:** DSC parameters of PP/R/H-031, PP/R/R-036 and PP/R/I-075.
10. **Table.2.1:** DSC parameters of PP/R/H-031, PP/R/R-036, PP/R/I-071 and PP/R/I-070 grades.
11. **Table.2.2:** DSC parameters of PP/R/R-036, PP/R/I-089, PP/R/I-027 and PP/R/I-066 grades.
12. **Table.3:** Oxidation induction Time of the 7 grades.
13. **Table.4:** The % Xylene Solubles and % mmmm sequences of PP/R/R-032, PP/R/I-70, PP/R/I-71, PP/R/I-75, PP/R/I-027 and PP/R/I-089 grades.

## **TABLE OF CONTENTS:**

Executive Summary.....	06
Lists of figures.....	07
List of tables.....	10
<b><u>Chapter-1</u></b> .....	<b>13</b>
1.1. Introduction.....	13
1.2. Stereoisomerism and Stereoregularity.....	14
<b><u>Chapter-2</u></b> .....	<b>17</b>
2.1. Introduction to Raffia grade polypropylene.....	17
2.1.1. Desirable resin characteristics.....	17
2.2. Raffia tape Manufacturing process.....	18
2.2.1. Extrusion of film.....	18
2.2.2. Quenching of film.....	20
2.2.3. Slitting of film.....	20
2.2.4. Orientation of tapes.....	21
2.2.4.1. Orientation and its effects on the morphology of PP.....	22
2.2.5. Annealing of tapes.....	23
2.2.6. Winding of films.....	24
2.3. Desirable characteristics of polypropylene raffia tapes.....	24
2.4. Application of polypropylene raffia tapes.....	25
<b><u>Chapter-3</u></b> Genesis of the problem.....	<b>27</b>
3.1. Genesis of the problem.....	29
3.1.1 Summary of the trial run.....	30
<b><u>Chapter-4</u></b> Experimental methods and conditions used for structural analysis.....	<b>31</b>
4.1. Xylene Solubles.....	32
4.2. Melt Flow Index.....	33
4.2.1. MFR (Melt Flow Rate).....	34
4.2.2. Calculation of shear-viscosity using power law equation.....	34
4.3. Capillary Rheometer.....	35

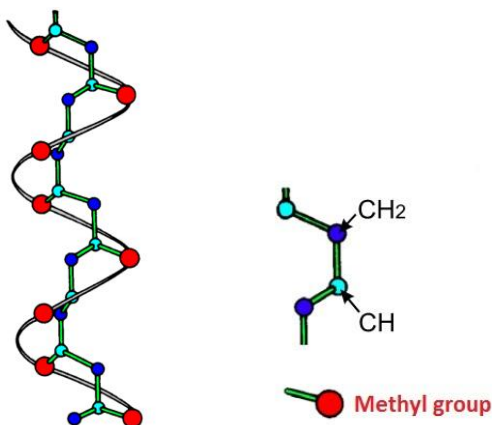
4.4. High Temperature Gel Permeation Chromatography.....	38
4.5. Dynamic Mechanical Rheometer (Parallel plate geometry).....	40
4.6. Differential Scanning Calorimetry (DSC).....	43
4.7. Oxygen Index Test (OIT).....	45
4.8. Dynamic Mechanical Analyzer (DMA).....	47
4.9. <sup>13</sup> CNMR (Nuclear Magnetic Resonance).....	50
<b><u>Chapter-5</u></b> Results and Discussions.....	53
<b><u>Chapter-6</u></b> Conclusion.....	100
<b><u>Chapter-7</u></b> References.....	103

## CHAPTER 1

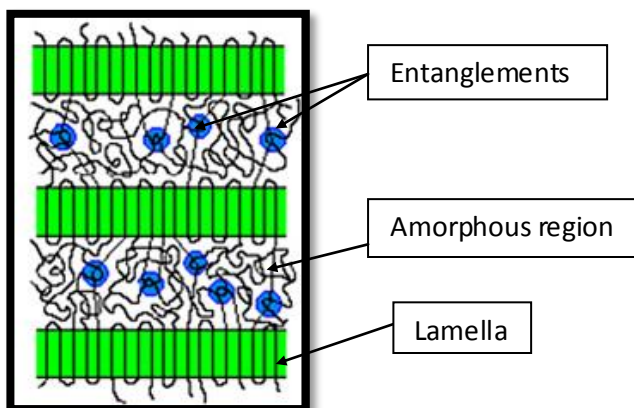
### 1.1 Introduction:

Polypropylene was discovered way back in 1950's by Giulio Natta [1]. In 1953 Ziegler, a German scientist, discovered that polyethylene could be prepared with a mixture of metal salts and transition metal salts (Busico *and* Cipullo (2001)). Giulio Natta succeeded in preparing polypropylene using the Ziegler catalyst and was able to obtain and characterize isotactic PP by fractionation (Salamone (1996)). In 1957 polypropylene was taken into commercial production (Karger-Kocsis (1995)) [2, 3], henceforth isotactic polypropylene became one of the fastest growing commodity thermoplastic in the world with different grades depending on their specific uses. The reasons behind its successful journey are the excellent properties such as high melting point (above 160°C), low density, stiffness, hardness and excellent chemical resistance.

However, one of the weaknesses of the polypropylene homopolymer is its low glass transition temperature range (-10°C to 0°C) [4]. Polypropylene has very broad spectrum of properties and can be significantly broadened by the introduction of comonomers, such as ethylene and butane to the main chain of polymer. The distribution of these comonomers depends on the type and composition of catalyst used. The most significant change by insertion of these comonomers is the reduction in the crystallinity and this brings about the improvement in the performance of the polymer. Crystallization from the melt or a solution usually starts from nuclei which can be the catalyst residues or purposely added nucleating agents. The polymer chains first folded into  $3_1$  helices (three monomer units from one rotation, as shown in figure.1 with a period of 6.5 °A [5, 6]. Those helices are the building blocks of the so-called lamellas (figure 1.1) which show a crystalline arrangement with unit cell parameters in the range of 6 - 20 °A. Four helical arrangements are possible by right or left-handed rotation about the central axis with unique (non-identical) "up" and "down" inclinations independent of the handedness (ref). The dominant crystallographic form for iPP is the  $\alpha$ -form [7, 8].



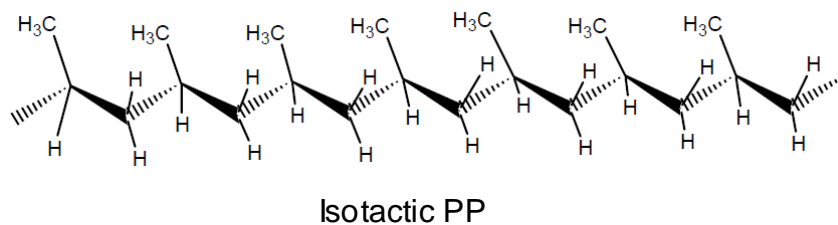
**Figure.1:**  $3_1$  helix structure of Polypropylene, (H. Batzer [9]).

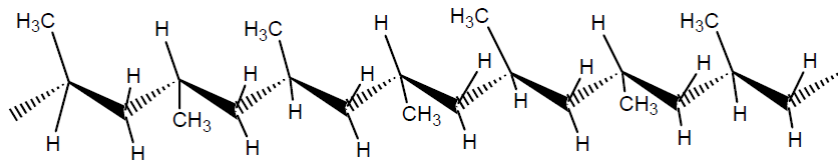


**Figure.1.1:** Chain folded lamella in semicrystalline polymers [10].

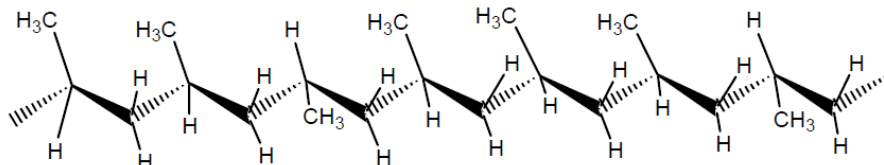
## 1.2 Stereo-isomerism and stereo-regularity

Polypropylene is a stereo-regular polymer. Three stereo-configuration of polypropylene can be possible based on the position of  $-CH_3$  group, namely the isotactic, syndiotactic and the atactic form.





Syndiotactic PP



Atactic PP

**Figure.1.2:** Isomerism in polypropylene. a) Isotactic polypropylene. b) Syndiotactic polypropylene. c) Atactic polypropylene as illustrated by Karger and Kocsis (1995).

In isotactic PP, each chiral center has the same configuration, i.e., all the -CH<sub>3</sub> groups are placed on the same side of the chain, while alternate chiral centers are identical in the syndiotactic PP and in the atactic PP, the arrangement of the methyl groups are completely random. NMR is the tool most commonly used to determine the degree of regularity within the polymer. The relative position of two CH<sub>3</sub> groups (a diad) can be described by an “m” (a meso-diad), known as isotactic or “r” (a racemic-diad), which is referred to as syndiotactic, which is shown in fig.1.3 below.



**Figure 1.3:** The m, meso-diad and the r, racemic diad, depending on the relative position of the CH<sub>3</sub>- group as described by Busico and Cipullo (2001) [11].

The degree of stereo-regularity in a sample is often defined as the percentage of isotactic- or syndiotactic-pentads, % mmmm or % rrrr, respectively. This represents the content of successive methyl-groups that are in the isotactic or syndiotactic-position with respect to each other, which is shown in the figure 1.4 below.



**Figure.1.4:** The isotactic pentad (mmmm), and the syndiotactic pentad (rrrr) (Busico and Cipullo, 2001)) [11].



## **CHAPTER 2**

### **2.1: Introduction to “RAFFIA” grade polypropylene:**

In the present study the focus is on the RAFFIA grade polypropylene, therefore it is necessary to define what raffia stands for and how the “RAFFIA” term associated with the polypropylene along with its properties and applications.

Raffia is the name of natural leaf fiber obtained from the enormous fan shaped leaves of raffia palm tree which is abundant in Africa, Madagascar, and Central and South America, mainly cultivated for commercial purposes. People there weave the strips of leaves to make fabric, known as “Raffia Cloth”, which reflect their social status, age, marital status, and also the person’s character. One of them is Indigo which is the most popular fabrics of Africa and is considered to be a symbol of affluence and prosperity.

**[12]**

Raffia polypropylene industry could be classified into six main categories such as; Woven sacks, FIBC (Flexible Intermediate Bulk Container), Leno Bags, Fibrillated Tapes, Monofilaments, Geo-textiles, Concrete reinforcement.

#### **2.1.1: Desirable Resin Characteristics [13]:**

The desirable resin characteristics for tape manufacturing are;

- ❖ The resin should have MFI (melt flow index) in the range of 2 to 4.
- ❖ The resin should have the ability to be easily processed into the film.
- ❖ The resin should have high melt strength and process stability, so as to eliminate melt flow breaks and thus deteriorating physical properties. The resin should have moderately broad molecular weight distribution.
- ❖ Resin cleanness is necessary to eliminate filter pack blockage and tape flaws.
- ❖ The resin should have the ability to orient readily to eliminate tape breakage during orientation at elevated temperature.
- ❖ Resin should have low water carry over when using quench bath. Water carry over is mainly related to the additive used in the resin.

## **2.2: Raffia Tape Manufacturing Process:**

Raffia tape manufacturing process mainly consists of the following steps:

- Extrusion of film
- Quenching of film
- Slitting of film into tapes
- Orientation of tapes
- Annealing of tapes
- Winding

### **2.2.1: Extruder and Casting of Film:**



**Figure 1.5: Extrusion Tape line [14].**

#### Screw Specification:

PP is extruded from the conventional extruder having three zones namely feed, compression, and metering. Output of an extruder depends on the L/D ratio of the screw. For PP recommended L/R ratio is 24:1 to 30:1.

#### Die specification:

Commonly Coat-hanger die is used because in coat hanger type of die, the design is of triangular preland section, which gives balanced pressure leading to uniform flow of the material. This minimizes the adjustment required to obtain uniform thickness of the film. Also the die gap is about 0.6 to 0.7 mm for Coat Hanger die.

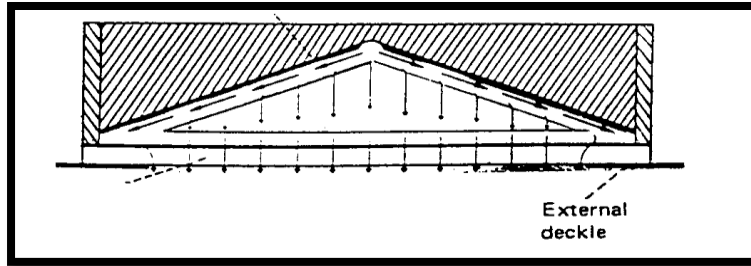


**Figure 1.6:** Coat Hanger Die

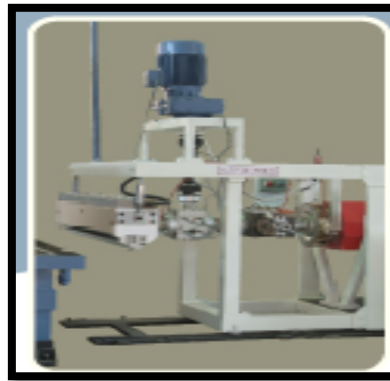


**Figure 1.7:** Screen Changer, Melt pump and Die [14].

Screen Changer: Screen changer is used to replace the screen pack when it is jammed with the foreign particles/melt lumps. Screen packs are attached with the breaker plate and the whole assembly resides in an adapter which is inserted between the ends of the extruder and die. The function of this assembly is to:

- Arrest the rotational flow of the melt and convert it into axial flow
- Removes any contaminants and un-melt.
- Improves mixing by increasing back pressure.
- Improves melt homogeneity by splitting and recombining the flow.

### 2.2.2: Quenching of film:

In cast film, the cooling is done by quenching the film in water tank. Film quality and end use performance of the resulting film mainly depends on the quenching conditions.

During the process of quenching the significant parameters which control the properties are air gap (Die-water distance), and quench water temperature.

The air gap should be lower in order to reduce the time for melt-relaxation. Moreover, a lower air gap produces a film with very fine crystal structure and very high strength.

Optimum condition for quenching: Air gap= 20 to 30mm.

Water tank temperature= 30°C to 40°C.

### 2.2.3: Slitting of film into tapes:



**Figure 1.8: Rotatory Slitter [14].**

The flat film after quenching is slit into tapes of specific width depends on the end use application. The slitting tools generally used are industrial or surgical blades with sharp edges. Slitting depends on the sharpness of the blades and its position to the film.

The recommended blade angle for slitting is 30 to 60 degree to the film.

#### 2.2.4: Orientation and Annealing of Tapes:

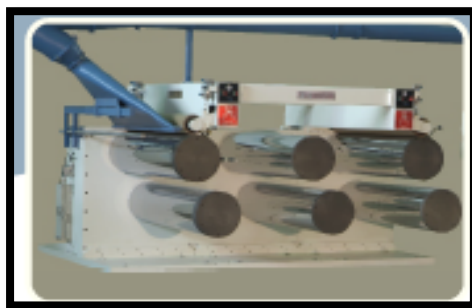


**Figure 1.9:** Stretching and Annealing Godets [14]

Orientation is accomplished by stretching the tapes by passing them through a hot air oven or hot-plate, maintained at a temperature just below the melting temperature of PP. The melting point of PP is 160-165°C, higher than HDPE; hence the orientation requires higher temperature to fully develop its mechanical properties, therefore, stretching at about 135°C to 155°C is recommended for hot air oven heating. Stretching of tapes is done by passing them over two sets of rollers, called godet rollers, placed on either side of the hot air oven / hot plate and operating at different speeds. Hot air oven heating is recommended in terms of improving end use product properties because it provides uniform heating to the tapes.

##### **Recommended condition for PP:**

**Stretch ratio:** Draw ratio between 5:1 to 6:1 is recommended to obtain tape with good combination of mechanical properties, non fibrillating tendency and curl free tapes. The draw ratio also determines initial cross-section of the slit strip/monofilament which is required for obtaining final width of the tape or size of monofilament.

#### **2.2.4.1: Orientation and its effects on the morphology of Polypropylene:**

In solidified PP, the macromolecules are arranged into crystalline and amorphous regions as shown in figure 1.1. In the melt phase, as the material leaves the die, the molecules are in a liquid state and there is no order (entangled form) [15]. During the orientation of the polymer melt in one direction the fibrillar structure can be formed and locked by subsequent cooling under pressure [16, 17]. It is generally believed that such systems with extended-chain crystals cause the high strength and modulus of elasticity [18]. This way of property modification, i.e. self-reinforcement, is appropriate namely for commodity polymers, such as polypropylene. It has low cost but unfortunately rather low mechanical properties, and therefore some improvement is desirable. On the other hand, these polymers possess high flexibility of the molecular chains allowing consequently to orienting them quite easily (19).

The decisive factor governing the change from this highly entangled form to the semi-crystalline arrangement is their molecular weight, molecular weight distribution, and their degree of long branching. In the stretched tape process rapid cooling crystallization is carried out at low temperature and this leads to higher crystallinity. In this type of crystallization chains are disentangled and the remaining entanglements are pushed into the inter-lamellar amorphous region and this leads to the higher entanglement density in the inter-lamellar amorphous region [20]. When semi-crystalline polymers are highly drawn, the shear forces destroy the spherulites. This is followed by the reorganization of the spherulitic morphology to another type of morphology mainly fibrillar in tapes. According to Peterlin et.al. [1973] the plastic deformation during the application of stress occurs in three stages. In the first stage, the plastic deformation of the original spherulitic structure occurs. The deformation occurs by strain of the interlamellar soft regions with a combination of interlamellar separation, lamellae stack rotation, interlamellar shear deformation and cavitation [Li1999, Lin1974, Zha 2000]. In the second stage, transformation of the spherulitic structure to fibrillar morphology takes place. During this stage, the lamellae are fragmented and the broken crystal blocks are incorporated into newly formed microfibrils.

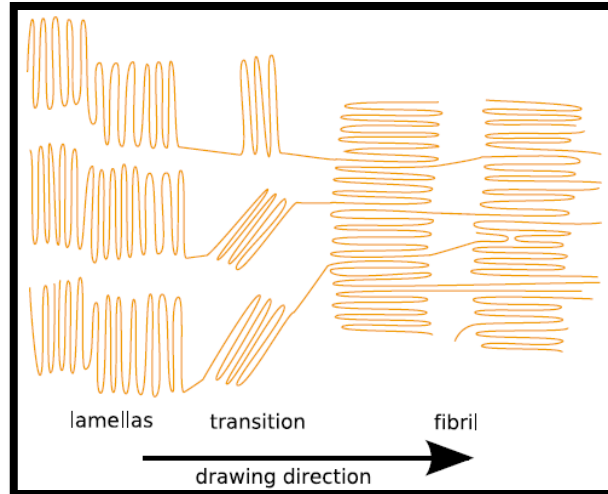


**Figure.2:** Transition from lamellar to micro-fibril morphology (peterlin [1973])

In uniaxial drawing, the blocks are not only oriented into the drawing direction, but also in the direction perpendicular to it [Bra1986]. The chains connecting the broken crystal blocks in the lamellae serve as intramicrofibrillar tie molecules [21].

It is generally believed that such systems with extended chain crystals cause the high strength and modulus of elasticity [19].

### **2.2.5: Annealing of tapes:**

This helps to minimize tape shrinkage which may occur as a result of residual stress in the oriented tapes. Annealing is done by heating the tape when it is passing from second to the third roller which revolves at a slightly slower speed than the second roller. Annealing temperature is about 5 to 10 deg lower than the orientation temperature i.e. 125-145 deg. (For PP).

### 2.2.6: Winding:



**Figure.2.1:** Tape Winding

After the end of annealing process, i.e., after passing the final godet the tapes pass to the winding strands where tapes are firmly wound with the help of bobbins.

### 2.3: Desired characteristics for polypropylene tapes:

Finished tapes should have the following properties:

- Finished tapes should have maximum width of 5mm.
- Finished tapes should have linear density (denier) of 600.
- Minimum tenacity should be 4.2 gm/denier, but the preferred performance range would be 5.0 to 6.0 gm/denier.
- Elongation at break should be in the range of 15-25%, but the preferred range will be 20-25%.



## 2.4: Application of polypropylene raffia tape:

### 1. Packaging application

#### a) Woven sacks:

Polypropylene woven sacks have significantly replaced the jute bags and paper bags for packaging cement, because of their distinct advantages over jute and paper bags in terms of high strength, lower bag weight, lower cost, resistance to fungus and low seepage of cement.



Sugar Bags



Postal Bags



Valve Bag

**Figure 2.2: Woven Sacks**

Previously HDPE woven sacks were predominantly used for cement packaging, but now days it has been mostly shifted to PP due to the following advantages:

- PP has lower density ( $0.90 \text{ g/cm}^3$ ) than HDPE ( $0.952 \text{ g/cm}^3$ ) therefore giving higher yield per unit weight.
- PP exhibits higher service temperature than HDPE, therefore when cement filled at a temperature of  $85^\circ\text{C}$  to  $90^\circ\text{C}$  and at a pressure of  $6 \text{ kg/cm}^2$ , the performance of PP woven sacks is better in terms of burst strength.
- Higher co-efficient of friction and hence higher stack ability during storage.
- PP has higher tensile strength than HDPE; hence unlaminated gusseted PP bags with a valve for filling cement are normally used. The bags are normally non-laminated to facilitate breathing of air during filling.
- Other applications of PP in the form of woven sacks are sugar bags, postal bags and tea bags.

## **FIBC (Flexible Intermediate Bulk Packaging):**

Flexible Intermediate Bulk Containers are large bags stitched from a woven PP fabric. These Fabrics are usually extrusion coated for additional barrier and also to prevent leak. It has accessories like handles and straps that provide easy handling. It is mostly used for the packaging of powders, granules, pellets, fertilizers, detergents and other free flowing products. The tape denier ranges from 2100 to 2600 for FIBC's.



**Figure 2.3: FIBC or Jumbo Bag [22].**

## **3. Monofilaments:**

### **Ropes and Nets:**

Ropes are made from PP exhibiting very good tensile strength, abrasion resistance, high inertia and excellent chemical resistance due to these properties therefore, PP ropes are used for the manufacturing of technical textiles. In fact it can be used as a container net for the agro-technical sector, or as protective netting, for shipping, ropes for trawling, mountaineering etc. Denier of monofilaments used for ropes and nets is usually between 500 to 800, and tenacity between 5.5 to 6 gm/denier.

PP monofilaments are also used for making nets. PP nets are used for high strength application due to its high tensile strength, wear resistance and knot strength.

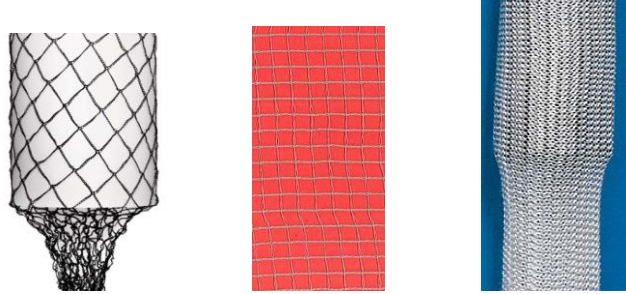


**Figure 2.4:** PP monofilaments rope [23].

**Furniture:**

Technical textiles are also widely employed in the furniture sector either for safety or for the comfort purposes.

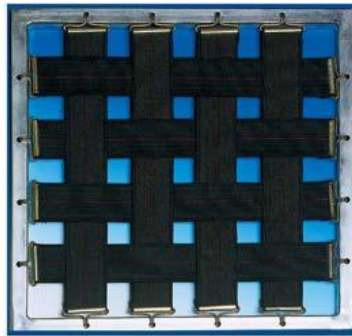


**Figure 2.5:** Furniture band made up of PP raffia [23].

**4. Leno bags:** These bags are made up from PP fabrics with a relatively open weave. It is a form of weave in which adjacent PP warp tapes are twisted around consecutive weft tapes to form a spiral pair, effectively locking each weft in place.



**Figure 2.6:** Weaving pattern of PP raffia leno bags.

These are mainly used for the packaging of fruits and vegetables. The capacity of Leno bags ranges from 50 kg to 70 kg. It is highly useful for products requiring cold storage and controlled temperature storage.



**Figure 2.7:** PP raffia leno bags.

## **CHAPTER 3**

### **3.1: Genesis of the problem:**

Successful trials were conducted at various locations with PP raffia grades namely, PP/R/R-036, PP/R/H-031, PP/R/I-071, PP/R/I-075, PP/R/I-027 and PP/R/I-089, to understand the material behavior in terms of processability and performance, and further, they were compared with the established grades viz, PP/R/R-036 and PP/R/H-031.

During the very first trial it was found that PP/R/I-071 raffia grade worked well up to a line speed of 300mt/min. The performance of PP/R/I-071 was then compared with that of PP/R/R-036 and PP/R/H-031. It was found that the grade has comparable tenacity (~5.03 gpd) than that of PP/R/R-036 but lower than PP/R/H-031 with elongation at break of 21.5% (higher than PP/R/R-036 and PP/R/H-031). Though the grade has lower power consumption than PP/R/R-036 and PP/R/H-031, however, significant tape breakages were found above the line speed of 300mt/min due to the presence of fish-eyes.

In another trial, which was conducted on the PP/R/I-075 grade, it was found that the grade has shown higher elongation with comparable tenacity. However, the film quality was found to be poor and hardly achieved a line speed of 300mt/min against the 415mt/min of PP/R/R-036.

The last two final trials were conducted on two different polymer grades, namely PP/R/I-027 and PP/R/I-089. It was observed that PP/R/I-027 grade has comparable tenacity (~4.5 gpd) with higher amount of elongation at break (23.1%). In addition to that the grade was found to be stable up to a line speed of 400mt/min with higher water carry over as compared to that of PP/R/R-036.

On the other hand, PP/R/I-089 achieved a line speed of 415mt/min, and PP/R/R-036 ran without any tape breakage along with comparable tenacity and elongation at break.

### 3.1.1: Summary of the Trial run:

Grade Name	Observations
PP/R/R-036	No tape breakage up to 415mt/min line speed, No water carry-over, Lower power consumption than PP/R/I-075 but higher than PP/R/I-071.
PP/R/I-071	Tape breakage beyond 300mt/min line speed, Non uniform distribution of filler, Poor film quality with Fish-eye. Comparable tenacity.
PP/R/I-075	Hardly 350mt/min line speed achieved, Higher power consumption, Higher water carry-over
PP/R/I-027	No tape breakage up to 400mt/min line speed, Higher tenacity than PP/R/R-036 (~ 4.95 gm/denier), Higher % elongation (~ 23.1%) than PP/R/R-036, High water carry-over, Higher neck-in
PP/R/I-089	No tape breakage up to 415mt/min line speed, Higher tenacity than PP/R/R-036 (~ 4.95 gm/denier), Higher % elongation (24%) than PP/R/R-036.

**Table.1:** Summary of the trial run on different polypropylene raffia grades.

## **CHAPTER 4**

### **Grade Details:**

<b>Sl.No.</b>	<b>Grade</b>
1	PP/R/R-036
2	PP/R/R-032
3	PP/R/H-031
4	PP/R/L-035
5	PP/R/I-070
6	PP/R/I-071
7	PP/R/I-075
8	PP/R/I-027
9	PP/R/I-089
10	PP/R/I-066

**Table.1.1:** Grade details of the samples used in the study.

### **Experimental Methods and Conditions used for Structural Analysis:-**

During the course of this project various experimental methods have been used for the characterization of the raffia grade polypropylene. All the characterization studies were carried out as per the ASTM standards wherever applicable.

#### **4.1: Xylene Soluble:**

The xylene soluble is the amount of polymer mass that is soluble in the xylene or that do not precipitate out when the solution is cooled from the reflux temperature to  $25^{\circ}\text{C} \pm 5^{\circ}\text{C}$ . The soluble fraction gives a relative measurement of soluble Polypropylene homopolymer or co-polymer. The soluble fraction can be correlated to the amorphous content in the polypropylene and also gives a good estimation of isotacticity of the polypropylene. This soluble fraction of polypropylene can be a good estimation of the performance of the product for specific applications, e.g. film and fibre.

Percent Xylene Soluble was determined as per the Basell test no. MTM-15558RE. 2 gm of sample was refluxed with o-Xylene (200 ml) for 45 min under Nitrogen atmosphere at  $135^{\circ}\text{C}$  and then solution was cooled in two stages. In the first stage solution temperature was reduced to  $100^{\circ}\text{C}$  over a period of 15 minutes under constant stirring. In the second stage, solution flask was transferred to a thermostatted water bath at  $25^{\circ}\text{C}$  for 30 minutes. During the first 20 minutes the temperature of solution was reduced to  $25^{\circ}\text{C}$  without stirring. For final 10 minutes, the temperature of solution was maintained at  $25^{\circ}\text{C}$  with stirring. The suspension was filtered through fluted filter paper which separated the Xylene soluble (XS) and Xylene insoluble (XIS). The Xylene soluble was expressed in weight percentage. A stabilizer Irganox 1010 was added to the Xylene and blank run was performed and the correction was carried out.



#### 4.2: MFI (Melt Flow Index):

The MFI test measures the rate of extrusion of a thermoplastic material through an orifice of specific length and diameter under specified condition of temperature and load. According to ASTM the die should have 2.095 mm internal diameter and 8.00 mm length.

MFI is still one of the most popular parameters in the plastic industries for distinguishing various grades of polymers. The higher the MFI the lower will be the viscosity and molecular weight while lower MFI correlates the low viscosity and high molecular weight. Polymer manufacturers have used it routinely to specify the most suitable end use of a particular grade of the polymer, MFI's of PP, in order to illustrate their various end uses, are shown below in table 1.1 below.

MFI (230°C/5kg) application	End use
2	Compression moldings, pipe
1-5	Extrusion blow moldings
5-15	Biaxially oriented film
5-15	Film tapes
5-15	Monofilaments

**Table.1.2:** End uses indication through MFI for various grades of polypropylene (Krassing et al (1984)).

The easiest polymer to flow is the material with low and uniform molecular weight distribution because the molecular weight of all polymer chains is similar. Therefore, the polymer with highest MFI will have the lowest average molecular weight.

Melt flow index of the PP granules was carried out as per the ASTM 1238 on CEAST Melt Flow Index machine at two different loads viz. 2.16 kg, and 20.6kg at 230°C. In the Melt Flow Index machine the PP granules were preheated at 230°C for 240 seconds without any load.

Then the samples were flowed through a die of 2.09mm diameter and 8mm long under the loading of two loads at 230°C and the extrudate were cut at a predetermined length (10mm). The extrudate was then weighed and the MFI was calculated.

#### **4.2.1 Melt Flow Ratio (MFR):**

MFR is the ratio of the MFI calculated at two different loads. MFR was calculated using MFI data collected from Melt flow tester. Higher the MFR value greater is the shear thinning in the resin. It is also used as a measure of the broadness of the MWD. Greater the value of MFR greater will be the broadness of the polymer. MFR is the ratio of the MFI at two different loads. MFR is also performed on the Melt flow tester. For this study, MFI has been evaluated at 2.16 kg and 20.6 kg load. The MFR at 20.6 kg load is calculated as,

$$MFR_{20.6 \text{ Kg}} = MFI_{20.6 \text{ Kg}} / MFI_{2.16 \text{ Kg}}$$

#### **4.2.2 Calculation of shear viscosity by using the MFI data at different loads:**

Shear Viscosity at various shear rates for different grades was calculated using the Power Law Model

$$\eta = m \times \text{shear rate}^{n-1} \quad (1)$$

Where n is the power law exponent or power law index, which can be calculated as follows:

$$n = \frac{\log(HL) - \log(LL)}{\log(HLMI) - \log(MI)} \quad (1.1)$$

and, m is the consistency index which is calculated as :

$$m = \frac{8982 \times (LL)}{\left(\frac{1838}{\rho} \times MI\right)^n} \quad (1.2)$$

Where,  $\rho$ , is the melt density at 2.16 kg load.

This power-law model gives a good fit of viscosity data at higher shear rates but not at low shear rates (because as shear rate goes zero, the viscosity goes to infinity). The smaller the value of  $n$  the greater will be the shear thinning of the polymer [24].

The values of consistency and power law exponent were calculated with the help of equation (1.1) and (1.2) from the MFI data obtained at two different loads.

#### **4.3: Capillary Rheometer:**

The common type of the capillary rheometer consists of a heated barrel and at the bottom of which a capillary die is fitted. The principle for capillary rheometer is that a polymer melt is extruded through a capillary die by the action of a piston which is driven at a constant speed. This gives a constant flow rate and hence a constant shear rate. A transducer is used to measure the melt pressure generated by the motion of the piston and is generally situated at the base of the barrel just above the die face.

In capillary rheometer, the apparent wall shear rate, ( $\dot{\gamma}_w$ ), apparent wall shear stress ( $\tau_w$ ), and apparent viscosity can be calculated as follows

Apparent wall shear stress, 
$$\tau_w = \frac{R\Delta P}{2L} \quad (2)$$

Where,  $R$  is the radius of the die,  $\Delta P$  is the pressure loss along the capillary, and  $L$  is the die length.

Apparent wall shear rate, 
$$\dot{\gamma}_w = \frac{4Q}{\pi R^3} \quad (2.1)$$

Where,  $Q$  is the volumetric flow rate and  $R$  is the radius of the die.

Measurement errors can occur at high shear rates in capillary rheometer, therefore, corrections should be required. Typical corrections include the Bagley end correction for pressure drop and the Rabinowitsch correction for a non-parabolic velocity profile through the capillary. Newtonian fluids possess a parabolic velocity profile, dilatants have

an extended parabolic profile, and pseudoplastics, a flattened parabolic velocity flow profile.

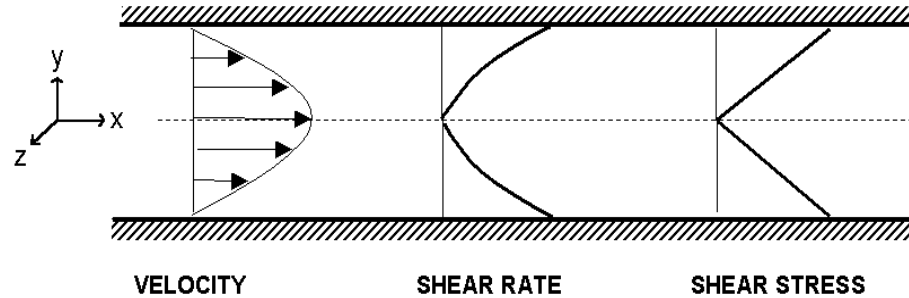


**Figure.3:** Velocity, shear rate and shear stress profiles for flow between two parallel plates [24].

**Bagley Correction (Shear stress correction):**

The velocity profile in the barrel is changed when the melt enters into the capillary die. This transfer of velocity profile needs energy and this energy is compensated by the abrupt decrease in the driving pressure. It was found by Bagley and Briks [1960] that the axial pressure drops suddenly and changes into linear form.

The Bagley correction involves measurements at various shear rates using at least two different dies of different length and same diameter. The corrected or true shear stress ( $\tau_{true}$ ) at the die wall is;

$$\tau_{true} = \frac{R\Delta P}{2(L+\Delta L)} \tag{2.2}$$

Where,  $\Delta L$  is the extrapolated die length,  $\Delta P$  is the pressure loss along the capillary and  $R$  is the radius of the die [25].

**Rabinowitsch Correction (Shear rate correction):**

The Rabinowitsch correction for the shear rate is account for the pseudoplastic nature of the polymer melt. The apparent shear rate corresponds to the Newtonian behavior i.e. assumed parabolic velocity profile but the polymer melt has flattened parabolic velocity profile as shown in the figure.3. Therefore, to obtain a true shear rate ( $\dot{\gamma}_{true}$ ) the apparent wall shear rate is modified (Equation 2.4).

From 
$$\gamma_w = \frac{4Q}{\pi R^3} \quad (2.3)$$

To 
$$\gamma_{true} = \left[ \frac{(3n+1)}{4n} \right] \left[ \frac{4Q}{\pi R^3} \right] \quad (2.4)$$

Where, n is the power-law index.

A twin bore rheometer (Bohlin RH-07 flowmaster, Malvern) was used. The rheometer has two cylindrical material reservoirs (barell) in which the PP raffia granules were melted and two pistons simultaneously force the melt through two different dies of different length at 200°C.

PP raffia granules were first inserted into the left and right barell and the granules were compressed to avoid any air entrapment. The test were carried out with the die of two different lengths i.e. 16mm and 0.25mm (zero length) respectively.

Die used: Capillary die (0.5×16×180-15) and Zero length die ((0.5×0.25×180-15).

The purpose of using two different dies is to remove the pressure differential error at the entrance and exit of the die (Bagley Correction) and that has given the corrected shear rate and shear stress. The pretest parameters were set in three consecutive stages. In the first stage the granules were compressed through piston up to 2Mpa pressure at the rate of 20mm/min, while in the second stage the granules were preheated for 3 minutes at 200°C and in the last and final stage the samples were compressed at much slower rate of 3mm/min. The shear viscosity was also measured at a very high shear rate between the ranges of 100s<sup>-1</sup> to 10000s<sup>-1</sup>. The melting point of PP raffia was found to be within the range of 160-168°C which was more prone to degradation as the experiment was being performed at 200°C, therefore the whole experiment were carried out under the atmosphere of Nitrogen gas.

#### **4.4: High Temperature Gel Permeation Chromatography:**

Gel Permeation Chromatography, also referred to as Size Exclusion Chromatography, is a mode of Liquid Chromatography in which the components of a mixture are separated on the basis of size or hydrodynamic volume. It is an important tool for the analysis of polymers. The essential results are molecular weight data and molecular weight distribution curves.

There is no upper limit in the molecular weight; even polymer analyses with molecular weight of several millions are possible. Demands on the instruments are very stringent due to a special calibration procedure using elution volume on the Y-axis.

#### **GPC-Separation Mechanism**

- Polymer molecules dissolve in solvent TCB to form spherical coils with size dependent on molecular weight.
- Polymer coils are introduced to the eluent TCB flowing through a column packed with porous gel beads.
- Smaller molecules pass through and around the beads while larger molecules are excluded from all but the largest pores.
- Size separation is converted to molecular weight separation by the use of a calibration curve constructed by the use of polymer standards (Polystyrene).

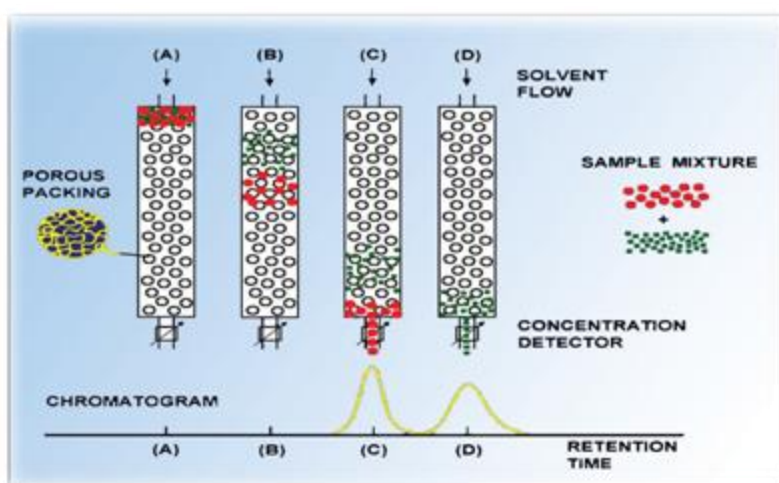


**Figure.3.1:** Typical GPC column with elution mechanism [26].

### **Sample Preparation**

Highly crystalline polymers such as PE and iPP are soluble only at high temperature. This is because elevated temperatures are required to break-down the ordered crystalline structure and on cooling the material will re-crystallize and precipitate from the solution.

For these applications, high temperature is required throughout the entire analysis to ensure that the samples remain in solution.

- The solvent used for PP was 1,2,4-Trichloro benzene and the samples were prepared at a concentration of 1-2 mg/ml in TCB.
- Elevated temperature was needed for the dissolution, typically at 140°C for 5hrs.
- The volume injected into the column was 200µl at a flow rate of 1 ml/min.
- The molecular weights were calculated against PS standard using conventional calibration (GPC-RI System).

### **Column Selection**

Column selection must be appropriate for the application in terms of molecular weight resolving range and efficiency of separation. The chromatographic columns used were two PLgel MIXED-B columns. Packed with 13 µm particles for maximum resolution with minimal polymer shear, the columns also operate upto 220 °C for the analysis of highly crystalline materials. The columns with 13µm particle size also give good efficiency. In addition, the 13µm particles size ensures no shear degradation.

#### 4.5: Dynamic Rotational Rheometer:

Dynamic oscillatory shear experiments deal with the state of the material in quiescent state. Therefore, dynamic test is usually carried out at small deformation and this type of test determines the linear visco-elastic properties of polymer. Dynamic rheological test in linear viscoelastic region usually involves with a small amplitude sinusoidal strain (Equation 3), measuring the resultant sinusoidal stress (3.1) at a predetermined frequency ( $\omega$ ).

$$\gamma(t) = \gamma_0 \cdot \sin(\omega t) \quad (3)$$

$$\tau(t) = \tau_0 \cdot \sin(\omega t + \delta) \quad (3.1)$$

Where,  $\gamma(t)$  is the sinusoidal strain, and  $\gamma_0$  is the strain amplitude,  $\omega$  is the frequency of oscillation, and  $\tau(t)$  is the sinusoidal varying stress,  $\tau_0$  is the stress amplitude and  $\delta$  is the phase angle.

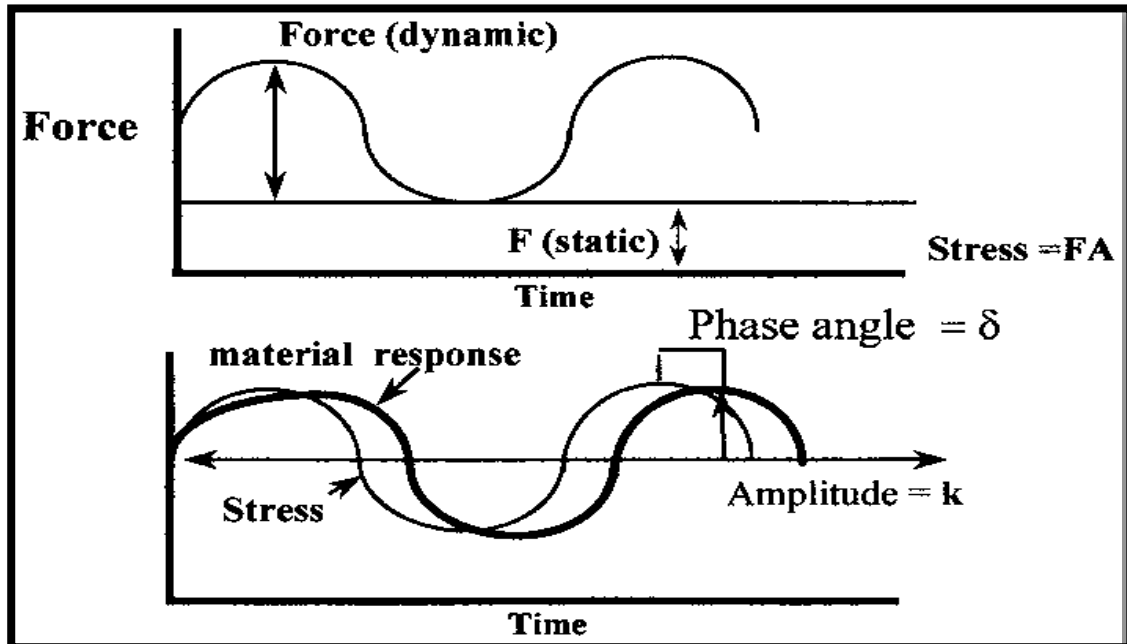


**Figure 3.2:** schematic of sinusoidal oscillating frequency to a sample and the corresponding sinusoidal response from the material [27].



Useful information that can be derived from the dynamic shear rheology is elastic (storage,  $G'$ ) modulus, viscous (loss,  $G''$ ) modulus and complex viscosity ( $\eta^*$ ).  $G'$  is a measure of the ability of material to store energy and the  $G''$  is a measure of its ability to dissipate energy. The ratio of the moduli is called damping, represented by  $\tan \delta$  (Equation 3.5).

$$G' = \frac{\tau_0}{\gamma_0} \cos \delta \quad (3.2)$$

$$G'' = \frac{\tau_0}{\gamma_0} \sin \delta \quad (3.3)$$

$$\tan \delta = \frac{G''}{G'} \quad (3.4)$$

The parallel plate geometry has an uneven strain field across the plate, where the material at the centre of the plate is strained very little, while the material at the edge of the plate is strained considerably.

Therefore the obtained strain value from this geometry is an average value. Comparing to other geometries, the parallel plate geometry is more straightforward, and hence it was selected.

Polymers are inherently visco-elastic in nature, therefore, there would be a critical point at which both moduli will be same. At this point  $G'=G''$ , and this is commonly referred to as the cross-over point of the material. From the cross-over point it is possible to get a good estimate of PDI ( $M_w/M_n$ ) for PP. PDI will give the good measure of broadness of the molecular weight distribution (shown in the figure 3.3 below). For this reason, polymers having different molecular weight and molecular weight distribution (MWD) are processed differently. Even if all the polymers had the same average molecular weight, they would undergo the process differently because the molecular weight distribution curves are not the same.

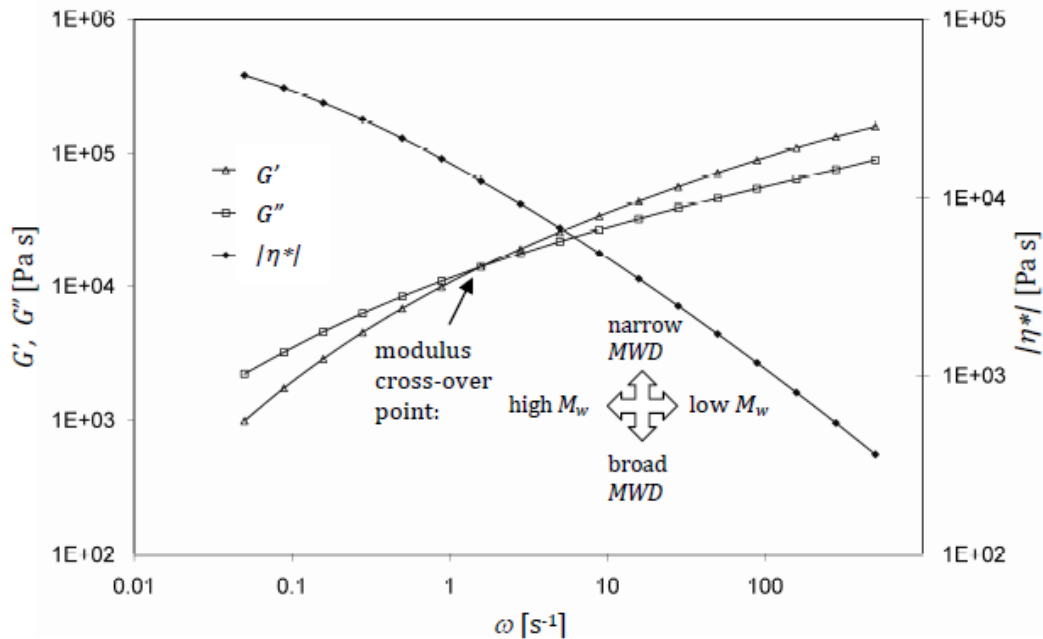


**Figure.3.3:** Location of the cross-over point of  $G'$  and  $G''$  gives information about the molecular weight and molecular weight distribution [28].

The elastic modulus ( $G'$ ), loss modulus ( $G''$ ) and complex melt viscosity, all were determined on a strain controlled oscillatory rheometer under frequency sweep mode using parallel plate geometry on a Dynamic rotational rheometer from *M/s Anton Paar*, at  $190^{\circ}\text{C}$ .

Linear visco elastic (LVE) region for the PP was found out by doing the strain sweep (from 0.01% to 100%) at  $190^{\circ}\text{C}$ , and 5 % strain was found to be in the LVE region.

The strain was kept at 0.05% and the frequency was varied between 0-100 Hz. Gap between the two parallel plate were maintained at 1 mm. Nitrogen was purged continuously to minimize the effect of degradation in the rheometric studies.

### **Test conditions for PP (Raffia Samples)**

Temperature –  $190^{\circ}\text{C}$

Preheat Time – 4 min

Strain – 5%

Frequency Sweep – 0.01-50 Hz

#### 4.6: Differential Scanning Calorimetry:

Differential scanning calorimetry (DSC) monitors heat effects associated with phase transitions and chemical reactions as a function of temperature. In a DSC the heat flow rate difference into the sample and a reference is measured as a function of temperature, while the sample is subjected to a controlled temperature program [29]. The reference is an inert material such as alumina, or just an empty aluminium pan. The temperature of both the sample and reference are increased at a constant rate. The basic principle involved is that when the sample undergoes a physical transformation such as phase transitions, more (or less) heat will need to flow to it than the reference to maintain both at the same temperature.

Whether more or less heat, must flow to the sample depends on whether the process is exothermic or endothermic.

Since the DSC is at constant pressure, heat flow is equivalent to enthalpy changes:

$$\left(\frac{dq}{dt}\right) = \frac{dH}{dt} \quad (4)$$

In an endothermic process, mostly in the cases of phase transitions, heat is absorbed and, therefore, heat flow to the sample is higher than that to the reference. Hence  $\Delta \frac{dH}{dT}$  is positive. In an exothermic process, such as crystallization, some cross-linking processes, oxidation reactions, and some decomposition reactions, the opposite is true and  $\Delta \frac{dH}{dT}$  is negative.

A flow of the Nitrogen gas is maintained on the samples to create a reproducible and dry atmosphere. The Nitrogen atmosphere also eliminates air oxidation of the samples at high temperatures. The samples are sealed into a small aluminium pan. The reference is usually an empty aluminium pan.

### **Degree of crystallinity:**

Degree of crystallinity is the content of the crystalline phase in the polymer that melts in the temperature range evaluated. If the enthalpy of the fusion of the fully crystalline polymer is known the degree of crystallinity of an unknown polymer sample can be determined as follows

$$\% \text{ Crystallinity} = \frac{\Delta H_s}{\Delta H_r} \times 100 \quad (4.1)$$

Where  $H_s$  is the heat of fusion of the sample and  $H_r$  is the heat of fusion of the 100% crystalline polymer, heat of fusion for 100% crystalline isotactic polypropylene is 209 J/gm [30].

Studies were carried out on Thermal Analyzer (Model-2960), TA Instruments, U.S.A and also on the Mettler Toledo 821E to get the heat flow pattern of the sample. The equipment was calibrated with Indium sample whose melting point is 156.6 deg C.

About 5 - 10 mg of the sample was taken in the aluminium pan (40 $\mu$ l) and heated in an inert atmosphere from 40 to 200 °C at 10°C/min; the whole process was carried out under the environment of Nitrogen gas in order to prevent any chance of thermal degradation. The samples are heated beyond the melting point @ 10°C/min to remove thermal history and then cooled down to room temperature. The cooled sample was again heated (second heating) @ 2°C/min to study the effect of crystallization and finally get the melting point ( $T_m$ ) and Enthalpy of heating ( $\Delta H$  j/g).

#### 4.7: Oxygen Index Test:

The Oxygen Induction Time (OIT) test is an accelerated aging test that is often used to predict the long term stability of hydrocarbon materials including plastics, rubbers, and adhesives. The OIT test can also be used to measure the level of effective antioxidant present or remaining in a polymeric material after some environmental exposure. Since thermal-oxidative degradation requires the presence of oxygen at elevated temperatures, the OIT test is designed to accelerate this degradation in order to get comparable results in a short period of time. The standard OIT test is performed according to ASTM D3895, and a Differential Scanning Calorimeter (DSC) is used. A few mg of the material to be tested are introduced into the DSC at room temperature, and the sample is heated to about 200°C under a nitrogen atmosphere. When 200°C is reached the cell is maintained in an isothermal condition, and the gas is changed from nitrogen to oxygen.

The flow rate of the oxygen is maintained at 50 ml/min. Under these conditions the stabilizer is consumed over time until it is totally depleted. At this point the polymer sample catastrophically degrades or oxidizes liberating additional heat (exotherm). The time it takes for this exotherm to appear from the time that the oxygen is introduced is reported as the OIT time, and is a measure of the thermal stability of the material.

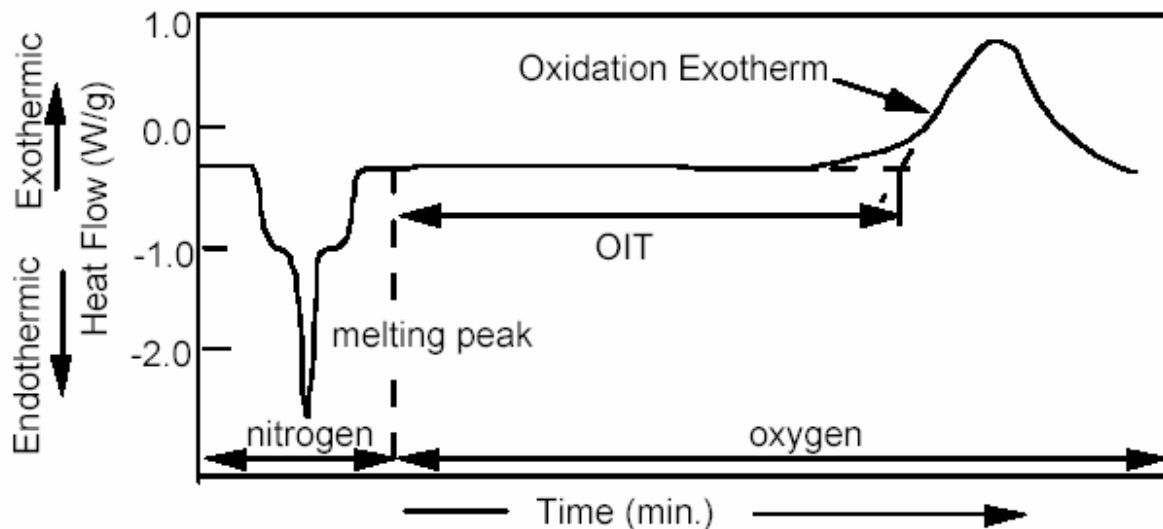


**Figure.3.4:** Thermal Curve of a Standard OIT Test

Oxygen induction time measurements provide a valuable characterization parameter associated with the long-term stabilities of polyolefin materials. Differential Scanning Calorimetry (DSC) provides an easy and sensitive means of characterizing the thermal properties of polyolefine materials. Test was carried out on a Thermal Analyzer (Model-2960) TA Instruments, USA.

OIT values were obtained as per ASTM D 3895. About 5 mg sample was heated under nitrogen atmosphere, at a standard purge flow rate of 50ml/min, from room temperature to 200°C at a rate of 20°C/min and held the sample under the nitrogen atmosphere at 200°C for 5 min. to allow the sample and DSC cell to thermally equilibrate at the target temperature. As the equilibrium temperature reached the gas flow was changed to flow oxygen at the same rate of 50ml/min. The oxygen purge was maintained at the same rate of 50ml/min until a significant oxidative exothermic response was obtained. Under these conditions the stabilizer has been consumed over the time until it is totally depleted. At this point the polymer sample catastrophically degrades or oxidizes liberating additional heat (exotherm). The time it takes for this exotherm to appear from the time that the oxygen is introduced is reported as the OIT time, and is a measure of the thermal stability of the material.

The time that is required for this to occur is dependent upon the relative stability of the material being tested. This is very useful for quality assurance purposes.

#### 4.8: Dynamic Mechanical Analyzer (DMA):

Dynamic mechanical analysis technique is defined as the application of an oscillating force to a sample and measures the visco-elastic properties over a wide range of temperatures and frequencies. This gives an insight of the structures and viscoelastic behavior of polymers for determining their stiffness and damping characteristics. DMA can be used for the evaluation of storage ( $E'$ ), loss modulus ( $E''$ ) and mechanical damping ( $\tan \delta$ ). The schematic diagram of sinusoidal oscillating deformation has shown in the figure.3.2; hence, not mentioned here.

Under an oscillating deformation the measured viscous component is known as the loss modulus ( $E''$ ), while the measured elastic component is referred to as the storage modulus ( $E'$ ). The ratio of the loss modulus to the storage modulus is known as the  $\tan \delta$  ( $E''/E'$ ). The term storage and loss modulus can be explained by the figure (3.4) given below.

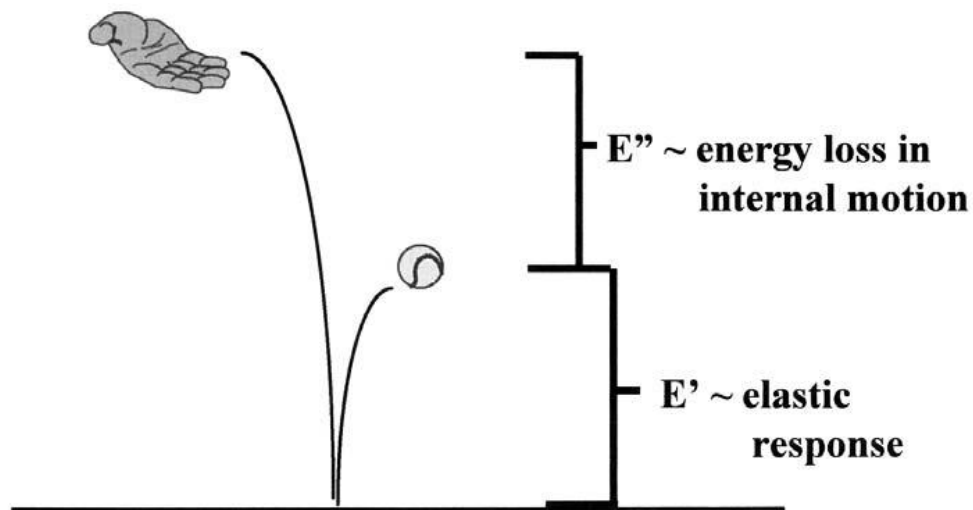


**Figure.3.5.** Storage and loss modulus,  $E'$  describes the stored energy while  $E''$  describes the loss energy due to internal motions and friction [27].

The storage modulus can be related to the amount of energy the ball gives back.

$$E' = \frac{\sigma_0}{\varepsilon_0} \cos \delta \quad (5)$$

$$E'' = \frac{\sigma_0}{\varepsilon_0} \sin \delta \quad (5.1)$$

The tangent of the phase angle (given in figure 3.3) is the tan delta. This gives a measure of how easily the material loses energy to molecular rearrangements and internal friction.

$$\tan \delta = \frac{E''}{E'} \quad (5.2)$$

The storage modulus  $E'$  can be related to the stiffness and increases with the increase in the crystallinity at a particular temperature. The stiffness reduces at higher temperature because of the higher molecular motions and any increase in the crystallinity reinforces the amorphous phase and thus reduces molecular mobility and consequently increases the elastic modulus  $E'$ .

Various relaxation phenomena occur in a given polymer and are completely associated with the motions of the different chain segments present in the different phases. Usually three relaxation peaks are observed in isotactic polypropylene namely,  $\alpha$ ,  $\beta$ , and  $\gamma$ . The relaxation which occurs at lowest temperature is associated with the  $\gamma$ -relaxation and it is due to the local relaxation in the amorphous phase. The  $\gamma$ -relaxation is mainly due to the rotation of the methyl groups present in the main or side chains, because this type of rotation requires less energy. In isotactic polypropylene  $\gamma$ -relaxation is mainly found at  $-100^\circ\text{C}$  [31].

The isotactic polypropylene relaxation occurs at about  $0^\circ\text{C}$  is mainly assigned to the  $\beta$ -relaxation. This is generally the glass transition ( $T_g$ ) of the iPP [32, 33]. The  $\beta$ -relaxation is mainly attributed to the co-operative segmental mobility of the disordered chains [34] and attributed to the amorphous region.

The iPP relaxation usually observed between the range of  $35-90^\circ\text{C}$  is attributed to the  $\alpha$ -relaxation and usually correlated to the crystalline phase.  $\alpha$ -relaxation has been



described as a consequence of local chain motion involving both the crystalline and amorphous phase.

It was found that the alpha relaxation either due to the orientation effect which occurs around 30°C. The temperature and the intensity of  $\alpha$ -relaxation peak increases with the increases in lamellar thickness [35].

### **Dynamic Mechanical Analysis:**

Polypropylene raffia grade samples were tested on DMA instrument. Samples for testing on DMA were prepared using Micro Injection Molding Machine (**Thermo Scientific, Haake, Mini jet**). Following conditions were used during the sample preparation.

Cylinder Temperature – 230°C

Mold Temperature – 60°C

Injection Pressure/Injection Time – 600 Psi/5 sec

Post Injection Pressure/Hold Time – 400 Psi/10sec

Samples thus prepared were conditioned in the conditioning chamber (at 23°C & 50% relative humidity) for 48hrs.

Instrument Used – Dynamic Mechanical Analyser (TA Instruments, TA Q800)

Assembly used for test – 3 point bending clamp

First linear viscoelastic region was determined using the amplitude/strain sweep from 1-200  $\mu\text{m}$  at 35°C & using 1 Hz frequency. LVE region was found at around 100  $\mu\text{m}$ .

Temperature sweep experiment were conducted using conditions (frequency 1 Hz, amplitude 100 $\mu\text{m}$ , ramp @3C/min, preload force 0.03N and force track 150%) from -50°C to 140°C. Storage modulus, loss modulus and tan delta values were obtained with respect to temperature.

#### 4.9. <sup>13</sup>C NMR-(Nuclear Magnetic Resonance):

The polymer samples show a large diversity in chain regularity. The regularity or the configuration of successive stereo centers (chiral carbon atoms) in the isotactic polypropylene chain determines the overall tacticity of the polymer. During polymerization tacticity can be disturbed by the incorporation of chain-defects. Possible irregularities can be divided into a category of stereo-defects and regiodefects respectively. In isotactic polypropylene tacticity play a major role to determine the structure and its properties.

Determination of Xylene Solubles and Xylene insolubles provides only a broad idea of tacticity of PP. The amount of polymer chains insoluble in xylene gives a rough measure of stereoregularity of the polymer while the soluble fractions can be assumed to be the atactic chains of the polymer. Usually in polypropylene low molecular weight isotactic chains along with slightly higher molecular weight chains are also present. The limitation of this method is that along with the high molecular weight chains the low molecular weight isotactic chains are also extracted in xylene and become part of xylene soluble. The xylene soluble part may contain some defects along with isotactic chains as shown figure 3.6 below.

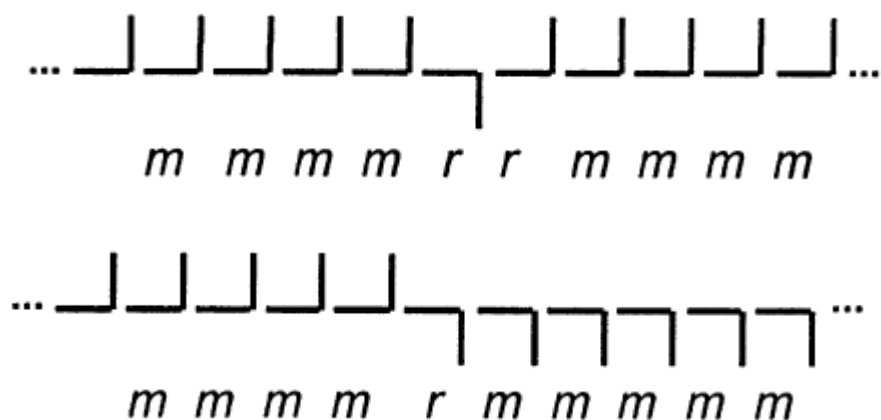


**Figure.3.6:** Stereodefects in polypropylene chains Busico and Cipullo (2001) [11].

Therefore, Xylene-solubles do not provide in-depth information of the real tacticity distribution i.e. microstructure of a PP chain.

In NMR, we measure the position (called chemical shift) of the groups in PP say position of methyl, methylene and methane groups. In the case of polypropene, the chemical shift of the methyl groups is highly sensitive to the relative stereochemistry of neighboring monomer units, that is, each methyl C has a different chemical shift depending on the configuration of the adjacent methyls, up to five on each side (a sequence length of 11 consecutive monomer units). Usually, the analysis is done at the Pentad level (i.e. sequence length of five consecutive monomer units).

Theoretically, there could be 10 Pentad sequences, as given below in figure.5.7.

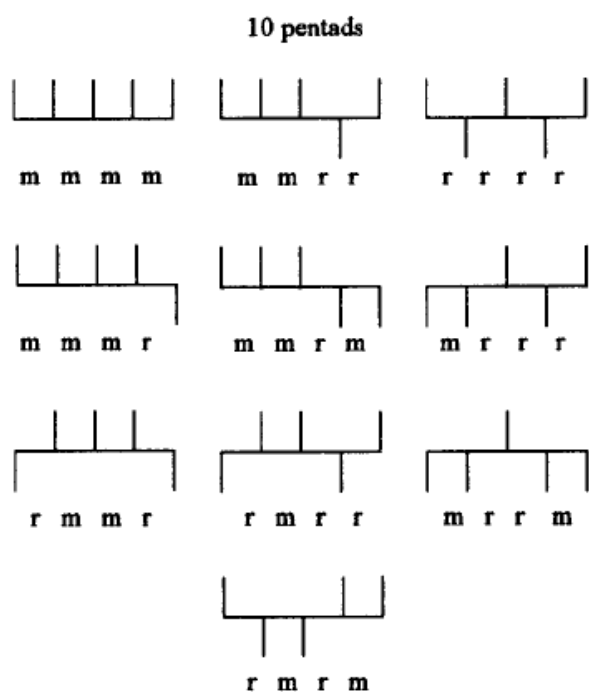


**Figure.3.7:** Theoretically possible ten non-equivalent steric pentads Busico and Cipullo (2001) [11].

### **Sample Preparation:**

Different grades of commercial polypropylene samples were taken for NMR studies. About 0.20-0.25 gm of sample was dissolved in 1,2,4-trichlorobenzene to prepare a concentration of ~20 wt./vol.% of polymer solution.

After swelling of polymers at 130<sup>0</sup>C for 1 h, deuterated solvents such as 1,1,2,2-tetrachloroethane-d<sub>2</sub> or 1,4-dichloro benzene-d<sub>4</sub> has been added as lock solvent. <sup>13</sup>C{<sup>1</sup>H} NMR spectra were acquired at 130<sup>0</sup>C on Varian Inova Unity 400 MHz at 100 MHz spectrometer for <sup>13</sup>C nuclei with various pulse angle and 5000 transients. Power gated pulse sequence was applied to ensure equal NOE throughout the NMR spectrum.

The internal standard most often used in high-temperature NMR studies of polymers in solution is Hexamethyldisiloxane (HMDS). It is preferred to report all polymer chemical shifts with respect to TMS by correcting the HMDS chemical shifts to a TMS standard. The chemical shift difference between TMS and HMDS is approximately 2 ppm, but the precise difference has been established independently. The chemical shifts were also referenced internally to the major backbone methyl carbon resonance, taken as 21.8 ppm from TMS.

Quantitative intensity measurements with high accuracy for <sup>13</sup>C nuclei require detailed attention and careful setup of experimental parameters.

### **Instrument Parameters:**

Pulse program, Zgig/Zgpg

Pulse angle, 90<sup>0</sup>

Pulse width, 8.4 μs

Pulse repletion, 10 s

Data size, 32 k

Sweep width, 200 ppm

Temperature, 398-403 deg K (120-130 deg C)

Number of scan, 500-4000

## **CHAPTER 5**

### **Results and Discussion:**

Polypropylene, which is used to make raffia tapes, undergoes a series of manufacturing processes. In the manufacturing processes microstructure of the PP plays a vital role. Raffia tapes are uniaxially oriented semi finished product with high weight to thickness ratio. These tapes are then converted in to twines, ropes woven or knitted fabrics etc. before reaching the market. In raffia tape production, PP is extruded in a single screw extruder, where melting, shearing of granules occurs and the melt viscosity of the PP plays the major role. The melt is then passed through a T-die and thereafter to a quench roll, to make a cast film where the crystalline morphology is developed. The crystalline morphology is the first critical stage, where it has a direct effect on the further processing, like stretching, slitting etc. Also this morphology determines the final product property like extent of orientation, tenacity, denier and also dictates the processing conditions like line speed.

The quenched films are then slit in to tapes and are then pre heated in an oven. Stretching is done between two goddet rollers running at different speeds and orientation of the tapes is done. Alignment of the polymer chain happens at this stage, where the morphology and microstructure of PP determines the properties. These tapes are then annealed to remove the residual stress and are then wound on bobbins and to the end application.

Different trials were conducted on the Raffia grades under study and it was found that PP/R/I-071 and lot PP/R/I-075 worked well with a line speed of 300 Mt/min and 350 Mt/min respectively without tape breakage while PP/R/I-071 grade has shown lower melt viscosity which was reflected in lower power consumption, though the grade was below the performance level with respect to the two grades namely PP/R/R-036 and PP/R/H-031, as tape breakages and fish-eyes were observed. While lot PP/R/I-075 was showing higher melt viscosity and hence required more energy in the trial.

Two different trial runs was conducted on lot PP/R/I-027 and PP/R/I-089 grades and it was found that the PP/R/I-027 has shown higher melt viscosity than PP/R/I-089, hence consumed more energy.

### **Xylene soluble fraction and isotacticity of PP:**

The properties of PP depend to a great extent on isotacticity of the chains which in turn affect the crystal type formed. The isotacticity depends on the catalyst system and the reaction temperature. The catalyst system which decides the addition of monomer units at the chain ends in head to tail fashion and such an arrangement results in the formation of isotactic polypropylene. At the molecular level isotacticity is measured by NMR, but another method i.e. percent Xylene Soluble fraction will give a rough estimation of the measure of atactic fraction. The soluble fraction can be approximately correlated to the amorphous fraction in the PP but also contain low molecular weight isotactic chains. The Xylene soluble %, calculated for all the 10 grades taking the average of two experiments are given in table 1.3.

Sl. no.	Sample Name	Exp (1) %	Exp (2) %	% XS (Avg.)
1.	PP/R/R-036	3.4	3.6	3.5
2.	PP/R/R-032	3.3	3.4	3.4
3.	PP/R/H-031	3.5	3.3	3.4
4.	PP/R/L-035	3.5	3.4	3.5
5.	PP/R/I-070	3.4	3.4	3.4
6.	PP/R/I-071	3.3	3.5	3.3
7.	PP/R/I-075	3.5	3.2	3.4
8.	PP/R/I-027	3.5	3.3	3.4
9.	PP/R/I-089	3.0	3.2	3.1
10.	PP/R/I-066	3.5	3.4	3.5

**Table.1.3:** Xylene soluble fractions of all the ten grades.

It is evident from the table that, though the grades are made from different manufacturing technologies, the Xylene Soluble fractions are comparable between 3.3 to 3.5 %. Conventionally, the raffia grade XS are maintained at 3 to 3.2%, but for the sake of the increase in line speed and of higher properties especially due to the advancement in the processing machines, the trend is slightly going up to keep a higher xylene solubles to 3.4-3.5% as can be seen in the case of PP/R/R-036 and PP/R/I-066.

**The percent xylene soluble of all the PP raffia grades remained similar within the range of 3.5% and no marked difference was found.**

**Melt Flow Index and Melt Flow Ratio:**

Melt flow index of all the ten grades of raffia PP were carried out as per the ASTM D 1238 at two different weights at the temperature of 230°C. The polymer granules were preheated for 240 seconds without load in all the experiments.

Sl. no	Grade	MFI @ 2.16 Kg	Shear rate [S <sup>-1</sup> ]	Melt Viscosity [Pa.s]
1	PP/R/R-036	3.9	9.9	1962
2	PP/R/R-032	3.4	8.6	2263
3	PP/R/H-031	2.8	7.0	2787
4	PP/R/L-035	3.4	8.5	2299
5	PP/R/I-070	3.4	8.5	2287
6	PP/R/I-071	2.4	5.9	3273
7	PP/R/I-075	2.7	6.3	3106
8	PP/R/I-027	3.1	7.7	2415
9	PP/R/I-089	3.3	8.4	2333
10	PP/R/I-066	3.5	8.7	2223

**Table 1.4:** MFI, shear rate and shear viscosity values at 2.16kg of all the grades at 230°C.

Sl. no	Grade	MFI @ 20.6 kg g/10min	Shear rate [S <sup>-1</sup> ]	Melt Viscosity [Pa.s]
1	PP/R/R-036	325	816	226
2	PP/R/R-032	306	768	241
3	PP/R/H-031	223	560	330
4	PP/R/L-035	249	621	297
5	PP/R/I-070	267	670	276
6	PP/R/I-071	177	441	419
7	PP/R/I-075	208	526	351
8	PP/R/I-027	233	579	319
9	PP/R/I-089	292	712	260
10	PP/R/I-066	284	698	265

**Table 1.5:** MFI values at 20.6kg of all the grades at 230°C.

Sl. no	Grade	MFI @ 2.16 Kg	MFI @ 20.6 kg g/10min	MFR @ 20.6 Kg
1	PP/R/R-036	3.9	325	83.2
2	PP/R/R-032	3.4	306	90.1
3	PP/R/H-031	2.8	223	79.7
4	PP/R/L-035	3.4	249	73.2
5	PP/R/I-070	3.4	267	78.6
6	PP/R/I-071	2.4	177	73.8
7	PP/R/I-075	2.7	208	83.3
8	PP/R/I-027	3.1	233	75.1
9	PP/R/I-089	3.3	292	88.04
10	PP/R/I-066	3.5	284	81.1

**Table.1.6;** MFI and MFR of all the grades at 230°C.



The data obtained for PP raffia grades at 2.16 kg and 20.6 kg showed that the PP/R/I-036 has high MFI, which reflects uniform distribution of low molecular weight and high molecular weight chains respectively, hence PP/R/I-036 has very large processing window than the other PP grades. In addition, when we compare the MFI value of PP/R/I-075, PP/R/I-071, PP/R/I-066, PP/R/I-027, PP/R/I-089, PP/R/I-070 PP raffia grades, PP/R/I-089 has shown lower MFI at 2.16 kg but higher at 20.6 kg than PP/R/I-075, PP/R/I-071, PP/R/I-066, PP/R/I-027 and PP/R/I-070 lots.

Further, PP/R/I-089 grade has higher MFR value when compared with that of PP/R/I-075, PP/R/H-031, PP/R/L-035 and PP/R/I-071. On the other hand PP/R/I-089 has also shown higher MFR value than that of PP/R/R-036, PP/R/R-066, and PP/R/R-027. While PP/R/R-036 has shown almost the similar MFR values when compared with that of PP/R/I-075 and PP/R/I-066, hence have similar molecular weight distribution.

Thus, from above comparison, we concluded that the PP/R/R-036 has better flowability amongst all the PP raffia grades. Moreover, as we increase the load the flowability of PP/R/R-036 increases due to the high shear thinning, though, PP/R/I-066 and PP/R/I-070 has shown comparable flowability at higher load but still far away from the PP/R/R-036. This could be the reason for better performance during trial runs.

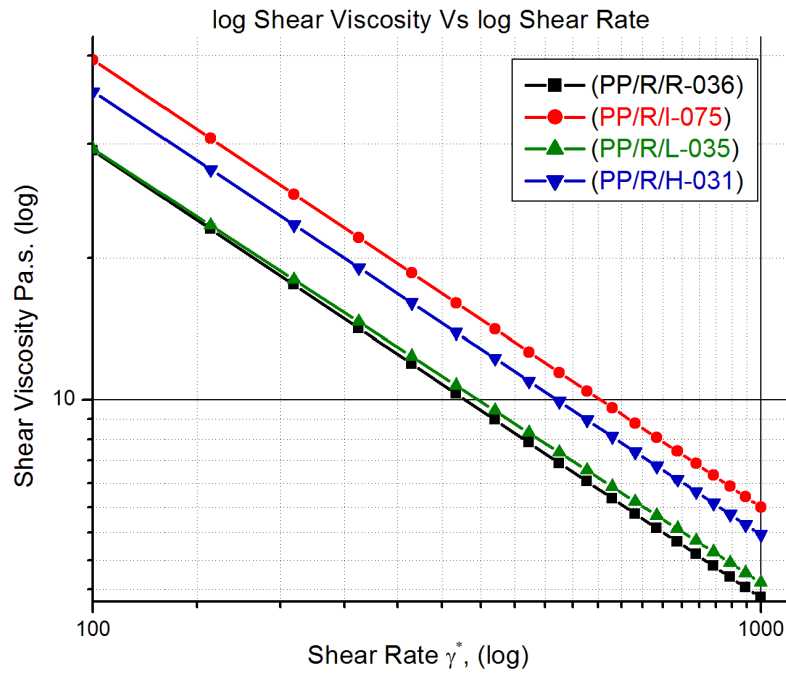
**The above comparisons have shown that the PP/R/R-036 has higher MFI at 2.16kg and 20.6kg, than all the other grades, respectively. Hence, the flowability of the grade was better and this could be further related to the lower power consumption during the trial run. The MFR value is a good estimation of broadness of the molecular weight distribution. From the above discussions it was also concluded that the PP/R/R-036 comparatively has similar molecular weight distribution as that of PP/R/I-066 and PP/R/I-075 while shown narrow molecular weight distribution than that of PP/R/I-089.**

In order to better apprise the values obtained from the higher load and low load MFI, the shear rate Vs shear viscosity graphs was generated using power law, and the constants can be derived from the MFI experiments.

The power law constants n and m were calculated for each of the grades and are given in the Table 1.6. From these m and n and substituting in power law equation, the viscosity for each shear rate from 100 to 1000 s<sup>-1</sup> for each grade was calculated.

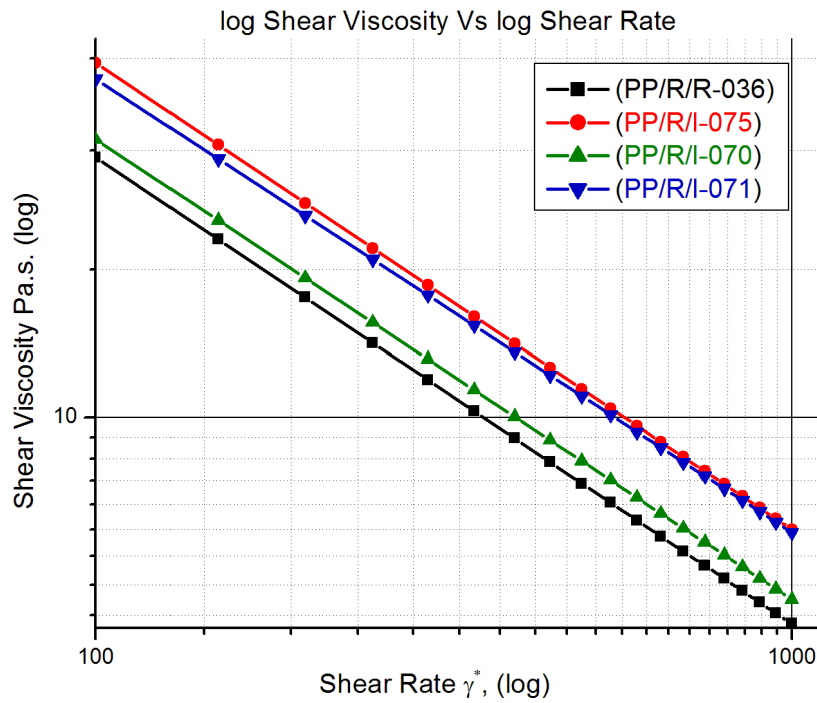
Sl. no	Grade	n	m
1	PP/R/R-036	0.510	178.98
2	PP/R/R-032	0.501	208.24
3	PP/R/H-031	0.515	202.81
4	PP/R/L-035	0.525	167.50
5	PP/R/I-070	0.517	180.84
6	PP/R/I-071	0.524	202.69
7	PP/R/I-075	0.510	225.01
8	PP/R/I-027	0.522	181.07
9	PP/R/I-089	0.504	206.93
10	PP/R/I-066	0.513	184.71

**Table 1.7:** power law constants n and m calculated from MFI at 2.16 kg and 20.6 kg.



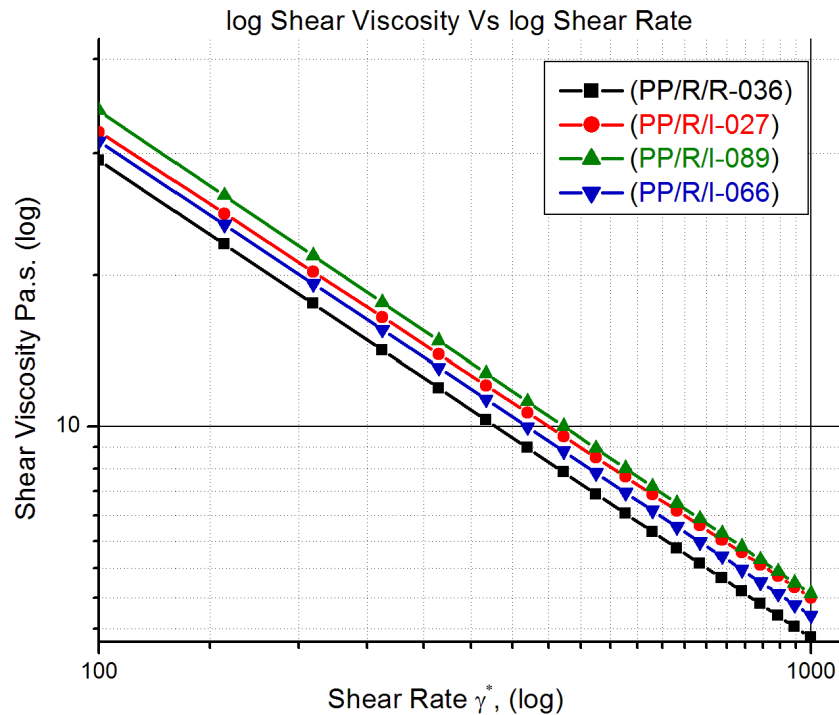
**Figure.4:** shear viscosity Vs shear rate graph of PP/R/R-036, PP/R/I-075, PP/R/H-031 and PP/R/L-035.

Figure .4 indicates that PP/R/R-036 and PP/R/L-035 has lower melt viscosity and the curves almost superimposing each other over the entire range of shear rate. While PP/R/I-075 has maximum melt viscosity over the entire range of shear rate, and this could be the reason for high power consumption during the trial runs in PP/R/I-075.



**Figure.4.1:** Shear viscosity Vs shear rate graph of PP/R/R-036, PP/R/I-075, PP/R/I-070 and PP/R/I-071.

Figure 4.1 showing that the PP/R/R-036 has lower melt viscosity than the other three PP grades. In spite of that PP/R/I-070 graph almost superimposing the PP/R/R-036 graph at lower shear rate, however, at higher shear rate PP/R/I-070 remained on the higher shear viscosity region, while the shear viscosity graph of PP/R/I-075 and PP/R/I-071 superimposing each other over the entire range of shear rate and have shown higher shear viscosity, consequently consumed more power during the trial run.



**Figure.4.2:** shear viscosity Vs shear rate graph of PP/R/R-036, PP/R/I-027, PP/R/I-089 and PP/R/I-066.

Figure 4.2, has shown that PP/R/I-089 and PP/R/I-027 showing higher melt viscosity over the entire range of shear rate and the curve superimposing at the higher shear rate. The superposition at the higher shear rate gives an indication that both PP/R/I-089 and PP/R/I-027 showing the same extent of power consumption, though showing the same extent of power consumption but the former has performed well and achieved a stable line speed of 415 Mt/min as compared to 400 Mt/min of PP/R/I-027. On the other hand PP/R/I-066 comparatively has better flowability hence it should have lesser amount of power consumed.

It is worth mentioning, however, that PP/R/R-036 is the better choice for processing at higher shear rates with minimum amount of power consumption.

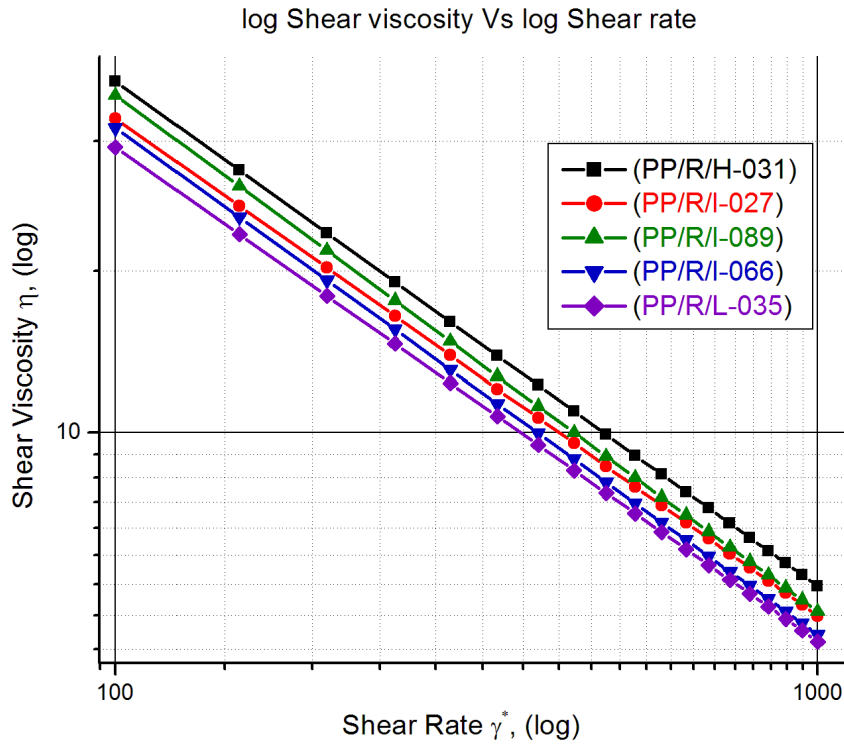


**Figure.4.3:** shear viscosity Vs shear rate graph of PP/R/H-031, PP/R/I-027, PP/R/I-089 and PP/R/I-066 and PP/R/L-035.

Figure 4.3, showing shear viscosity vs shear rate comparison graph of two other polymer viz., PP/R/H-031 and PP/R/L-035 which are remain untouched under this discussion. In this graph PP/R/L-035 showing the least shear viscosity over the entire range of shear rate, though, it is superimposing the PP/R/I-066 curve at higher shear rate. The compensation of loss of higher power consumption at lower shear rate supposes to occur at higher shear rate by superposition of PP/R/I-066 by PP/R/L-035. While , on the other hand PP/R/H-031 is significantly out of league amongst the five PP- raffia grades, because it is showing very high shear viscosity over the entire range of shear rate and hence showing poor flowability and leads to higher power consumption.

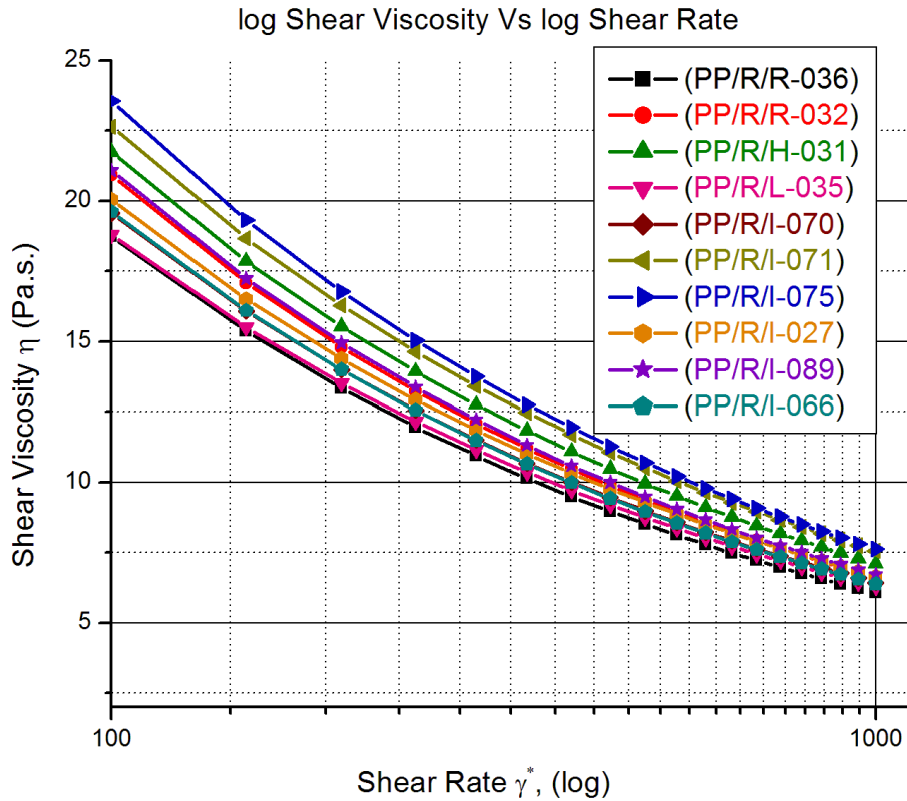


**Figure.4.4:** shear viscosity Vs shear rate graph of all the PP raffia grades.

In the said comparisons from figure.4 to figure.4.4, it can be concluded that PP/R/I-075 and PP/R/I-071 has found to be the grades with highest melt viscosities followed by the PP/R/R-036 which could be the reason for comparatively higher power consumption over the entire range of shear rate. PP/R/I-089 has shown higher melt viscosity as compared to PP/R/I-027 and PP/R/R-032 at lower and higher shear rate respectively. However, PP/R/I-089 has performed well and achieved a line speed of 412mt/min as compared to 400mt/min of PP/R/I-027. Interestingly, the flow curve of PP/R/I-066 overlap with that of PP/R/I-070 over the entire range of shear rate, hence should have better flowability. Above all, the two polymer grades viz, PP/R/R-036 and PP/R/L-035 has shown similar effects at low shear rate, however, PP/R/R-036 comparatively has the best combination of better flowability with lower power consumption over the entire range of shear rate.

### Capillary Rheometer Analysis:

Shear viscosity and corrected shear rate values was obtained from Capillary Rheometer and plotted against each other for PP/R/R-036, PP/R/I-027, PP/R/I-066 PP/R/H-031 and PP/R/I-089 samples.

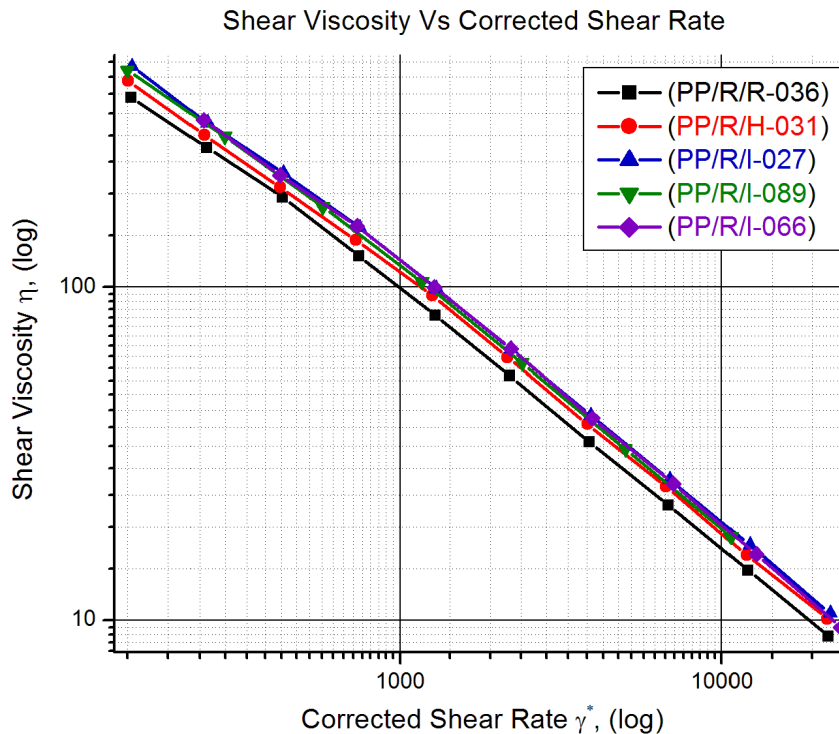


**Figure.5:** Shear viscosity Vs corrected shear rate graph for PP-raffia grades.

In figure.5; it was found that PP/R/I-027, PP/R/I-089 and PP/R/I-066 grades have almost similar shear viscosity, as can be seen in the curves, are overlapping, over the entire range of shear rate ( $100 \text{ S}^{-1}$  to  $10000 \text{ S}^{-1}$ ). On the other hand PP/R/R-036, PP/R/H-031 polymer grades have distinctively different shear viscosity behavior over the entire shear rate. Moreover, the PP/R/R-036 grade comparatively has lowest shear viscosity over the entire range of shear rate than all the grades this further strengthen the power law shear viscosity Vs shear rate graph. Hence, PP/R/R-036 has shown better flowability over the entire range of shear rate.



## Rheological and Molecular Analysis of PP raffia Grades from Dynamic Rotational rheometry and High Temperature GPC.

In frequency sweep experiments, the response of the material is found out against the small oscillatory strain applied. Since the melt is in shearing mode from the top plate, complex shear modulus and complex viscosity are obtained in these experiments. The loss modulus ( $G''$ ) and storage modulus ( $G'$ ) are obtained as a function of frequency.  $G'$  for the storage component and  $G''$  for the loss component,  $G'$  represents the characteristic elastic modulus of the system and  $G''$  measures the viscous response. Loss modulus is the viscous response of the melt while storage modulus is the elastic response of the material. The polymer molecular weight and MWD directly affect the extrusion process. The polymer with high molecular weight will require more energy to process i.e., high drive torque due to higher melt pressure, as already been explained in shear viscosity vs shear rate from power law.

In order to understand the relationship between the molecular weight and MWD with the processing characteristics of all the PP raffia grades, HT-GPC characterization have been carried out and the graphs are correlated.

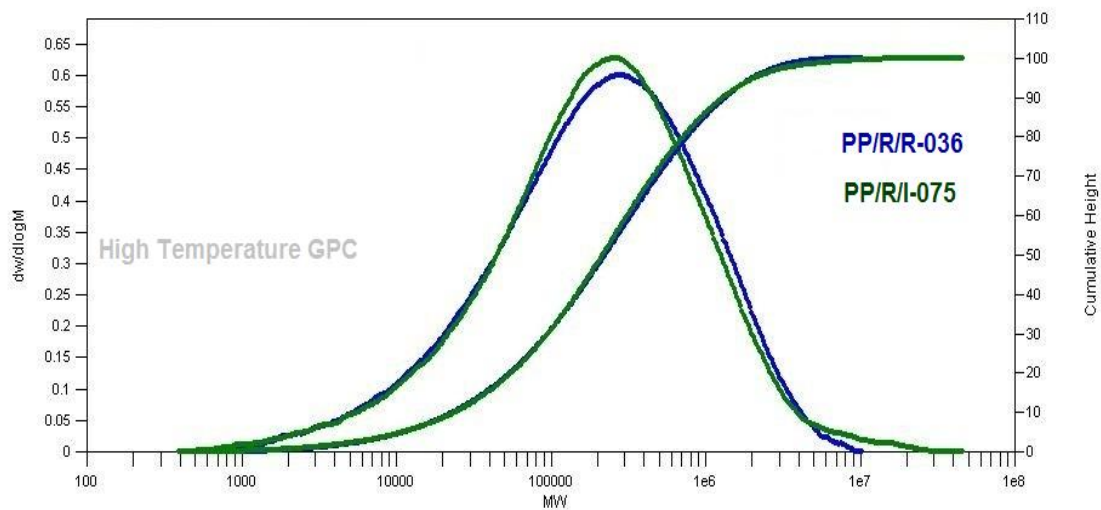


**Figure.5.1:** HT-GPC MWD Chromatogram of PP/R/R-036 Vs PP/R/I-075.

In figure.5.1; high temperature GPC chromatogram of PP/R/R-036 and PP/R/I-075 is compared. From MWD chromatogram it is evident that the PP/R/I-075 grade has a long tail of very high molecular weight fractions ( $1 \times 10^7$  to  $4 \times 10^7$ ) and very low molecular weight fractions as compared to PP/R/R-036.

The high concentration / fraction of this high molecular weight chains, will not form the required lamellar morphology on cast film, and this could lead to the tape breakage while stretching.

The PP/R/R-036 has a very definite MWD pattern, therefore, limiting the very high molecular weight fraction and the limited high molecular fraction will give rise to a morphology, which will assist in stretching at higher speeds. When the melt is cooled on a quenched roll, the very high molecular weight chains will come out from the melt and will act as nucleating back-bone and on to it daughter lamellas will grow [8]. This morphology is very critical in stretching and, the increase or decrease in this very high molecular weight fraction will deteriorate the performance of the polymer resulting in lower line speeds. From the graph it is evident that the high molecular weight fraction of PP/R/R-036 at lower concentration also influences the  $M_z$  (Z-Average Molecular weight) value leads to higher mechanical strength which is reflected in the higher line speed of 415mt/min.

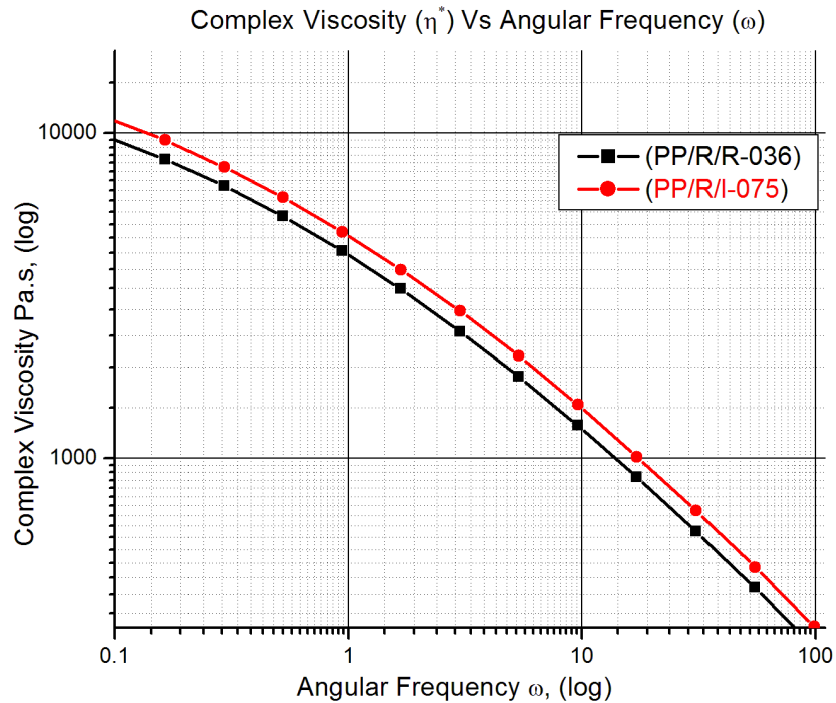


**Figure.5.2:** Complex Viscosity Vs Angular Frequency of PP/R/R-036 and PP/R/I-075.

Further, on comparing the GPC curve of PP/R/R-036 and PP/R/I-075 with complex viscosity graph (figure.5.2), the high molecular weight chains of PP/R/I-075 can be correlated to higher melt viscosity which could also be the reason of higher power consumption and poor performance during the trial.

Though, GPC gives relative MWD chromatogram of the polymer, therefore, for better appreciation of result MWD chromatogram from GPC is correlated with MWD chromatogram obtained from rheometry by calculating zero shear viscosity in figure 5.3. It is clearly shown in figure 5.3; that there is a hump in the high molecular weight region in the lot PP/R/I-075 which in turn related to the high molecular weight tail in the GPC chromatogram (right hand side in red circle).

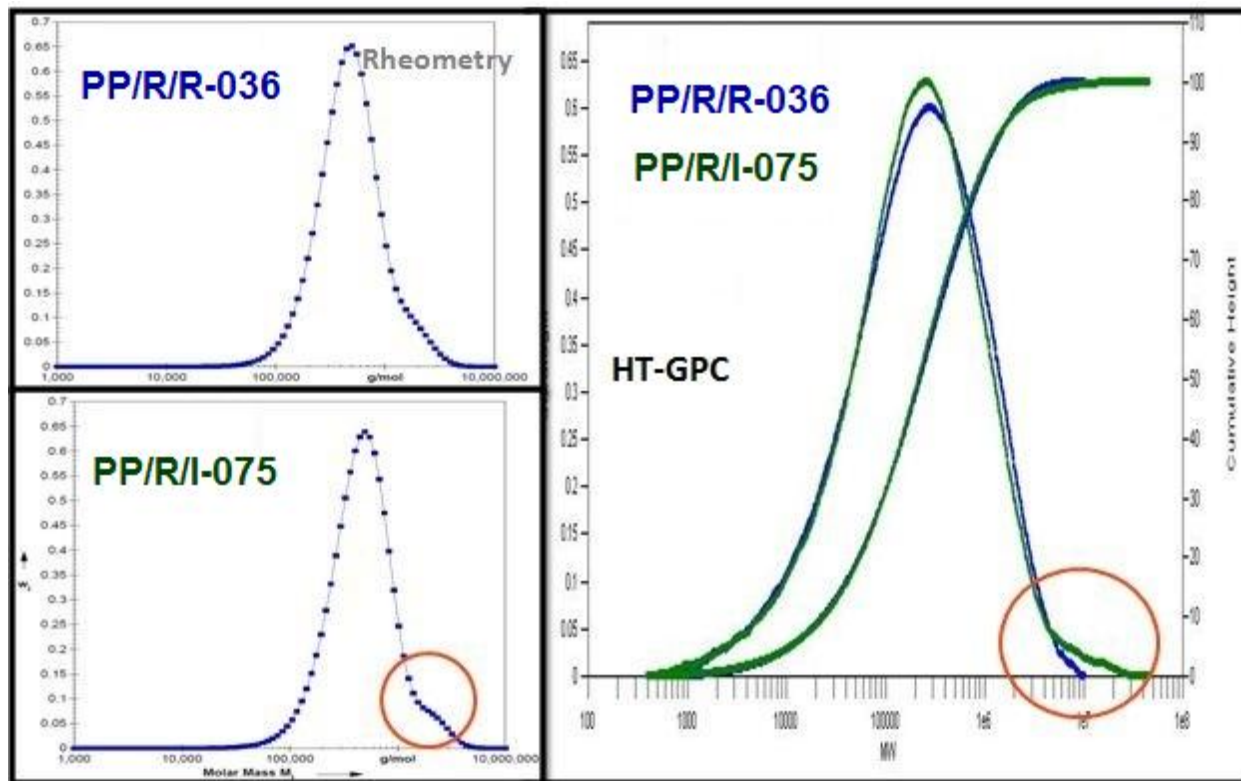


**Figure.5.3:** MWD Chromatogram from rheometry and HT-GPC of PP/R/R-036 Vs PP/R/I-075.

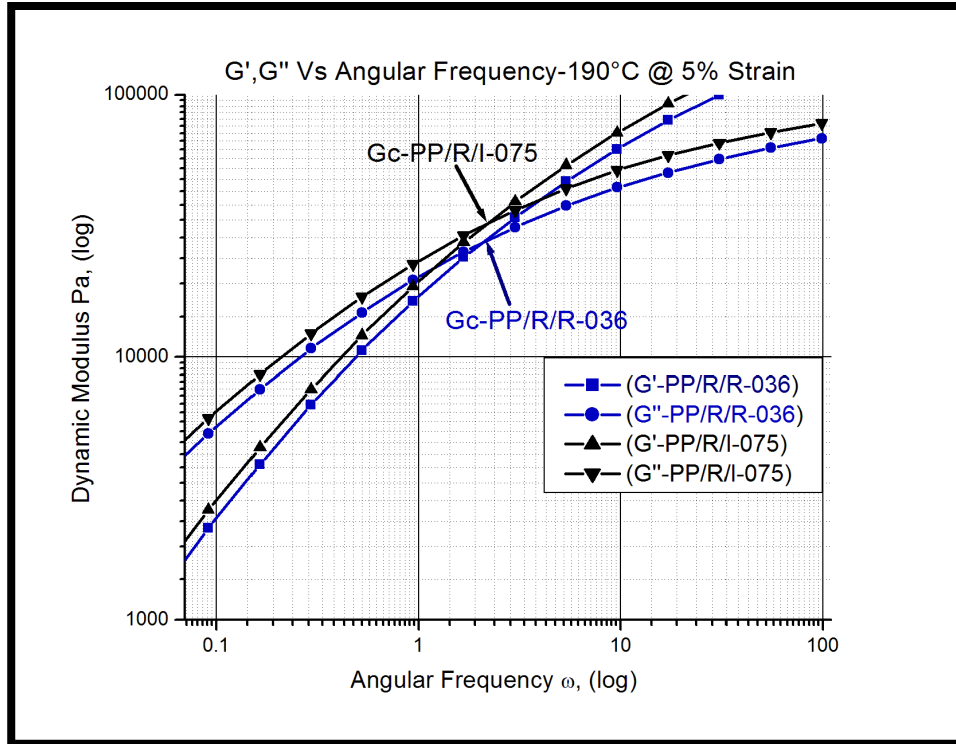


**Figure 5.4:** Storage Modulus ( $G'$ ) and Loss Modulus Vs Angular Frequency of PP/R/R-036 and PP/R/I-075.

In figure 5.4; storage modulus ( $G'$ ) and loss modulus ( $G''$ ) data against angular frequency is compared. It can be seen clearly that the cross-over modulus, which is the good measure of molecular weight distribution, of PP/R/R-036 is lower than the PP/R/I-075 showing broad MWD of the former. This further supports the better performance of PP/R/R-036 during the trial.

**It was found that the PP/R/R-036 has very limited tail of high molecular weight chains as compared to PP/R/I-075 at the same time PP/R/R-036 has higher amount of high molecular weight chains at very low concentration which was found to be very detrimental at higher line speed (415mt/min). It can also conclude that PP/R/R-036 has lower complex viscosity and complex modulus over the entire range of angular frequency and hence performed well during the trial.**

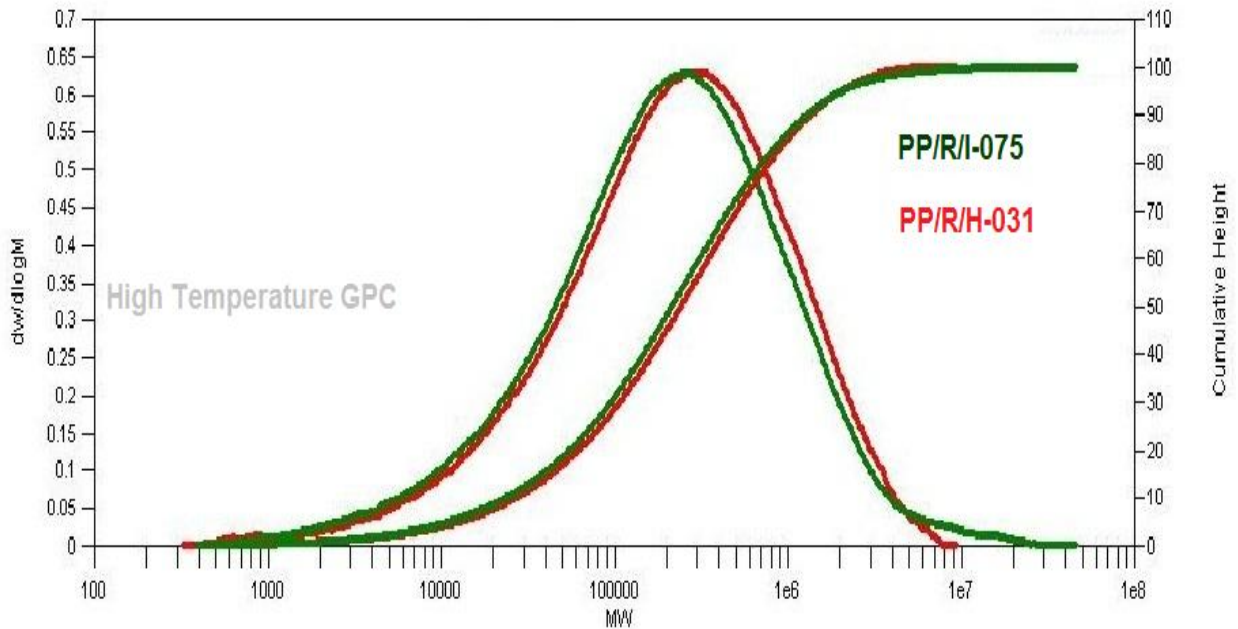


**Figure 5.5:** HT-GPC MWD Chromatogram of PP/R/H-031 Vs PP/R/I-075.

In the figure 5.5; MWD chromatogram of PP/R/I-075 is further compared with PP/R/H-031. It can be seen that, the PP/R/I-075 grade has very high molecular weight tail which may be the cause of poor performance in the trial.

As graph has shown that the PP/R/H-031 has high fraction of high molecular weight content at very low concentration, this may be the reason for line speed up to 365mt/min as compared to 350mt/min of PP/R/I-075 grade.

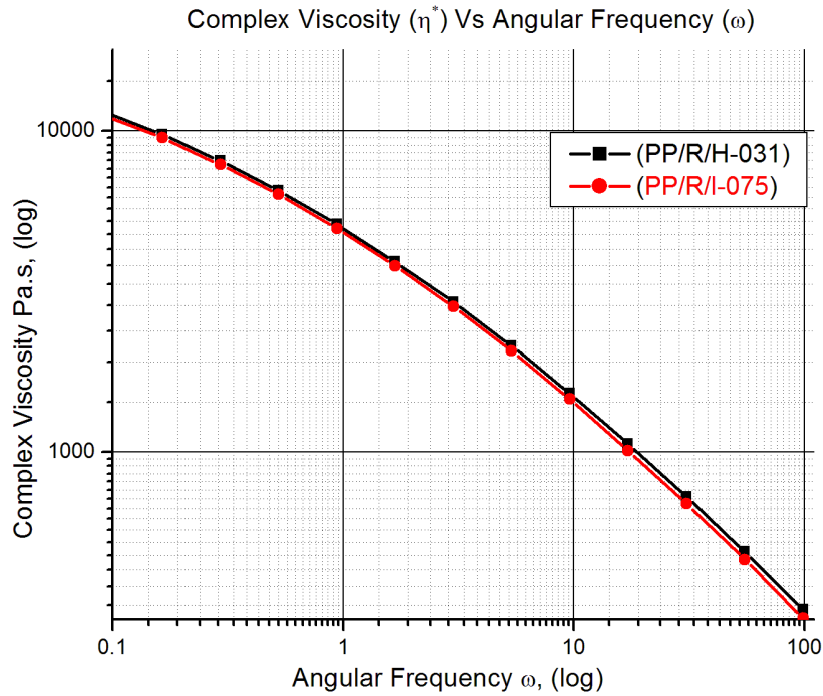


**Figure 5.6:** Complex viscosity Vs Angular frequency of PP/R/H-031 and PP/R/I-075.

This very high molecular weight tail has very limited effect on the complex viscosity over the entire range of angular frequency, as can be seen in the figure 5.6; that the PP/R/H-031 superimposing the PP/R/I-075 grade.

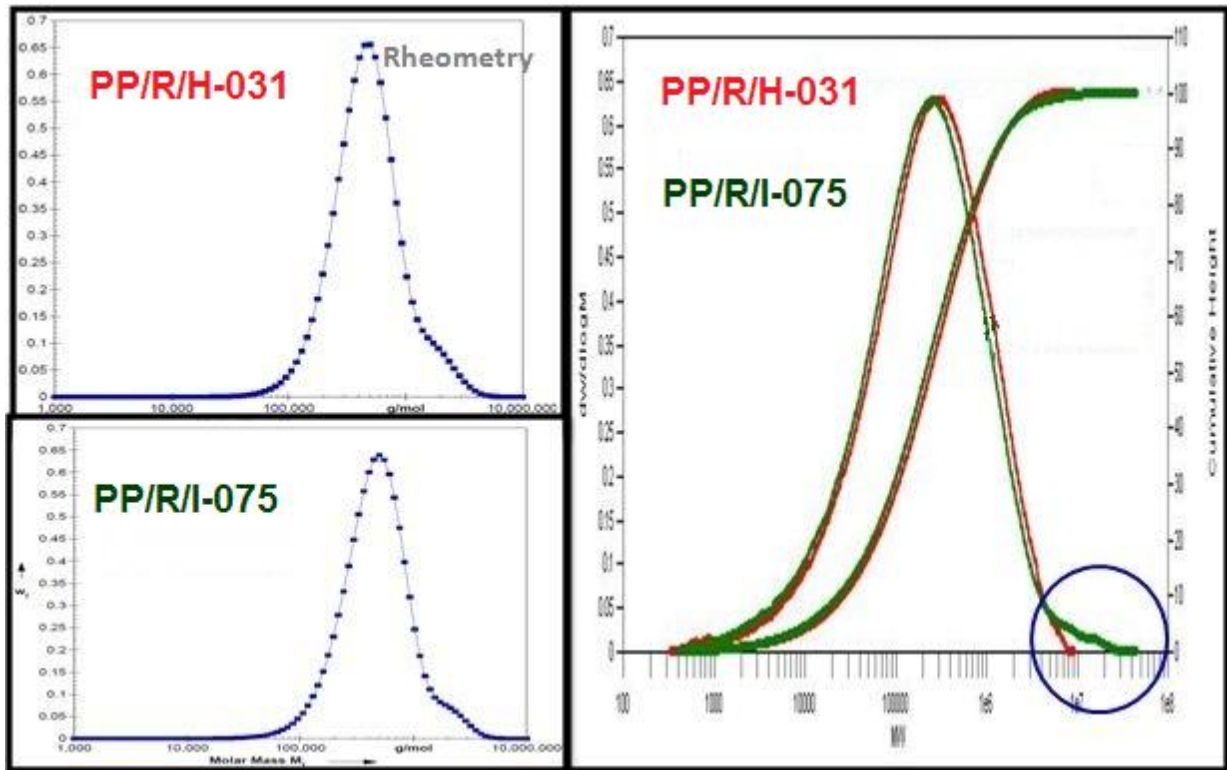


**Figure 5.7:** MWD from rheometry and HT-GPC of PP/R/H-031 Vs PP/R/I-075.

In the figure 5.7; the MWD from GPC and rheometry for PP/R/H-031 is complementing each other. As it is showing that there is a more pronounced hump in the PP/R/I-075 compared to PP/R/H-031.



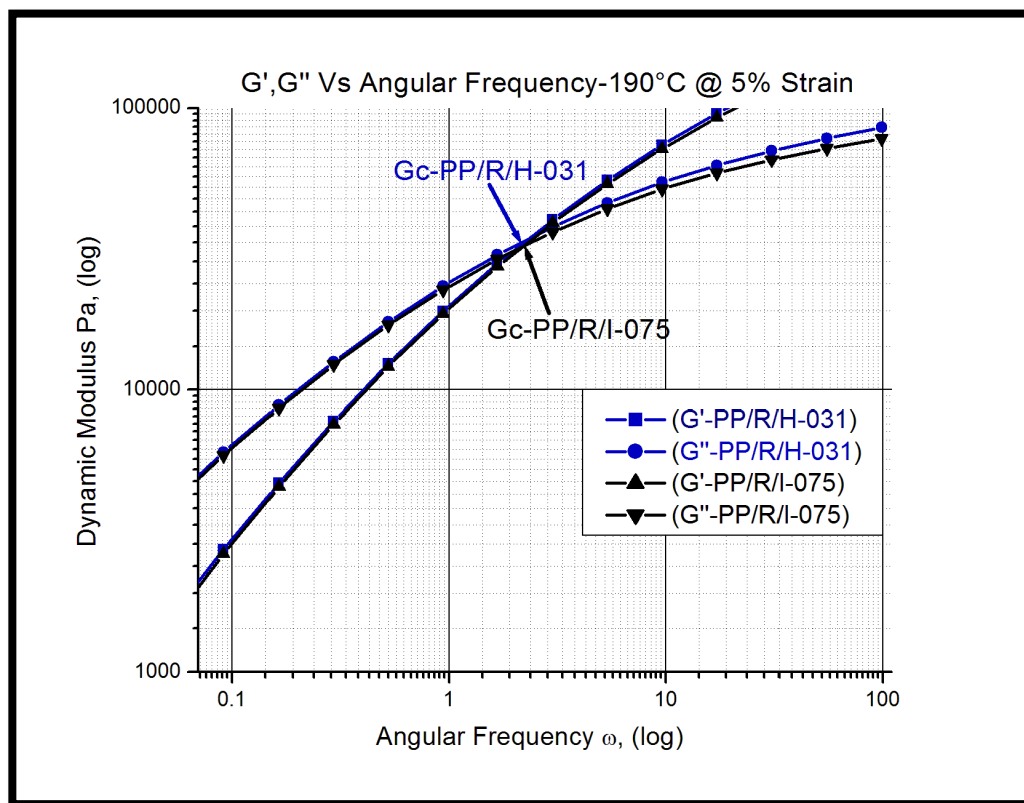


**Figure 5.8:** Storage Modulus ( $G'$ ) and Loss Modulus Vs Angular Frequency of PP/R/H-031 and PP/R/I-075.

In the figure 5.8; storage modulus and loss modulus has been compared and it was found that both the grades have shown hardly any difference over the entire frequency range and thus have comparable values.

It was found that the PP/R/H-031 comparatively has very limited high molecular weight tail than that of PP/R/I-075. In addition, the PP/R/H-031 has higher amount of high molecular weight chains at very low concentration which is in agreement with the line speed of 365m/min, while no difference was found in the storage modulus, loss modulus and complex viscosity values.

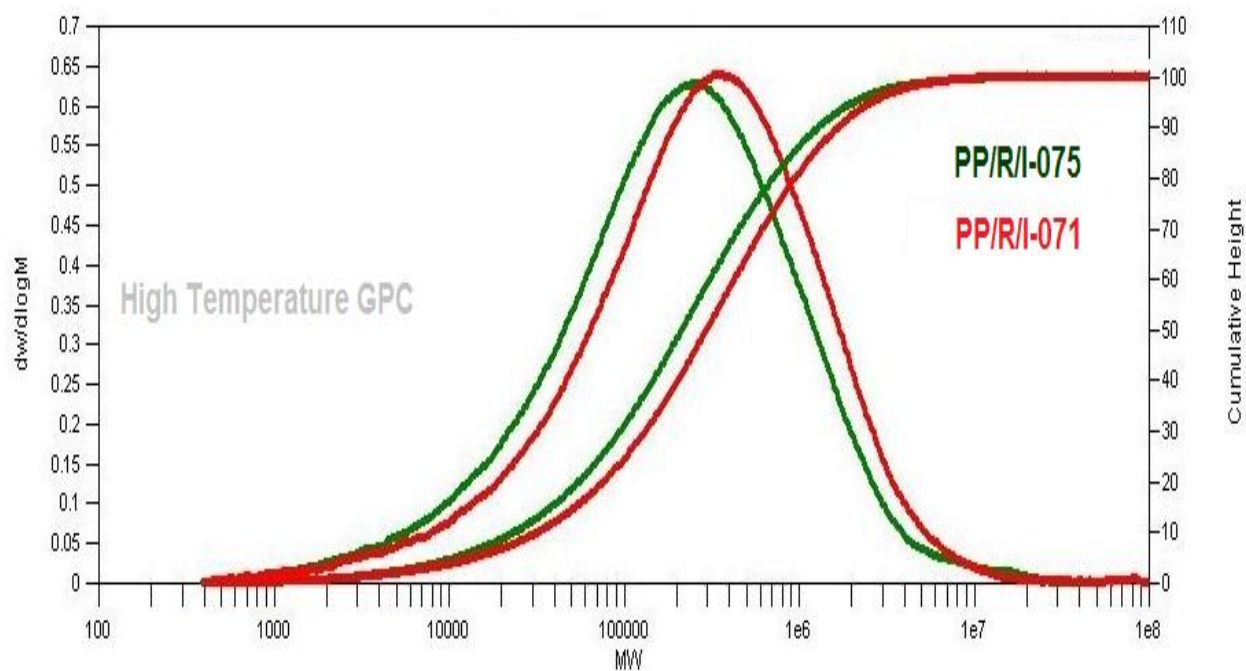


**Figure 5.9:** HT-GPC MWD Chromatogram of PP/R/I-075 Vs PP/R/I-071 .

In the figure 5.9, GPC chromatogram of PP/R/I-075 and PP/R/I-071 has shown a very large difference in the MWD pattern. It is apparent from the figure that PP/R/I-071 showing very long high molecular weight tail which reached up to  $10^8$ . If PP/R/I-075 is considered as a base chromatogram then it easy to say that the PP/R/I-071 chromatogram has been shifted toward higher molecular weight region, this very high molecular weight tail may be the reason for comparable tenacity to that of PP/R/I-075. On the other hand both the grades have limit their low molecular weight tail within the range of  $2 \times 10^2$ , but the PP/R/I-075 has higher amount of low molecular weight content which significantly lowers the value of number average molecular weight and consequently increases the PDI, gives an estimation of broad molecular weight

distribution. That was further confirmed by the complex viscosity and angular frequency graph in the figure.6, that PP/R/I-071 has very high molecular weight, showing very high complex viscosity over the entire range of angular frequency.

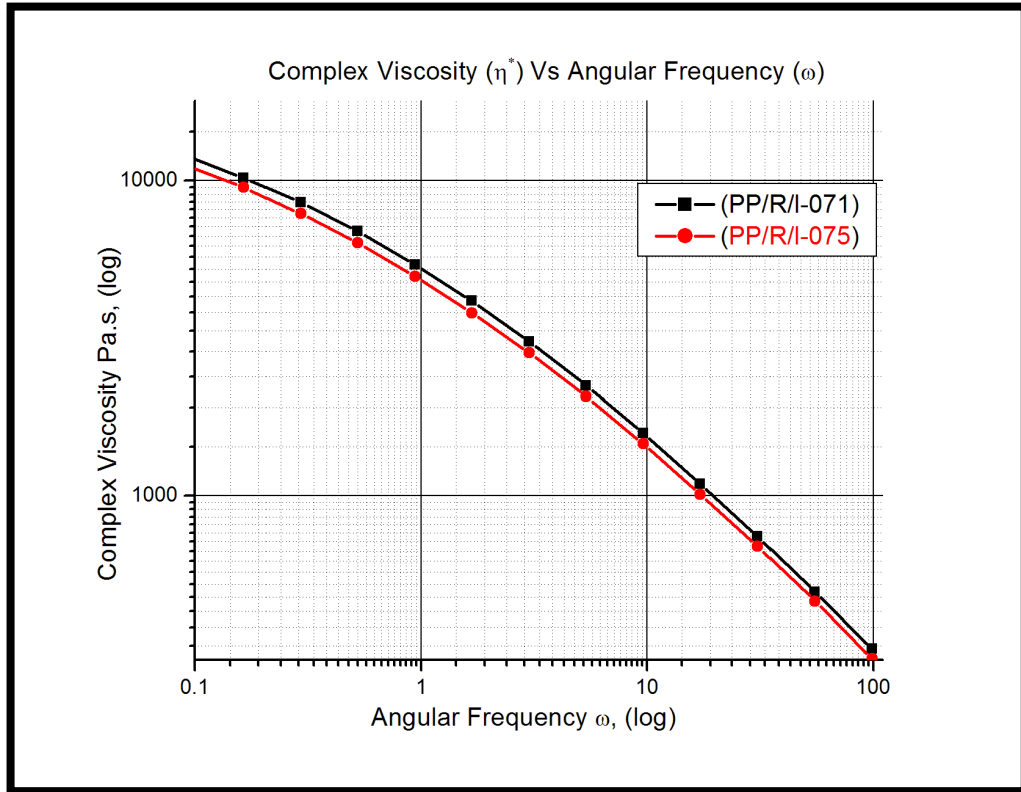


**Figure.6:** Complex viscosity Vs Angular frequency of PP/R/I-071 and PP/R/I-075.

In figure.6.1, the GPC and rheometry MWD chromatogram is compared. As the graph has shown that both the chromatogram have a hump in their high molecular weight region, this further complementing the GPC MWD chromatogram.

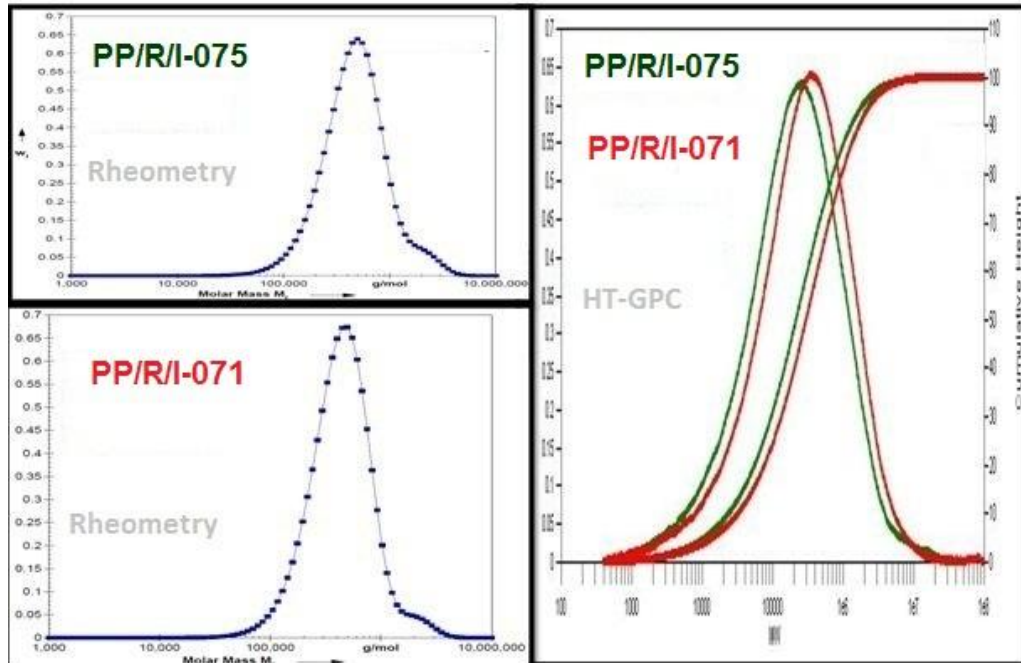


**Figure.6.1:** MWD Chromatogram from GPC and rheometry of PP/R/I-071 Vs PP/R/I-075.

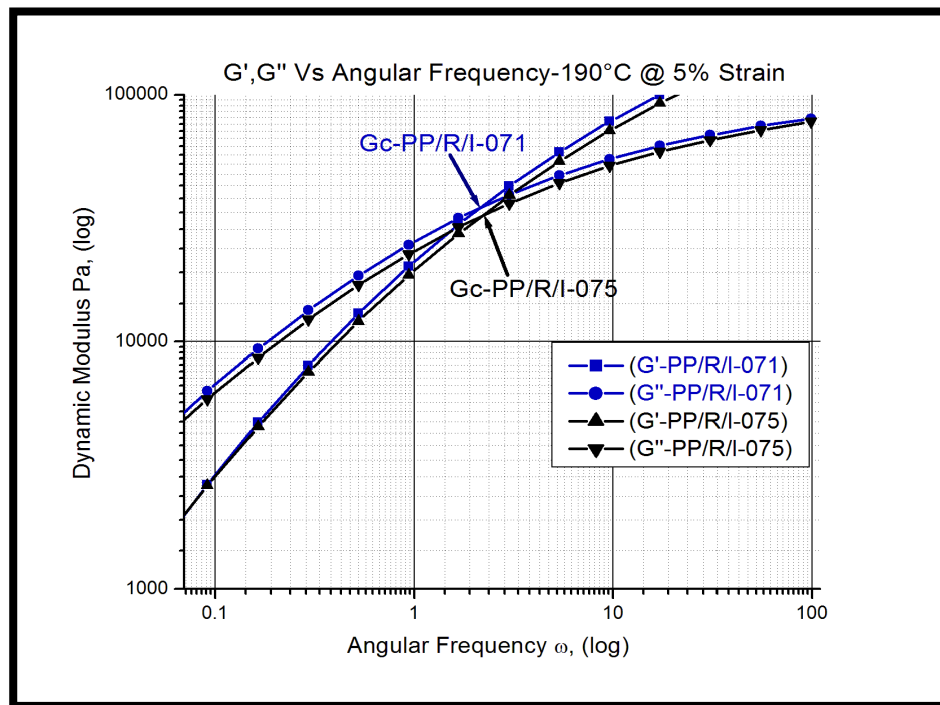


**Figure.6.2:** Storage Modulus ( $G'$ ) and Loss Modulus Vs Angular Frequency of PP/R/I-071 and PP/R/I-075.

It is evident from figure 6.2, that PP/R/I-075 has shown slightly lower cross-over modulus which is an indication of broader MWD and has shown better flow-ability during the trial and reached a line speed of 350 mt/min as compared to 300 mt/min line speed of PP/R/I-071. On the other hand PP/R/I-071 has slightly higher storage modulus but this effect is overshadowed by the difference in MWD between the two. In addition, this effect could be partially related to a greater number of tie molecules between the lamellae in the broad MWD in PP/R/I-075 [36].

**In spite of higher molecular weight tail of PP/R/I-071 has shown comparable tenacity along with PP/R/I-075 grade this could be attributed to very high molecular weight content, while PP/R/I-075 has higher amount of low molecular weight content at very low concentration than PP/R/I-071.**

**The overall effect of lower molecular weight content also reflected in complex viscosity graph as the former have shown more shear thinning which in turn reflected in broad MWD of the same (PP/R/I-075) in dynamic modulus Vs angular frequency graph and could be the reason of 350mt/min line speed compared to PP/R/I-071.**

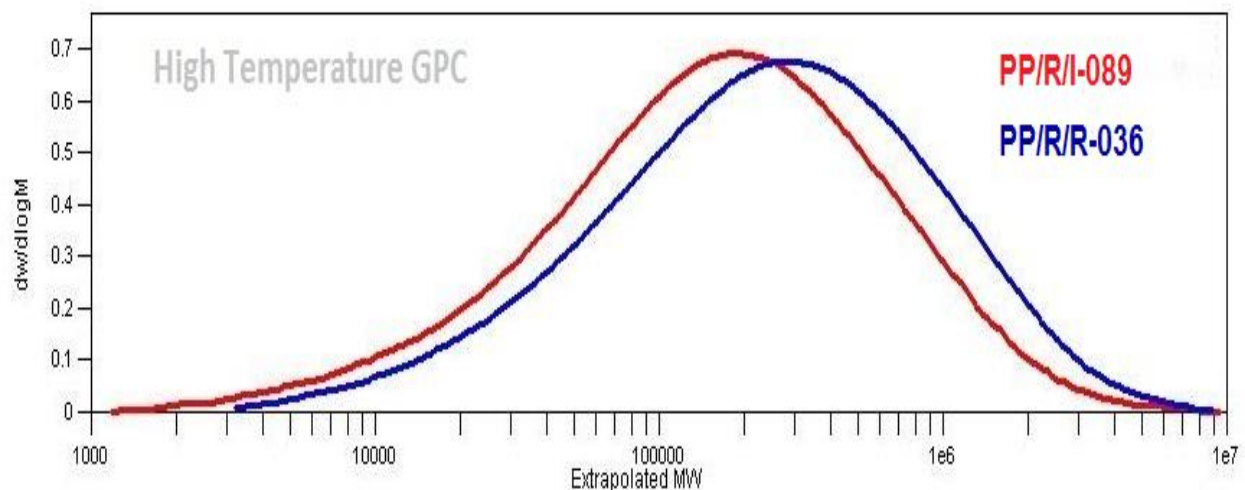


**Figure 6.3:** HT-GPC MWD Chromatogram of PP/R/R-036 Vs PP/R/I-089.

In figure 6.3; GPC chromatogram of PP/R/I-089 and PP/R/R-036 is compared and it was found that both the grades restrict their high molecular weight tail within the limit of  $10^7$ . However, if PP/R/R-036 is considered as a reference curve, then it can be seen that PP/R/I-089 grade curve shifted to the left and showing higher amount of low molecular weight chains than PP/R/R-036 grade at all concentration which significantly affects the processability and could be able to reach a comparable line speed of 412mt/min against the line speed of 415mt/min of PP/R/R-036 during the trial run. On contrary when complex viscosity graph (figure 6.4) of PP/R/R-036 was compared with that of PP/R/O-089 it was found that graph does not complement the GPC chromatogram.

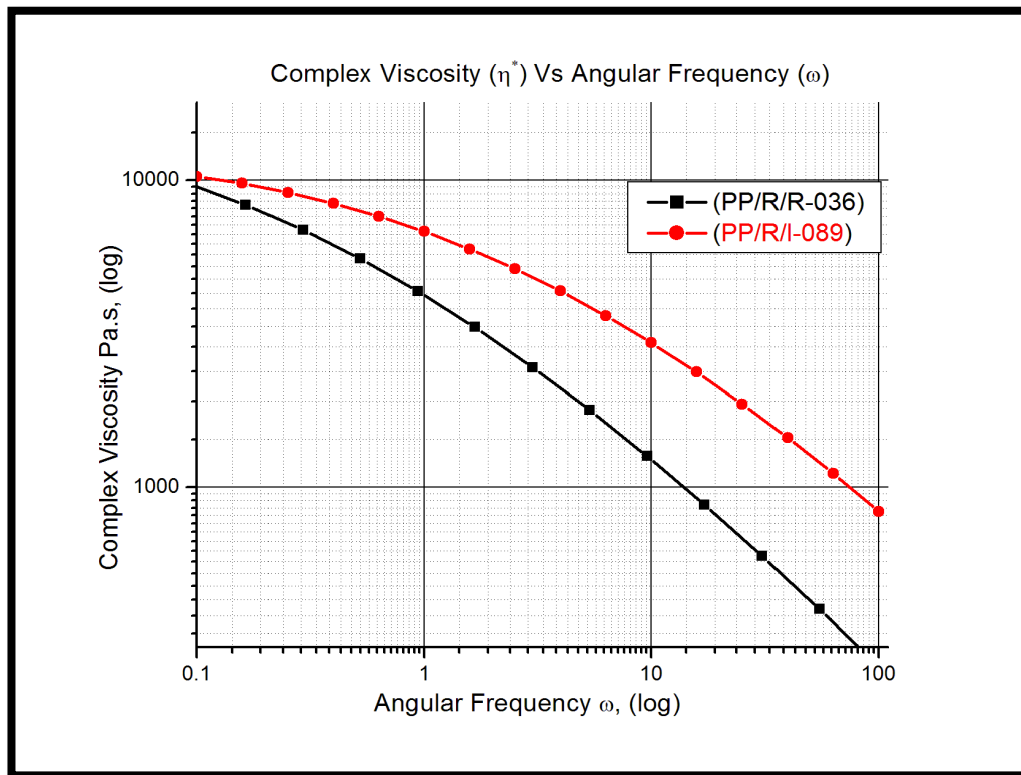


**Figure.6.4:** Complex viscosity Vs Angular Frequency of PP/R/R-036 Vs PP/R/I-089.

However, when we look into the effect of very high molecular weight chains on the  $M_z$  (Z-average molecular weight) value, this very high molecular weight significantly increases the value of  $M_z$ .

When the tape is stretched at higher temperature, this higher  $M_z$  molecules once oriented, are less likely to lose their orientation due to stress relaxation and hence increases the modulus [36]. This could be the reason of 415m/min line speed of PP/R/R-036. The above discussion is further strengthened by the dynamic modulus vs angular frequency graph which is shown in the figure 6.5; below.

Further, when the storage and loss modulus curves are compared in figure 6.5; it was found that both the polymer grades have similar cross-over modulus. Therefore, in this case the effect of  $G_c$  (cross-over modulus) is overshadowed and hence not considered (I.B. Kazatchkov et al, 1999). While the effect of molecular weight has shown significant shift of storage modulus curve to the left hand side at lower frequency. This could be the determinantal effect during the orientation at elevated temperature.

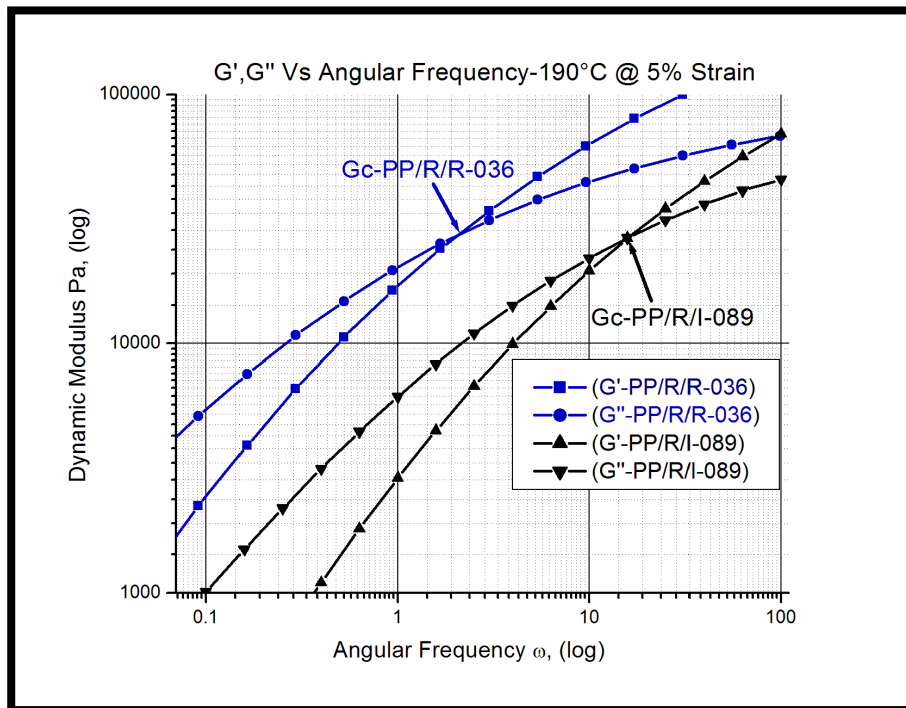


**Figure 6.5:** Storage Modulus ( $G'$ ) and Loss Modulus Vs Angular Frequency of PP/R/R-036 Vs PP/R/I-089.

It was found that in the above discussion that both the grades limit their high molecular weight tail within the range of  $10^7$  while on the low molecular weight region, PP/R/I-089 has higher amount of low molecular weight content which could be attributed to the better performance in the trial and accomplished a line speed of 412mt/min as compared to 415mt/min of PP/R/R-036.

PP/R/I-089 raffia grade was compared with PP/R/I-027 for GPC MWD and the Chromatogram is given in Figure 6.6.

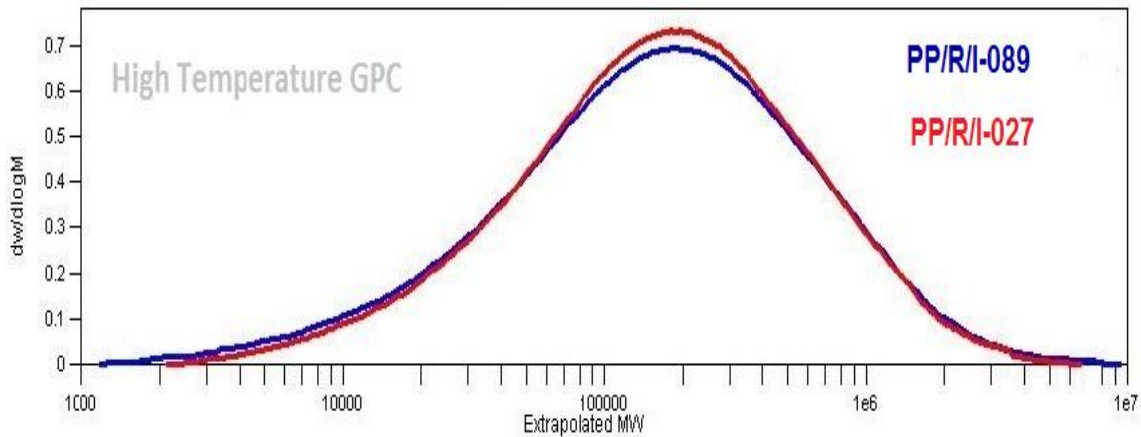


**Figure 6.6:** HT-GPC MWD Chromatogram of PP/R/I-089 Vs PP/R/I-027.

In figure 6.6; GPC Chromatogram of PP/R/I-027 and PP/R/I-089 is compared. The graph is itself explanatory and showing that PP/R/I-027 superimposing PP/R/I-089 at high molecular weight region. Both the grades showing very limited high molecular weight tail. On the other hand PP/R/I-089 has slightly higher amount of low molecular weight chains at very low concentration (0.1-0.15). This very low molecular weight facilitates the processing. However, it is worth mentioning here that PP/R/I-089 achieved a line speed of 412mt/min than PP/R/I-027 of 400mt/min during the trial run.



This is further illustrated by complex viscosity versus angular frequency graph in the figure 6.7. It is clearly shown that PP/R/I-089 showing more shear thinning as the frequency increases than that of PP/R/I-027 due to higher amount of low molecular weight chains in PP/R/I-089.

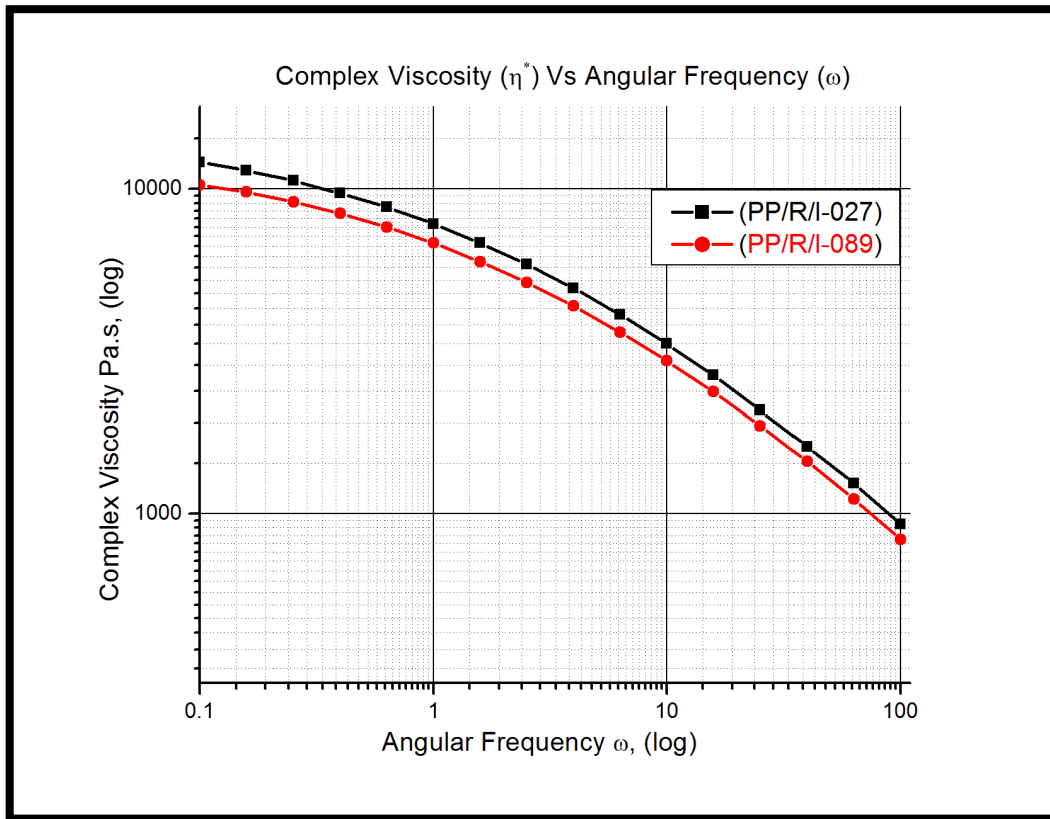


**Figure 6.7:** Complex viscosity Vs Angular Frequency of PP/R/I-089 Vs PP/R/I-027.

The storage modulus and loss modulus dependency of angular frequency shown in figure 6.8; and the graph were compared.

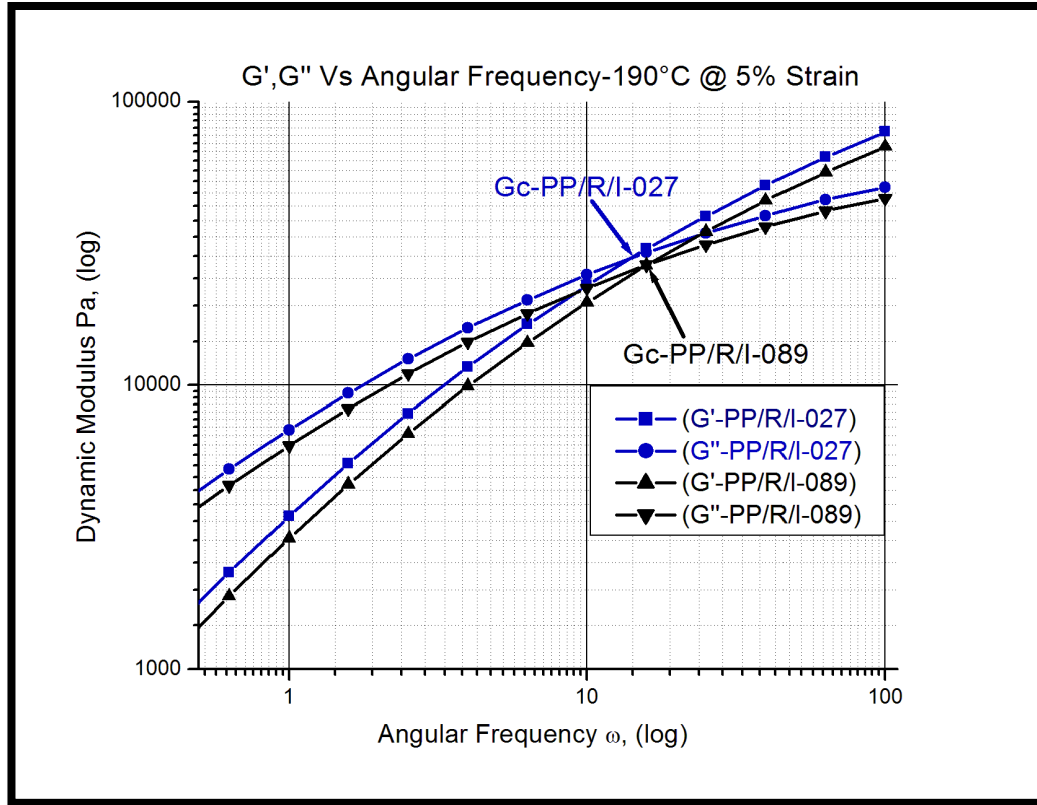


**Figure 6.8:** Storage Modulus ( $G'$ ) and Loss Modulus Vs Angular Frequency of PP/R/I-089 Vs PP/R/I-027.

As we can see in the figure 6.8; which shows the storage modulus and loss modulus dependency of frequency of the two grades PP/R/I-089 and PP/R/I-027. There is slight difference in the cross-over modulus and cross-over frequency; hence PP/R/I-089 has shown slight broad molecular weight distribution than the PP/R/I-027. Therefore higher the MWD better will be the flowability as is the case for PP/R/I-089.

**It was found that the PP/R/I-089 and PP/R/I-027 polymer samples have similar amount of high molecular weight chains and overlapping each other in the high molecular weight region, however, PP/R/I-089 has slightly higher amount of low molecular weight chains which was also complementing the complex viscosity where PP/R/I-089 grade has shown more shear thinning and also complementing the dynamic modulus graph in the figure.6.8.**

## **Micro structure Analysis of Grades from Thermal analysis of PP raffia grades using Differential Scanning Calorimetry (DSC) and Dynamic Mechanical Analyser (DMA).**

### **DSC (Differential Scanning Calormetry):**

Differential Scanning Calorimeter is used to evaluate the microstructure of the different grades. Melting of polypropylene has been studied to correlate melting temperature with the tacticity and molecular weight of the polymer. Sometimes multiple melting peaks also found in the thermogram. The multiple melting peaks were affected by various factors such as tacticity, heating rate, molecular weight. The origin of the melting peak in isotactic polypropylene has been discussed by Samules [1975] [37], he found that at least two crystalline species are responsible for multiple melting peaks, either different disordered crystals or different crystal sizes, or different crystal types. In the recent past decades it was also evident from the studies [Hikoska; 1973 and Corradini, Giunchi, Petraccone, Pirozzi, Vidal; 1980] [38, 39, 40] that the  $\alpha$  -modification of isotactic polypropylene may show various degree of disorder in the position of chains that could be the reason for multiple melting peaks, but this discussion is out of the scope of this work. The data was obtained from the DSC thermogram and was further correlated with the percent crystallinity.

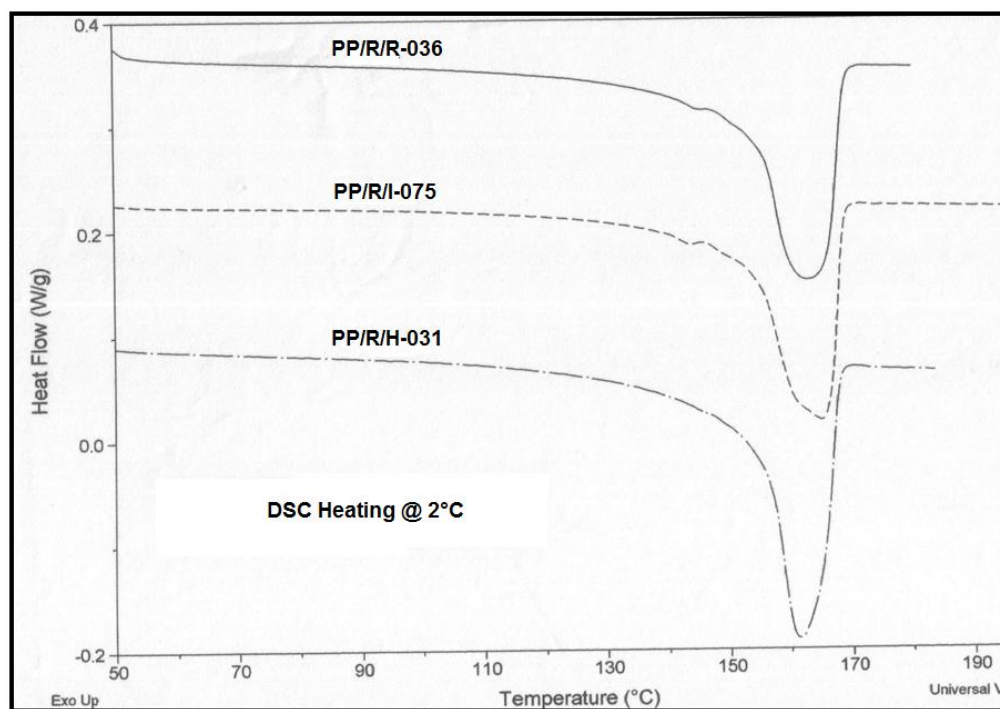
In this experimental work the first heating and cooling carried out at the same rate of 10°C/min while the second heating were carried out at the rate of 2°C/min. The heating rate is very low for better observation of the thermogram. The basis of slow heating rate is that, as we slow the heating rate actually we were giving more time for the crystals to reorganize to thicken in lamella and show an increase in melting temperature ( $T_m$ ).

Table.2; describes the major DSC values where it compares between PP/R/R-036, PP/R/H-031 and PP/R/I-075 grades taken from the thermogram which is shown in Figure.7. It can be seen that, PP/R/I-075 has highest peak melting point indicating that it has higher concentration of large spherulites as compared to PP/R/R-036 and PP/R/H-031.

Also onset of PP/R/I-075 is higher compared to PP/R/H-031 and PP/R/R-036 grades. Yet, on comparing the enthalpy, PP/R/I-075 is having the lowest value. It is worth to recall that PP/R/I-075 has a long tail of very high molecular weight fraction compared to PP/R/H-031 and PP/R/R-036. The long molecular chains will reduce the overall crystallinity, as can be seen here, by reducing the enthalpy.

**Table.2:** DSC parameters of PP/R/H-031, PP/R/R-036 and PP/R/I-075.

Sl. No.	Grades	T <sub>m2</sub>	Onset T <sub>m2</sub>	ΔH <sub>1</sub> - Area up to T <sub>m2</sub>	ΔH <sub>2</sub> - Area after T <sub>m2</sub>	ΔH=(ΔH <sub>1</sub> + ΔH <sub>2</sub> ) (J/g)	% Crystallinity (%)
1	PP/R/R-036	163	154	72.3	29.7	102	48.8
2	PP/R/I-075	165	155.2	81.2	16.8	98	46.9
3	PPR/H-031	162	155	72.3	35.8	108.1	51.8



**Figure.7:** DSC melting thermograms of PP/R/R-036, PP/R/I-075 and PP/R/H-031.

Figure.7; has shown that the PP/R/I-075 grade has three melting peaks at 143°C, 163°C, and at 165°C. On the other hand, PP/R/R-036 grade has shown melting peaks at 145°C and at 163°C while PP/R/H-031 has shown only a single intense melting peak at 162°C.

This reveals that the PP/R/R-036 grade has spherulite of less oriented lamella which was melted at 144°C, while PP/R/I-075 grade showing more heterogeneous spherulitic structure, hence the less stable and less oriented lamella of thin spherulite were first melted at 144°C and a larger one of more stabilized and thick spherulite melted at 163°C while the PP/R/H-031 grade showing more homogeneous spherulite which is stable up to the single melting peak at 161.2°C.

The above observed data has shown the presence of more heterogeneous spherulites in the PP/R/I-075 grade. The DSC thermograms here very well compliment the microstructure from GPC/ Rheometer to the extent that PPR/H-031 and PP/R/R-036 grades shows similar onset and crystallinity.

DSC thermogram data of four different grades have been shown in the table 2.1; followed by their DSC thermogram in the figure.7 and subsequently compared.

Sl. No	Grades	T <sub>m2</sub>	Onset T <sub>m2</sub>	ΔH <sub>1</sub> -Area up to T <sub>m2</sub>	ΔH <sub>2</sub> -Area after T <sub>m2</sub>	ΔH=(ΔH <sub>1</sub> +ΔH <sub>2</sub> ) (J/g)	% Crystallinity (%)
1	PP/R/R-036	163	154	72.3	29.7	102	48.8
2	PP/R/I-071	164	153.6	69.3	20.4	99.4	47.5
3	PP/R/H-031	162	155	72.3	35.8	108.1	51.8
4	PP/R/I-070	166	153.2	86.3	16.4	102.7	49.1

**Table.2.1:** DSC parameters of PP/R/H-031, PP/R/R-036, PP/R/I-071 and PP/R/I-070 grades.

Similarly, The PP/R/R-036 and PP/R/H-031 grades have been compared with PP/R/I-070 and PP/R/I-071. On the basis of obtained data from the DSC experiment, which is shown in the table.2.1; it is evident that PP/R/I-071 has shown  $T_{m2}$  at 164°C and for PP/R/I-070 at 166°C, while  $T_{m2}$  of PP/R/R-036 and PP/R/H-031 are at 163° C and 162°C respectively.

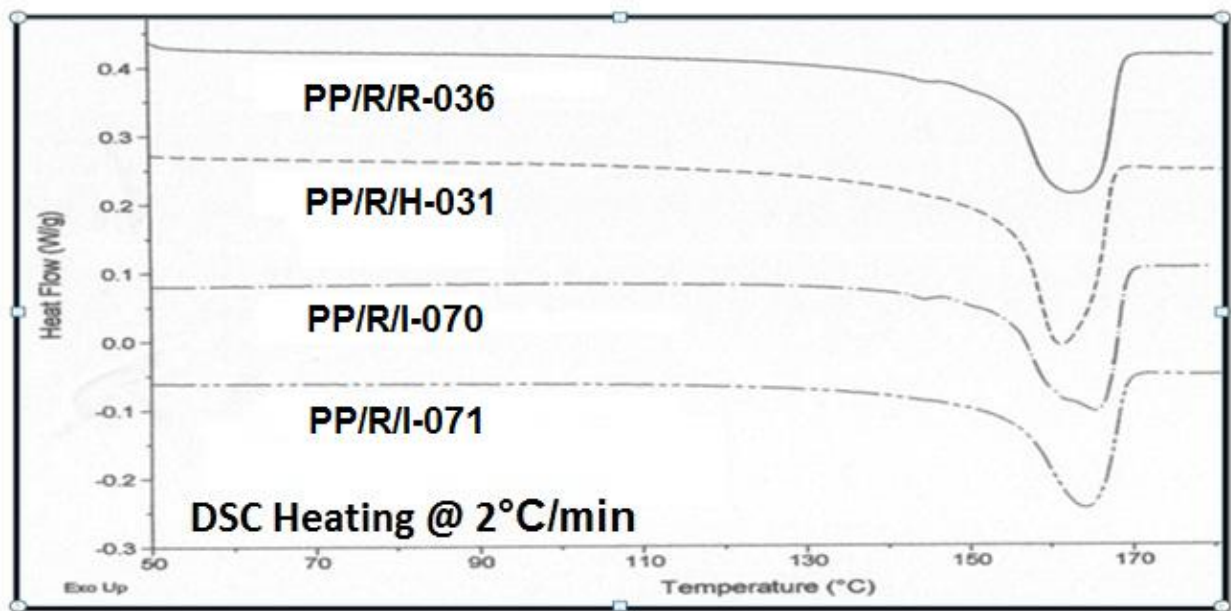


**Figure.7.1:** DSC melting thermograms of PP/R/R-036, PP/R/I-071, PP/R/H-031 and PP/R/I-070.

In the above figure.7.1 PP/R/I-070 has shown three peaks, first at 144°C, second at 158°C and the last one at 166°C, showing that a less stable thin spherulite melted at 144°C and a large stable spherulite melted at 158°C, on the other hand PP/R/H-031 has a single peak at 164°C showing much stable spherulite composed of much thicker lamella. It is apparently shown in the figure.7.1; that the PP/R/I-070 grade has more heterogeneous spherulites.

DSC thermogram data of four different grades have been shown in the table 2.2; followed by their DSC thermogram in the figure.7.2, 7.3, and 7.4 and subsequently compared.

Sl. No	Grades	T <sub>m2</sub>	Onset T <sub>m2</sub> (°C)	ΔH <sub>1</sub> -Area up to T <sub>m2</sub>	ΔH <sub>2</sub> -Area after T <sub>m2</sub>	ΔH=(ΔH <sub>1</sub> +ΔH <sub>2</sub> ) (J/g)	% Crystallinity (%)
1	PP/R/R-036	163	154	72.3	29.7	102	48.8
2	PP/R/I-089	168	153	84.82	15.18	98.52	47.1
3	PP/R/I-027	168	157	84.76	15.24	94.9	45.4
4	PP/R/I-066	168.	158	84.96	15.04	95.56	45.8

**Table.2.2:** DSC parameters of PP/R/R-036, PP/R/I-089, PP/R/I-027 and PP/R/I-066 grades.

Table 2.2; showing the DSC parameters obtained during thermal analysis of four different grades namely, PP/R/R-036, PP/R/I-089, PP/R/I-027 and PP/R/I-066. It is very much clear that the later three grades showing the same value of T<sub>m2</sub> but different onset temperature.

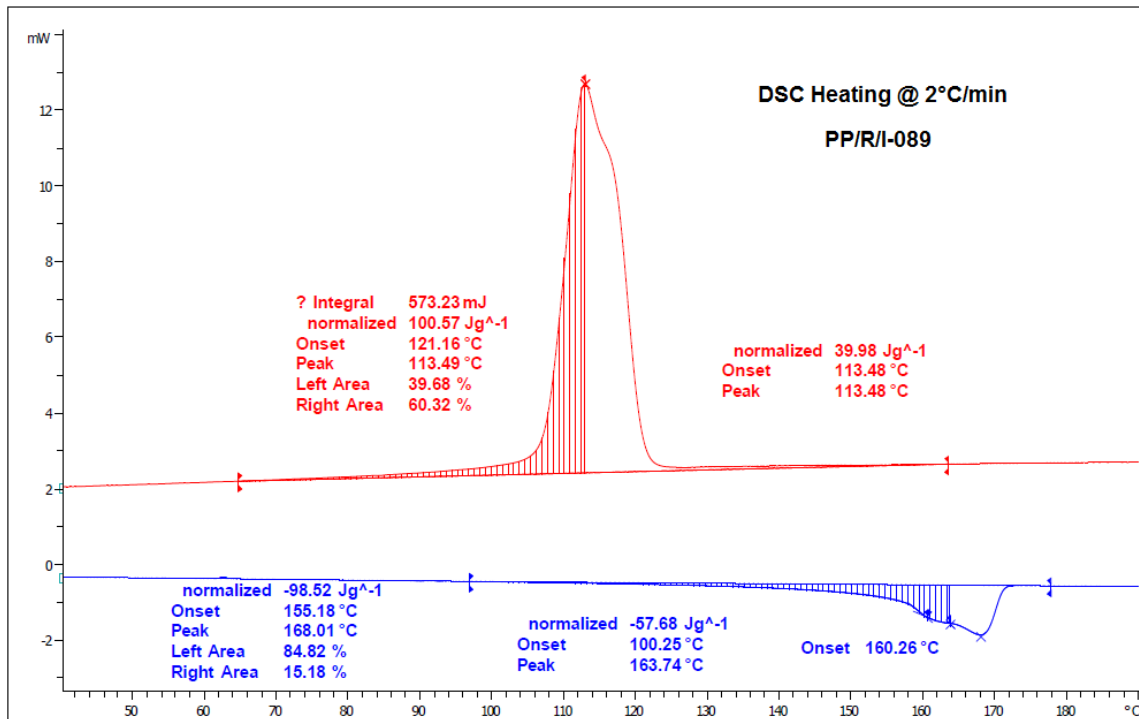


**Figure 7.2:** DSC melting and cooling thermogram of PP/R/I-089 grade.

On comparing the graph of three grades namely, PP/R/I-089, PP/R/I-027 and PP/R/I-066 with PP/R/R-036 it was found that all the four grades showing different lamellar thickness distribution in their melting thermogram, which is clear from the figure.7 and further from figure 7.2, 7.3 and 7.4. Moreover, it is very interesting to note that the PP/R/R-036 grade has two melting peaks, first at 145°C and the second one at 163°C corresponding to very thin and thicker lamella respectively. On the other hand all the later three grades have shown first melting peak (thin lamella) same as the  $T_{m2}$  of the PP/R/R-036, this reveals that much stable and thicker lamellar distribution in the later three grades namely, PP/R/I-089, PP/R/I-027 and PP/R/I-066.

In addition to that, on comparing the value of enthalpy, PP/R/R-036 and PP/R/I-089 grades has shown a comparable value of % crystallinity. It is necessary to recall the GPC curve of the two in figure 6.3; in which both the grades limit their high molecular weight tail within the value of  $10^7$  that may be the cause of comparable value of enthalpy.



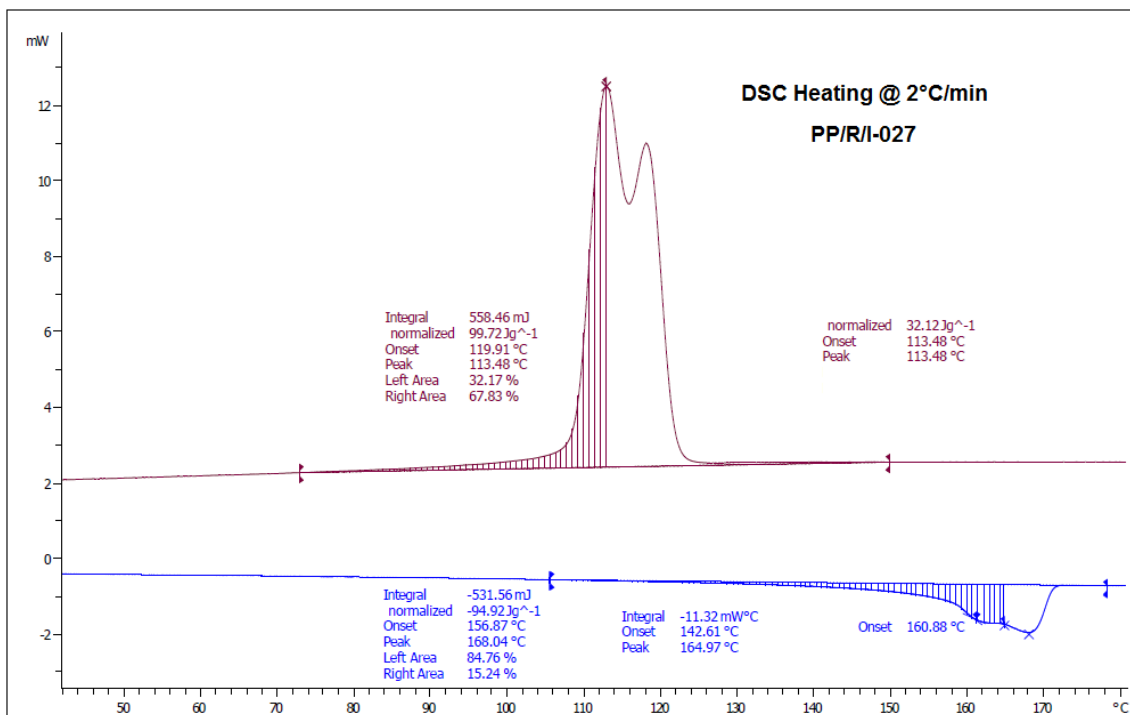


**Figure7.3:** DSC melting and cooling thermogram of PP/R/I-027 grade.

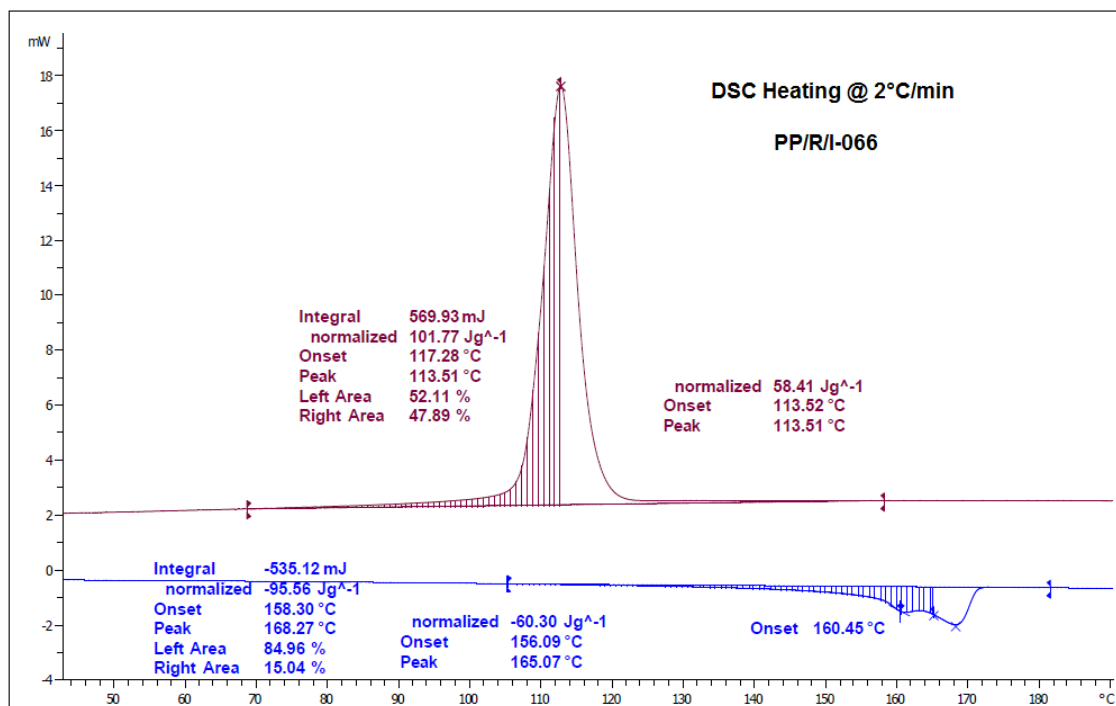


**Figure7.4:** DSC melting and cooling thermogram of PP/R/I-066 grade.

It was observed that the PP/R/R-036, PP/R/I-071, PP/R/I-070, PP/R/H-031 and PP/R/I-075 grades have same onset melting temperature and found within the limit of 155°C. The melting points of all the grades were found to occur between the ranges of 162°C to 166°C. It was also found that the PP/R/I-075 and PP/R/I-070 have shown three melting peaks while PP/R/R-036 has shown two melting peaks and thus altogether have shown more heterogeneous lamellar distribution. On the other hand PP/R/H-031 and PP/R/I-071 have shown single melting peak hence shown more uniform distribution of the lamella. At the same time PP/R/I-089, PP/R/I-027 and PP/R/I-066 grades have shown same  $T_{m2}$  melting peak at 168°C while have shown different onset  $T_m$  i.e. 153°C to 158°C.

PP-raffia grades PP/R/R-036 and PP/R/I-070 found to have similar melting enthalpy of 102J/g and consequently have the same % crystallinity, i.e. 48%, while PP/R/H-031 comparatively has higher melting enthalpy consequently higher % crystallinity, i.e. 51.8%; on the other hand PP/R/R-036 and PP/R/I-089 have comparable % crystallinity within the range of 47-48% and could be correlated to the comparable line speed of 412mt/min to 415mt/min.

### **Oxidation Induction Time (OIT) Analysis :**

The Oxygen Induction Time (OIT) test is an accelerated aging test that is often used to predict the long term stability of hydrocarbon materials including polyolefin materials. The OIT test can also be used to measure the level of effective antioxidant present. The OIT test is designed to accelerate this degradation in order to achieve meaningful comparisons in a short period of time

<b>S.NO</b>	<b>Grades</b>	<b>OIT (minutes)</b>
1	PP/R/R-036	9.7
2	PP/R/R-032	15.8
3	PP/R/H-031	14.3
4	PP/R/L-035	12.6
5	PP/R/I-075	14.0
6	PP/R/I-071	12.3
7	PP/R/I-070	7.9

**Table.3:** Oxidation induction Time of the 7 grades.

The OIT value generally follows a linear relationship with antioxidant concentration; this behavior makes the OIT test a useful quality control procedure for tracking the concentration of the antioxidant.

In the case of above seven Raffia polypropylene grades, shown above in the table.3, the maximum OIT limit was reached to a value of 15.8 min for the PP/R/R-036. Therefore, PP/R/R-036 is the most stable grade in terms of its oxidation stability at a predetermined temperature (i.e., 200°C) i.e., one may conclude that the PP/R/R-036 grade may have the highest concentration of antioxidant. It was also found that the three grades namely PP/R/I-071, PP/R/I-070 and PP/R/I-075 have significantly large difference in their OIT values.

Although, the PP/R/I-075 grade has the highest OIT (14.0) compared to PP/R/I-071, PP/R/I-070 and has the comparable OIT value with that of the PP/R/R-036 (OIT = 14.3). The reduction / difference in AO (Anti-Oxidant) loading also could effect in poor performance of the melt, but it is evident from the table.3 that, all the grades taken for benchmarking are stable having OIT 8 minutes or more.

**The stability of PP raffia grades, which could arise from the difference in the loading of AO (Antioxidant) additive, was evaluated by OIT measurements and conclusively proved that all the grades were stabilized well.**

### Dynamic Mechanical Analysis:

The loss tangent ( $\tan\delta$ ), storage modulus ( $E'$ ) and loss modulus ( $E''$ ) as a function of temperature for the five PP raffia samples were shown and compared in the figure.8; and figure.8.1, two transitions  $\alpha$  and  $\beta$  in the order of decreasing temperature, were observed, the third transition,  $\gamma$ , usually occurs at much lower temperature than the range of temperatures used in this experiment ( $-100^\circ\text{C}$ ).

The  $\beta$ -transition which was found to occur between the ranges of  $5.7^\circ\text{C}$  to  $7.5^\circ\text{C}$ . As previously discussed in the experimental method section that the  $\beta$ -relaxation is mainly due to the co-operative segmental mobility of the disordered chains and attributed to the amorphous region. In fact, a decrease in the  $\beta$ -transition is related to the decrease in the mobility of the chains in the amorphous region (ref).

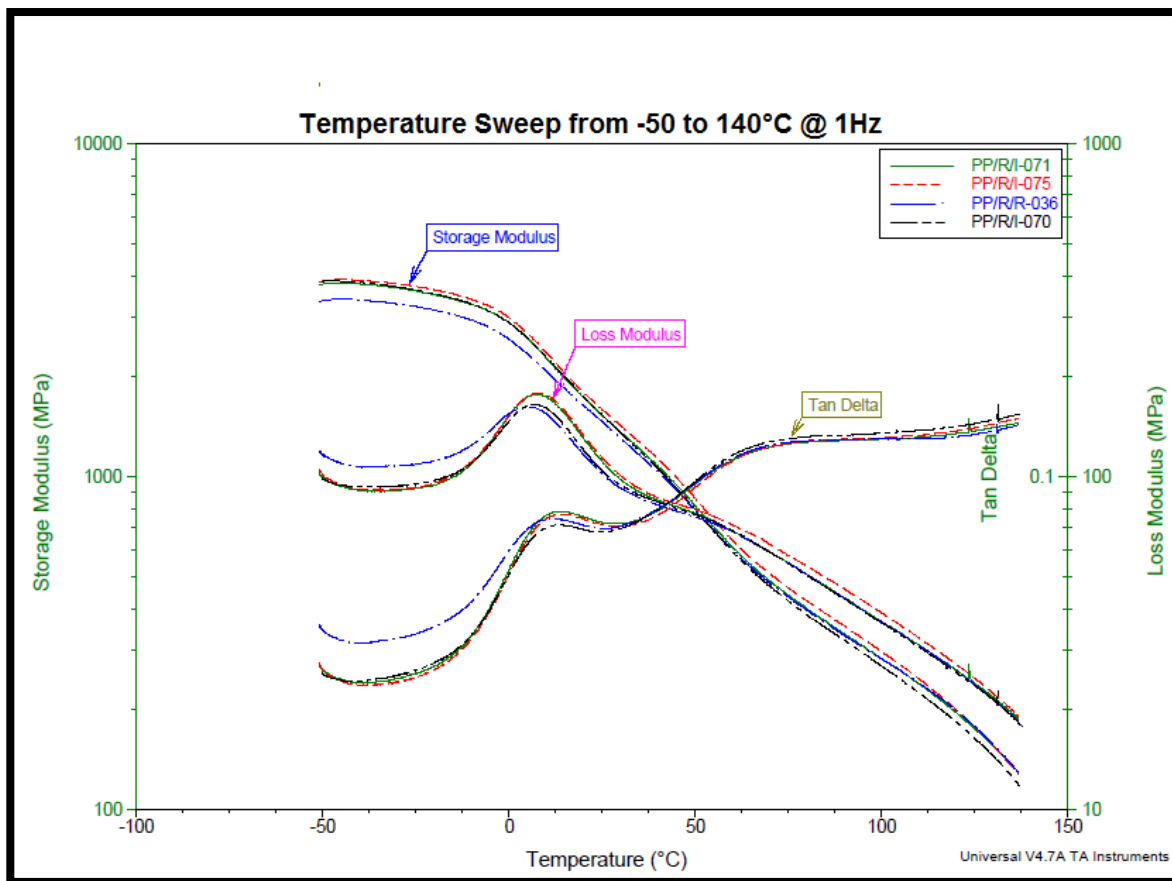


**Figure.8.** Storage modulus, Loss modulus and Tan delta curves of PP-raffia samples.

In the figure.8; comparatively slight decrease in the  $\beta$ -relaxation were observed in the PP/R/R-036 and PP/R/I-070 samples and that could solely be attributed to the slight increase in the crystallinity which was found in the DSC analysis of the same. Conversely, it was found that PP/R/I-071, PP/R/H-031 and PP/R/I-075 have slightly higher  $\beta$ -relaxation as can be seen in both the figure.8 and figure.8.1.

The  $\alpha$ -relaxation peak observed in all the PP raffia samples under the study and found to occur between the temperature range of 63°C and 67°C. There is always a relation between the  $\alpha$ -relaxation and crystallinity, and the intensity of the transition increases with the increase in crystallinity. In our case hardly any difference was found in the intensity of  $\alpha$ -relaxation peak and position of the  $\alpha$ -relaxations are almost overlapping each other.

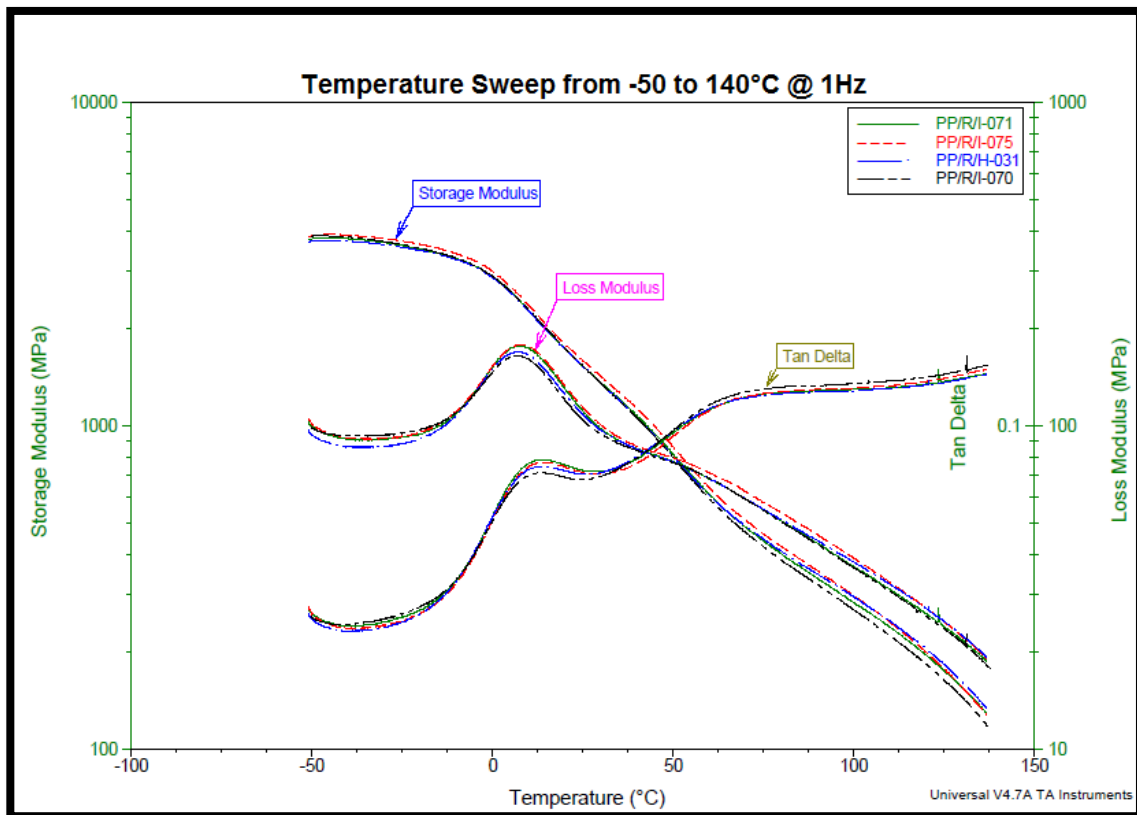


**Figure.8.1** Storage modulus, Loss modulus and Tan delta curves of PP-raffia samples.

Two relaxations namely  $\alpha$ -relaxation (63°C-67°C) and  $\beta$ -relaxation (5.7°C to 7.5°C) were found in our experiments. A slight shift in the  $\beta$ -relaxation were observed in three samples i.e. PP/R/I-071, PP/R/H-031 and PP/R/I-075 while hardly any difference found in the  $\alpha$ -relaxation peak in all the samples.

### <sup>13</sup>C-NMR (Nuclear Magnetic Resonance):

The distribution of the sequences, shown in table.4; originated from the <sup>13</sup>C-NMR analysis of the polymer. The difference of the %mmm pentad amount exhibits relatively higher values around 92%.

Polymer Grades	% Xylene Solubles	% mmmm
PP/R/R-032	3.4	83
PP/R/I--70	3.4	92
PP/R/I--71	3.4	90
PP/R/I--75	3.4	84
PP/R/I--027	3.4	86
PP/R/I--089	3.1	88

**Table .4:** The % Xylene Solubles and % mmmm sequences of PP/R/R-032, PP/R/I-70, PP/R/I-71, PP/R/I-75, PP/R/I-027 and PP/R/I-089 grades.

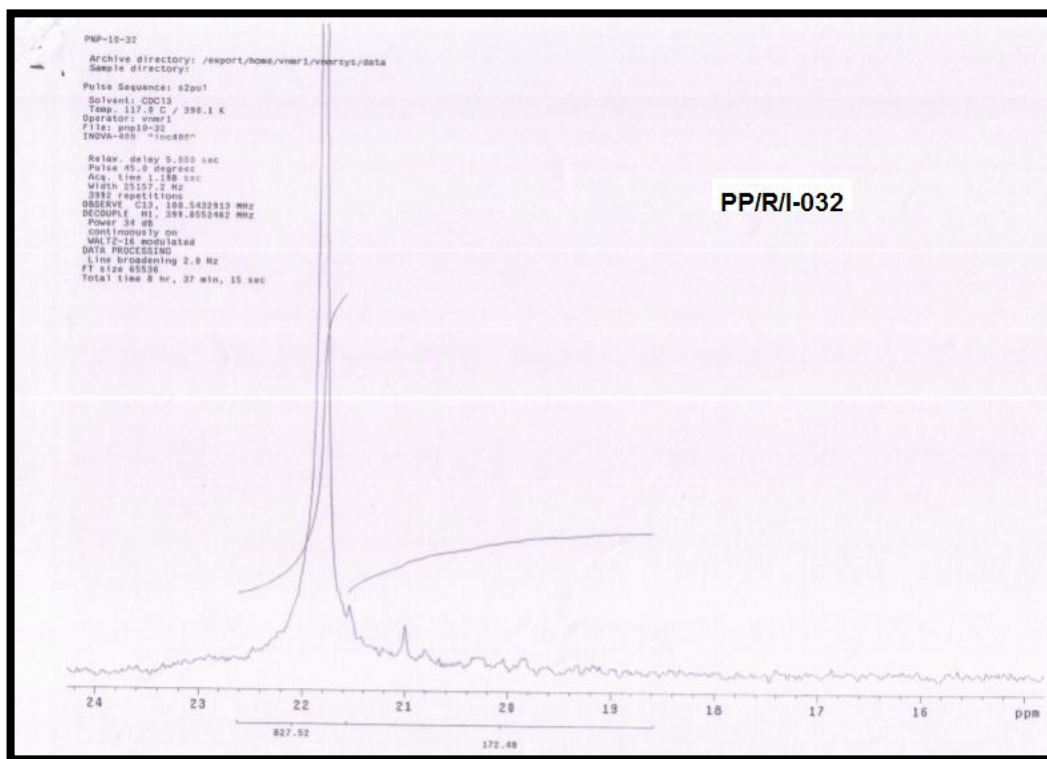


**Figure.9:** <sup>13</sup>C-NMR spectra of PP/R/R-032



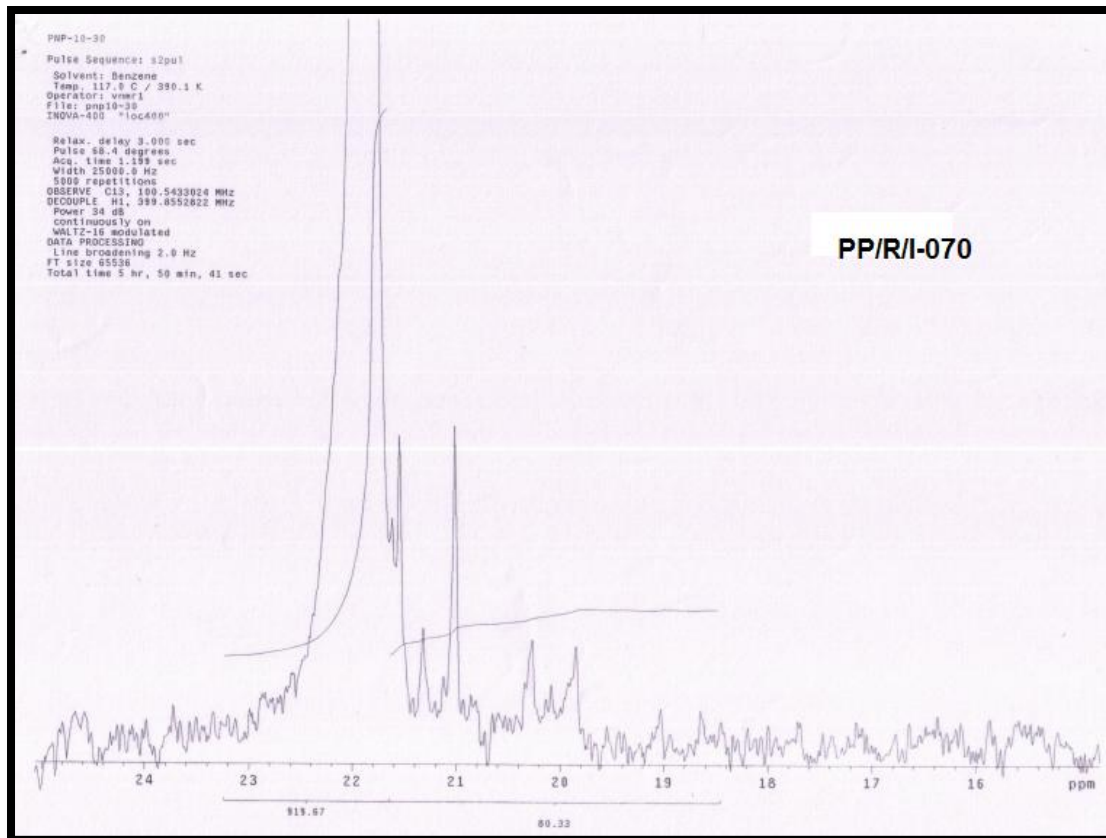


**Figure.9.1:**  $^{13}\text{C}$ -NMR spectra of PP/R/I-070.

In figure .9, 9.1, 9.2, 9.3, 9.4 and 9.5; it is found that the  $^{13}\text{C}$ -NMR spectra of PP/R/R-032, PP/R/I-70, PP/R/I-71, PP/R/I-75, PP/R/I-027 and PP/R/I-089 grades are predominantly isotactic in nature. However, the isotacticity i.e. %mmmm has been found to be 83% in PP/R/R-032, 92% in PP/R/I-70, 90% in PP/R/I-71, 84% in PP/R/I-75, 86% in PP/R/I-027 and 88% in PP/R/I-089. This shows that PP/R/I-70 grade has slightly higher concentration of isotactic sequences as compared to PP/R/I-71 and PP/R/I-089 respectively. While a marked difference were found in the results of % mmmm sequences as compared to that of PP/R/R-032, PP/R/I-75 and PP/R/I-027 grades.

On the other hand the results of xylene soluble contents found to be in the experimental error of 3.4% and therefore do not correspond to the % mmmm sequences obtained from the NMR-spectra.

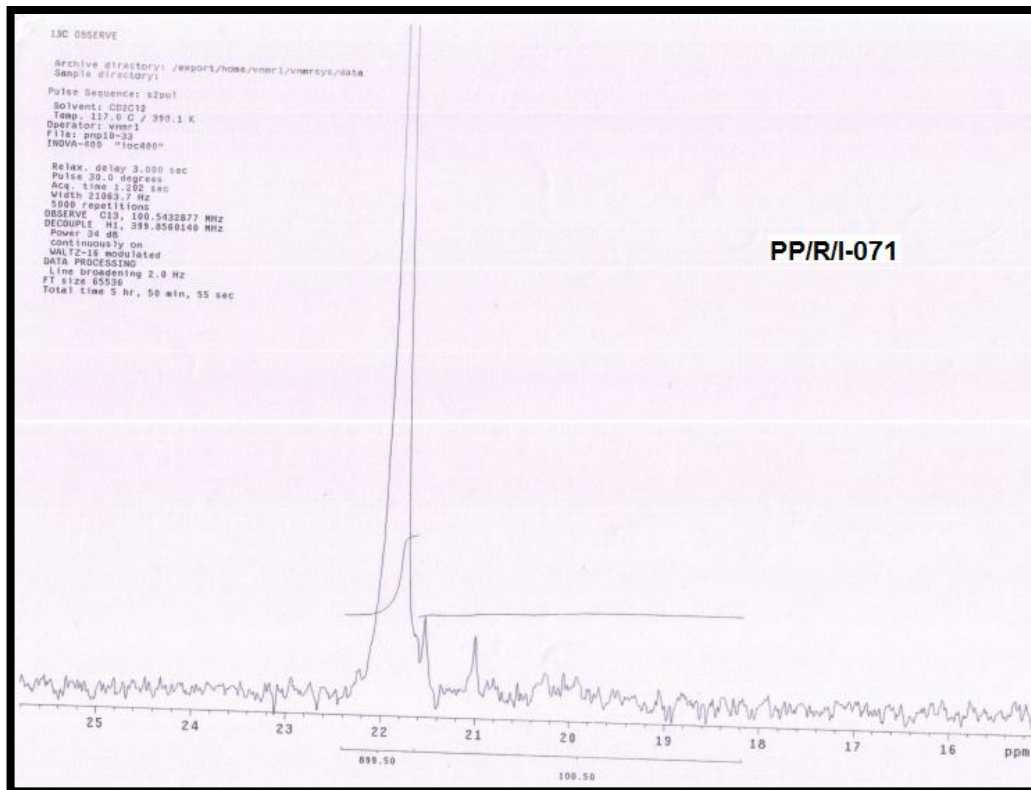


Figure.9.2:  $^{13}\text{C}$ -NMR spectra of PP/R/I-071.

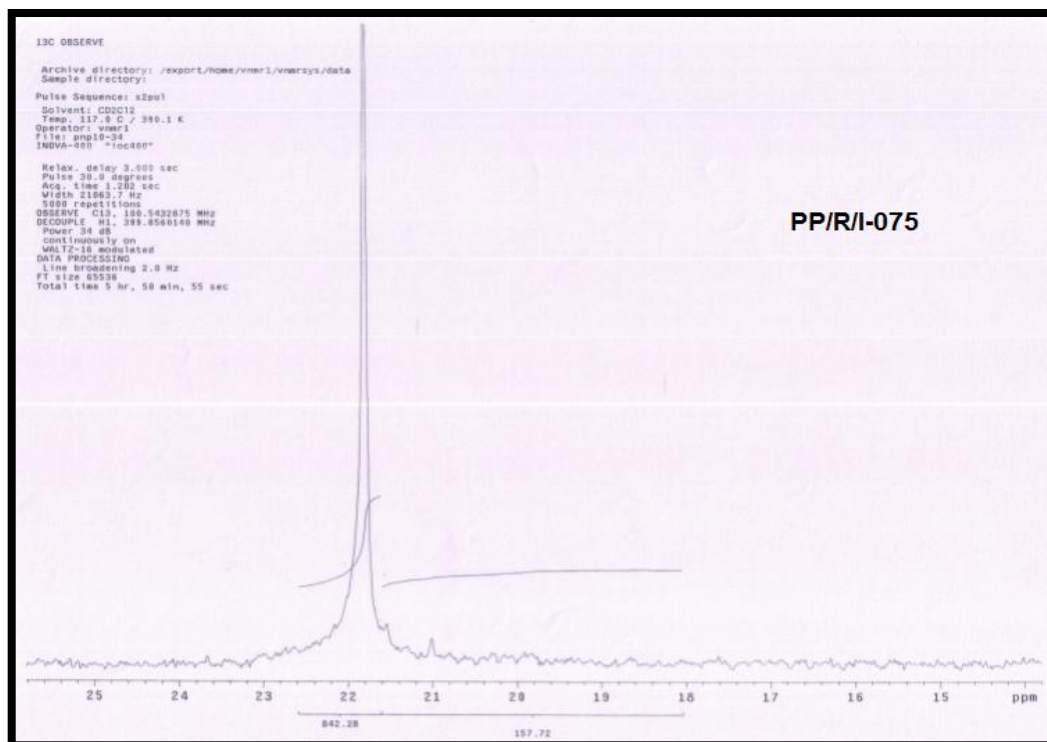
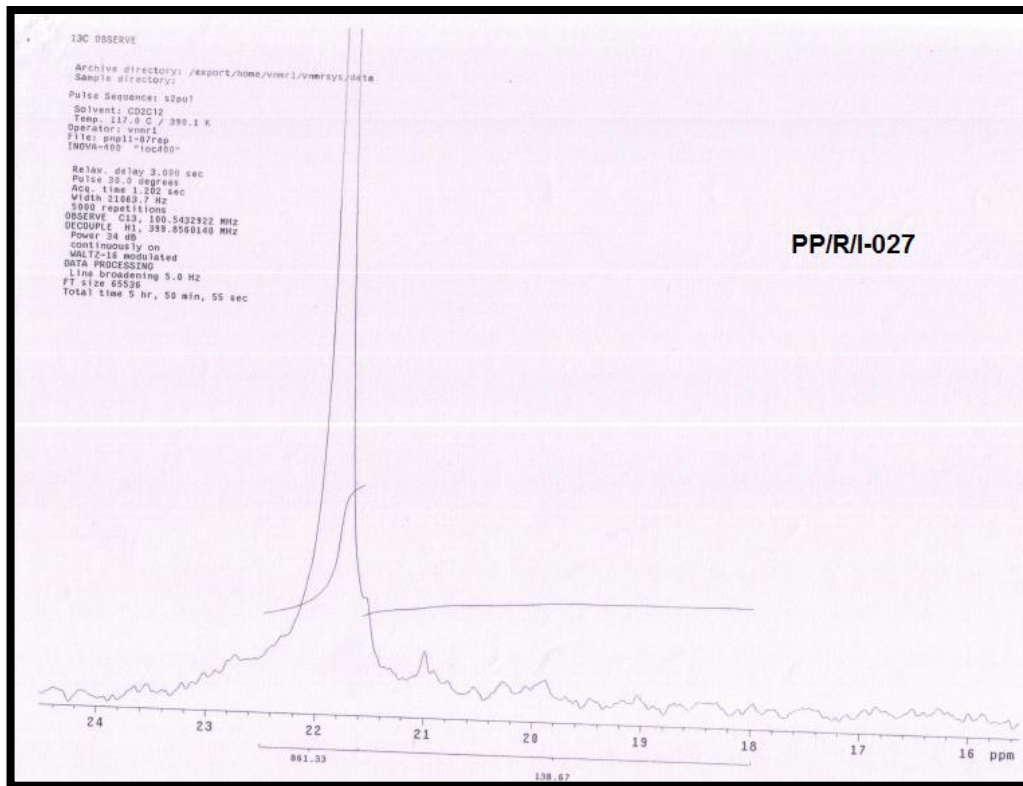
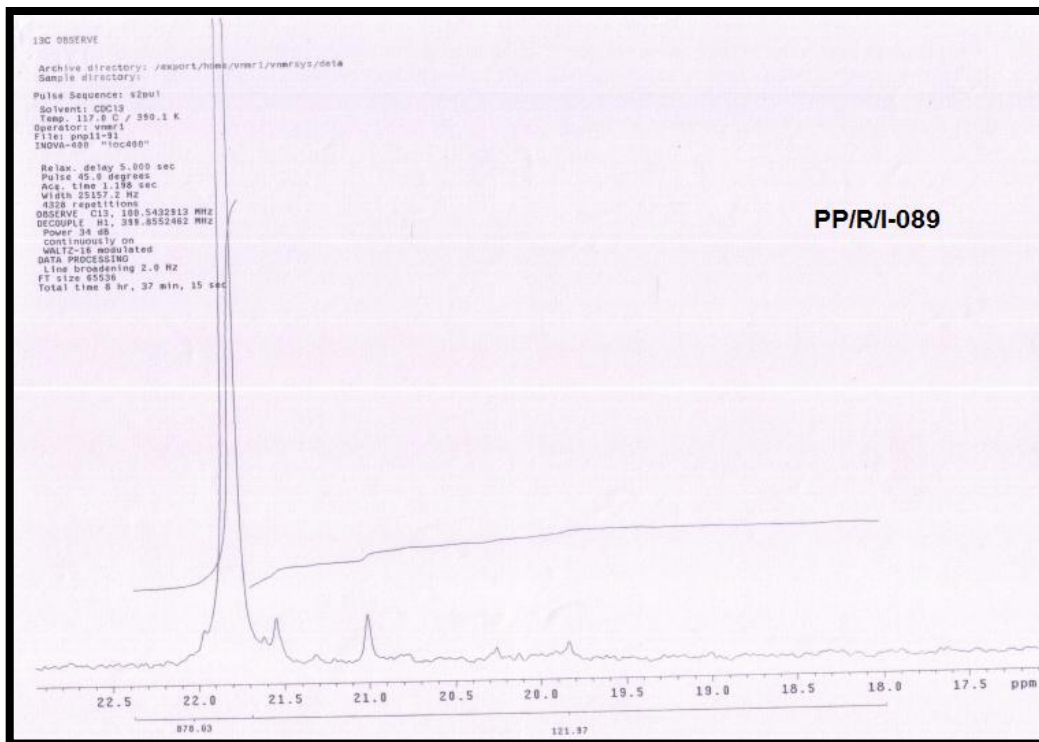


Figure.9.3:  $^{13}\text{C}$ -NMR spectra of PP/R/I-075.



**Figure.9.4:**  $^{13}\text{C}$ -NMR spectra of PP/R/I-027.



**Figure.9.5:**  $^{13}\text{C}$ -NMR spectra of PP/R/I-089.

## **CHAPTER 6**

### **Conclusion:**

A total of ten Polypropylene homopolymer Raffia grades were taken and a detailed “Benchmarking” study was carried out on the bases of various problems observed during the various field trials. Consequently, all the results were compared for each of the grades and reasons for inferior performance of some of the grades (PP/R/I-070, PP/R/I-071, PP/R/I-075, PP/R/I-027) compared to other performing grades (PP/R/R-036 and PP/R/H-031) were established.

- Xylene soluble was performed for all the ten grades, which is an estimation of the isotacticity. The results were found to be between the ranges of 3.1 to 3.5%, hence, no marked difference concluded.
- MFI of all the grades were carried out at different loads as per the ASTM D1238 and the results were found to be in the range of 3.9 to 2.4 at 2.16 kg load. On comparing the data, PP/R/R-036 has better flowability than PP/R/H-031 PP/R/I-071, PP/R/I-075, PP/R/I-027 and PP/R/I-089 grades up to third trial. This was further corroborated with the Power law index curves. On the other hand on comparing Power law graph of PP/R/H-031 with PP/R/I-089, it was found that both the grades have shown comparable flowability as it was also observed during the trial run where tape breakages occurred beyond 415mt/min.
- Power law constants were calculated for each grade and then by substituting the values in power law equation the viscosity for each grade were calculated for each shear rate ranging from 100 to 1000  $s^{-1}$ . Further, on comparison it was found that PP/R/I-075 has highest melt viscosity amongst all the other PP raffia grades over the entire range of shear rate. This was further correlated with the higher power consumption during the trial run. While on the other hand PP/R/I-066 overlap with that of PP/R/I-070, hence shown more shear thinning over the entire range of shear rate, except PP/R/R-036 which was found to have better flowability with lower power consumption during the trial run.

- Rheological characteristics of the melt were determined by the capillary rheometer. It was found that PP/R/I-027, PP/R/I-089 and PP/R/H-031 grades have higher shear viscosity over the entire range of shear rate ( $100\text{s}^{-1}$  to  $10000\text{s}^{-1}$ ) as compared to PP/R/R-036 and PP/R/H-031. Moreover, PP/R/R-036 grade comparatively has shown distinctively lowest shear viscosity over the entire range of shear rate.
- Molecular analysis of PP raffia grades at micro-level determined by HT-GPC (High Temperature Gel Permeation Chromatography) and the MWD data were generated and was further compared with that of MWD obtained from rheological analysis tool, Parallel Plate Rheometer. It was found that PP/R/I-075 and PP/R/I-071 have relatively high molecular weight tails than PP/R/R-036 and PP/R/H-031 which could be the reason for poor performance of the grades during the trial run. On the other hand PP/R/I-089 comparatively has lower amount of high molecular weight fractions while significantly has higher amount of low molecular weight fractions, this likely to be the reason for good performance of PP/R/I-089 during the trial (415mt/min). In addition to that PP/R/I-027 was the another grade on to which trial run were conducted and it was found that the grade performed well and achieved a line speed of 400mt/min with poor film quality and high water carry over along with the higher power consumption as compared to PP/R/R-036 and PP/R/I-089.
- DSC of all the ten grades was performed and the results were compared. It was found that the PP/R/I-075 and PP/R/I-071 grades relatively have high molecular weight fractions as the overall crystallinity was lower as compared to PP/R/R-036 and PP/R/H-031. The endotherm of the PP/R/I-075 has shown comparatively more heterogeneous lamellar distribution while PP/R/I-071 has shown more uniform melting endotherm. Moreover, it was found that PP/R/I-089 has similar trend of high molecular tail as that of PP/R/R-036 i.e. up to  $10^7$  (shown in figure 7.1.) but having higher amount of low molecular weight fraction with comparable crystallinity (shown in table 2.2).

- The stability of PP raffia grades, which could arise from the difference in the loading of anti-oxidant (AO) additive, was evaluated by OIT measurement and conclusively found that all the grades were stabilized well.
- Thermal analysis of PP raffia grades was performed on DMA (Dynamic Mechanical Analyzer) to analyze the different relaxation phenomena at micro-level. Two relaxation peaks namely  $\alpha$ -relaxation (63°C to 67°C) and  $\beta$ -relaxation (5.7°C to 7.5°C) was found. A slight shift in the  $\beta$ -relaxation were observed in three samples viz, PP/R/I-071, PP/R/H-031 and PP/R/I-075 while no such difference was found in the  $\alpha$ -relaxation in all the PP-raffia samples under study.
- $^{13}\text{C}$ NMR (Nuclear Magnetic Resonance) of PP raffia grades was performed on Varian Inova Unity spectrometer T 400 Mz to determine the % mmmm pentad sequence in the polymer. The % mmmm values found to in the range of 83% to 92%. It was found that PP/R/I-70 grade has higher in % mmmm pentad sequence values as compared to all other grades and consequently cannot further corroborated with the % xylene soluble values.

## **REFERANCES:**

1. Triplett KB. The evolution of Ziegler-Natta catalysts for propylene polymerization. *Appl Ind Catal* 1983; 1:177-205.
2. J. Huang, G. L. Rempel, *Prog. Polym. Sci.* **1995**, 20, 459.
3. K. Soga, T. Shiono, *Prog. Polym. Sci.* **1997**, 22, 1503.
4. Harding. G. The structure property relationships of polyolefines, *Ph.D. thesis, Stellanbosch University, 2009*
5. Frank P.T.J. van der.B. Crystallization of isotactic polypropylene: The influence of stereo-defects - *Eindhoven: Technische Universiteit, Eindhoven, 2002. Proefschrift. - ISBN 90-386-2674-6*  
*NUR 952.*
6. Androsch R , Di Lorenzo M L , Schick C , Wunderlich B. Mesophases in polyethylene, polypropylene, and poly(1-butene), *Polymer* **51** (2010) 4639-4662.
7. Mark, H.F, Bikels, N.M, Overbayer, C.G. Menges, G, *Encyclopedia of polymer science and engineering- Vol.13, John Wiley & Sons, Inc. Canada, 1988.*
8. B. Lotz, J. C. Wittmann, and A. J. Lovinger, *Polymer* **37**, 4979 (1996).
9. Batzer, H; *Polymere Werkstoffe, Band I, Chemie und Physik. Georg Thieme Verlag Stuttgart New York, 1985.*
10. F. Zuo et al. The role of interlamellar chain entanglement in deformation-induced structure changes during uniaxial stretching of isotactic polypropylene/, *Polymer* **48** (2007) 6867-6880
11. V.Busico, R.Cipullo, *Prog in Polymer sci* (2001), 26,443.
12. [www.technicaltextile.net/packaging-textiles/indian-raffia-industry/supplier.aspx](http://www.technicaltextile.net/packaging-textiles/indian-raffia-industry/supplier.aspx).
13. [www.ril.com/downloads/pdf/raffia%20and%20monofilaments.pdf](http://www.ril.com/downloads/pdf/raffia%20and%20monofilaments.pdf)
14. [www.jpextrusiontech.com/brouchers/tapeline/tape\\_stretching\\_line.pdf](http://www.jpextrusiontech.com/brouchers/tapeline/tape_stretching_line.pdf)
15. Culter, J; *Optimizing packing performance through polymer choice. Part 1. Basic polymer chemistry, 1999.*
16. B. Pornimit, G.W. Ehrenstein, *Adv Polym Tech*, **11**, 91 (1992)
17. H.X. Huang, *J Appl Polym Sci*, **67**, 2111 (1998)

18. G.K. Elyashevich, E.A. Karpov, O.V. Kudasheva, E. Rosova; *Mech Time-Depend Mat*, **3**, 319 (1999)
19. Vychopnova, J.; Cermak. R., Obadal. M., Morphology variations of polypropylene, *Modern Research and Educational Topics in Microscopy*, 2007.
20. Fischer, S; Physical properties of novel polypropylenes, *Ph.D. thesis, Institute for experimental physics, Ulm University, Augsburg, 2009.*

Same 20

21. Hedesiu, C.E; Structure-property-relationships in polyolefines, *Ph.D. dissertation, RWTH Aachen, Germany, 2007*
22. [www.fibcindia.com](http://www.fibcindia.com)
23. [www.comez.com](http://www.comez.com)
24. Vlachopoulos, J.; Strutt. D., The role of rheology in polymer extrusion, [www.polydynamics.com/Role\\_of\\_Rheology\\_in\\_Extrusion.PDF](http://www.polydynamics.com/Role_of_Rheology_in_Extrusion.PDF).
25. Schramm, G.; A practical approach to rheology and rheometry, *Gebrueder HAAKE GmbH, Karlsruhe, Germany, 2000.*
26. [www.viscotek.com](http://www.viscotek.com)
27. Menard, K. P.; Dynamic mechanical analysis: A practical introduction, *CRC press, Boca Raton, USA, 1999.*
28. Aho, J., Rheological characterization of polymer melts in shear and extension: Measurement reliability and data for practical processing, *Ph.D. thesis, Tampere University of Technology, 2011.*
29. Menczel, J. D; Prime. R. B, Thermal analysis of polymers: Fundamental and applications, *John Wiley & Sons, Inc., 2009.*
30. Wunderlich, B; *Macromolecules physics, vol 2. New yourk, Academic Press; 1976.*
31. Kolesov, I.S ;Androsch,R ; Radosch, H.J ; *Macromolecules*, **2005**, 38, 445
32. Stehling, F.C;Mandelkern, L; *Macromolecules*, **1970**, 3, 242
33. Nouri, M.R; *Iranian Polymer Journal*, **2005**, 14, 5, 485
34. Boyer, R.F ; *Macromolecules*, **1973**, 6, 288
35. Kolesov, I.S ;Androsch,R ; Radosch, H.J ; *Macromolecules*, **2005**, 38, 445



36. Flood, J.E; Nulf, S.A; How molecular weight distribution and drawing temperature affect polypropylene physical properties and morphology; *Polym Engg and Sc*, 1990, vol 30, No.23
37. Samuels, R.J; *J. Polym. Sci., Polym. Phys. Ed.* **13, 1417 (1975)**
38. M. Hikosaka, T. Seto, *Polym. J.* **5, 111 (1973)**
39. P. Corradini, G. Giunchi, V. Petraccone, B. Pirozzi, H. M. Vidal, *Gazz. Chim. Ital.* **110, 413 (1980)**
40. Corradini, P.; Napolitano, R.; Oliva, L.; Patraccone, V.; Pirozzi, B.; Guerra, G.; *Makromol. Chem., Rapid Commun.* **3, 753-756 (1982).**